System Modeling and Applications Based on Information in Time and Frequency Domains

Xinyu LIU

February 2022

The University of Kitakyushu Doctoral Thesis

System Modelling and Applications Based on Information in Time and Frequency Domains

Xinyu LIU

Graduate School of Environment Engineering, The University of Kitakyushu

February 2022

Abstract

System modeling is one of the fundamental issues in practical applications where dynamic characteristics are required for system design and analysis. Sometimes the system dynamics vary rapidly with time. Sometimes sufficient information such as the model structure, time difference, cannot be extracted from the uninformative experimental data by the conventional methods. Therefore, effective system modeling should work well under these complicated conditions to satisfy the practical requirements. This work focuses on the new approaches to deal with such system modeling problems based on information in time and frequency domains, and illustrates their applications in time-varying channel identification and localization system.

In the time-varying system, if the variation is too fast, most of the conventional methods fail to track the variation satisfactorily unless the prior information is available. It requires an efficient approximation of the fast varying parameters under less variation information, for example, a sum of cosines of various frequencies. Moreover, the insufficient frequency components of band-limited signals will lead to ambiguities in parameter estimation. As a result, the accuracy of the localization system for band-limited signals degrades largely.

This thesis illustrates how to solve the identification problem of insufficient information in system models. For the rapid time-varying system with less variation information, using the orthogonality of the trigonometric functions, more time-domain variation information can be obtained by estimating the coefficients of the cosine series with respect to each degree of the cosine harmonic term in a recursive manner. For the localization system with insufficient frequency components, both the spectral characteristics including phase information in frequency domain and the information evaluation in time domain are applied to improve the convergence performance.

The thesis contains the following six chapters as follows.

Chapter 1 first introduces the significance of system modeling and gives the general account of the system identification and its applications, respectively. Then, the existing methods for system identification and their methods under insufficient information conditions are summarized. At last, challenges are listed from the modeling perspective.

Chapter 2 gives some basic mathematical formulas and reviews the main preliminaries for time-varying model, parameter approximation based on cosine series, Gibbs effect at the rapid changing points, multi-path model, and multi-path interference.

Chapter 3 proposes a new recursive algorithm for the system with rapid variation but less variation information. The recursive identification using cosine series based approximation is introduced to remove the discontinuity of the model parameters by expanding the varying parameters into even periodic functions to remove the Gibbs effect at the time window edges. Numerical experiments exhibit the effectiveness of the proposed method, and it has a higher convergence rate than the conventional methods.

Chapter 4 proposes the extension of identification system using time-varying model. Some efficient approximation is used to reduce the computational complexity. The weight factor is imposed on the output and parameters to reduce the series degree. And a smoothing technique is considered to reduce the influence of the noise term. Moreover, to mitigate the fluctuation caused by Gibbs effect in the parameter estimates, the compensation of time-domain variation information through detecting the rapid changing is introduced. The experimental results validate the effectiveness of the proposed method, and it can track the true time-varying parameters faster than the conventional methods.

Chapter 5 proposes a localization system using multi-path model for band-limited signals. The function defined by following the signal band limitation is designed. Moreover, a time-domain information evaluation based genetic algorithm is introduced to avoid ill-conditioned numerical optimization. Simulation results confirm that the proposed algorithm performs with some advantages over the other conventional algorithms.

Chapter 6 concludes the thesis and gives future works. To conclude, this thesis shows the system models for the problem of insufficient information and proposes new approaches based on information in time and frequency domain. Numerical simulation results demonstrate the effectiveness of the new approaches. In future work, sparse identification will be considered to deal with the problem of insufficient data.

Preface

The general theme of this thesis is to show the system models under insufficient information conditions and elaborate on the process of system modeling through leveraging information from the time and frequency domains. This thesis is organized into six chapters. Most of the materials have been published in the following listed journal papers and conference papers.

The material in Chapter 3 is related to

- [P4] X. Liu and L. Sun, "Recursive Identification of Time-varying Systems with Rapid Changing", in *Proceedings of 13th International Conference on Innovative Computing, Information and Control*, August, 2018.

which has been extended into a journal paper and formulated the major content of this chapter

- [J3] X. Liu and L. Sun, "Recursive Identification Algorithm based on Cosine Basis for Rapid Time-varying Systems", *International Journal of Innovative Computing, Information and Control*, Vol.15, No.2, pp.617-628, April, 2019.

The material in Chapter 4 are related to

- [P3] X. Liu, L. Sun and J. Liu, "Trigonometric Basis Functions based Time-Varying Identification Algorithm with Output Weight Factor", in *Proceedings of 2019 12th Asian Control Conference (ASCC)*, pp.1072-1077, June, 2019.

- [P1] L. Sun, X. Liu and J. Zeng, "Recursive Identification of Time-varying Systems with Rapid Changing", in *Proceedings of 15th International Conference on Innovative Computing, Information and Control*, September, 2021.

which formulate the major content of this chapter.

The material in Chapter 5 is related to one research about a localization system for band-limited signals.

Acknowledgements

Time flies by, the past few years at the University of Kitakyushu have been full of rewarding. Many helped me along the way on this journey. I want to take a moment to thank them.

Foremost, I would like to express my deep and sincere gratitude to my research supervisor Lianming Sun for the continuous support of my Ph.D. study and research, for his patience, motivation, enthusiasm, and immense knowledge. He went above and beyond to help me reach my goal.

Besides, I would like to thank the rest of my thesis committee.

My sincere thanks also go to my love Yanni Ren for her companionship, encouragement, and guidance in writing my doctoral thesis.

Last but not least, I would like to thank my mum Lixin Xu: your love and understanding helped me through the dark times. Without you believing in me, I never would have made it. It is time to celebrate; you earned this degree right along with me.

Kitakyushu, Japan

Xinyu LIU

October 22th, 2021

Contents

List of Figures

List of Tables

Abbreviations

DPD	Direct Position Determination
TPM	Two-step Positioning Method
ML	Maximum Likelihood
ToA	Time of Arrival
TDoA	Time Difference of Arrival
AoA	Angle of Arrival
LS	Least Squares
WLS	Weighted Least Squares
CRLB	Cramér Rao Low Bound
EM	Expectation Maximization
WRELAX	Weighted Fourier Transform and RELAXation
JML	Joint Maximum Likelihood
MUSIC	MUltiple SIgnal Classification
ESPRIT	Estimating Signal Parameter via Rotational Invariance Techniques
RTLS	Real-Time Locating Systems
SNR	Signal-to-Noise Ratio
DoA	Direction of Arrival
WSF	Weighted Subspace Fitting
LPV	Linear Parameter Varying
FRFs	Frequency Response Functions
RLS	Recursive Least Squares
LMS	Least Mean Square
NLMS	Normalized Least Mean Square
AP	Affine Projection

BOP	Block Orthogonal Projection
GA	Genetic Algorithm
ACO	Ant Colony Optimization
PSO	Particle Swarm Optimization
SEM	Singularity Expansion Method
SGPOF	Sparse Generalized Pencil-Of-Function
SCE	Shuffled Complex Evolution
DFT	Discrete Fourier Transform
FFT	Fast Fourier Transform
MSE	Mean Square Error
CS	Cosine series
RCS	Recursive identification based on Cosine series approximation
WCS	recursive identification with output Weighted Cosine Series
RSS	Received Signal Strengthg
AP-ML	Alternation Projection Maximum Likelihood
RML	Refined Maximum Likelihood
IEGA	Information Evaluation based Genetic Algorithm
RMSE	Root Mean Square Errors
CRB	Cramér Rao Bound

Symbols

$u(\cdot), s(\cdot)$	input
$y(\cdot), a(\cdot)$	output
$e(\cdot), v(\cdot)$	noise
h	path attenuation coefficient
ϕ	correlation vector
κ	variation rate
$E\{\cdot\}$	mean
$cov(\cdot)$	covariance function
σ^2	mean square error
c	coefficients of cosine series
θ	coefficient vectors
$\mathbf{I}$	identity matrix
$\mathbf{W}$	diagonal matrix
$\mathbf{\Phi}$	correlation matrix
$\mathbf{P}$	the inverse of the correlation matrix
$\mathbf{g}$	gain vector
ε	error
λ	forgetting factor or coefficient
$\eta(\cdot)$	compensation function
Y	cross power spectral ratio
$w(\cdot)$	weight coefficient
f, F	fitness function
γ	individual chromosomes

Chapter 1

Introduction

1.1 System Modeling and its Application

System modeling is generally accepted as an executable system description that allows the analysis and measurement of system behavior. In scientific research, in order to simulate, predict and control the system, the object to be studied is usually abstracted into a certain mathematical model and then, according to certain experiment and analysis means, the relationship between internal and external factors of the system is obtained by testing the observed input and output information. That is, the input-output relationship described by the mathematical relationship reflects the characteristics of the system model, which is shown in Fig.1.1.

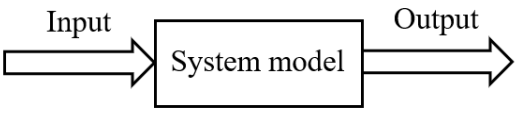

FIGURE 1.1: The schematic chart of system model

System identification is an important data-driven approach to constructing a mathematical model for the practical system. Mathematical models can be divided into static and dynamic mathematical models according to time factors. System identification is mainly to study the modeling method of the dynamic mathematical model. The mathematical model of the dynamic system can be divided into a time-varying system

and a time-invariant system according to whether the parameters vary with time. A time-varying system is a system whose parameters change with time. Compared with the estimation of constant parameters, time-varying parameters are much more difficult to be estimated.

In many practical systems, due to the various internal and external forces, the system model parameters are difficult to remain unchanged and often vary with time. Sometimes the impact of such changes cannot be ignored. The time-varying characteristics of parameters often make the dynamic and static characteristics of the system change significantly and even threaten the stability of the whole system. Or due to large uncertainty such as system noise, incomplete test information, and missing benchmark models, system models often encounter problems of insufficient information, which will lead to ambiguities in parameter estimation. As a result, system model identification faces significant challenges. Consequently, how to obtain a relatively accurate system model under these complicated conditions will be a considerable research direction.

This thesis focuses on the new approaches based on information in time and frequency domains to deal with the above system modeling problems, and their applications in time-varying channel identification and localization system in system identification.

1.1.1 System identification

System identification has been successfully applied in many practical applications, which are mainly reflected in the following aspects:

(1) For the design and analysis of the control system [1]. After the mathematical model of the controlled process is obtained by using the identification method, a more reasonable control system can be designed based on this model or used to analyze the performance of the original control system in order to put forward an improvement scheme.

(2) For online control [2]. In engineering practice, a large number of systems are time-varying systems. Through system identification, the mathematical model of

the controlled object is established online, and the parameters of the controller are continuously adjusted to implement adaptive control of the controlled object so as to obtain a better control effect.

(3) For monitoring process parameters [3] and realizing fault diagnosis [4]. Many practical processes, such as aircraft, missiles, nuclear reactors, mechanical engineering, large metallurgical equipment, etc., hope that possible faults can be monitored and detected frequently in order to eliminate them in time and avoid faults. This means that it is necessary to continuously collect information from the process, and infer the changes in the dynamic characteristics of the process, and then determine whether the fault has occurred, when it occurred, the size of the fault, the location of the fault, and so on based on the changes in the process characteristics [5].

(4) For forecasting weather, population, energy, and passenger flow [6–8]. When the model structure is determined, a time-varying model is established, and time-varying model parameters are estimated. Then the process is forecasted on this basis.

1.1.2 Localization system

Localization systems has been successfully applied in many practical applications, which are mainly reflected in the following aspects:

(1) For the military field. In maritime affairs, submarines use sonar systems to search, track, locate and identify targets [9, 10]. In the army and air force, localization technology can be used in artillery location, airspace enemy aircraft monitoring, and other scenes [11, 12].

(2) For noise detection and health monitoring of mechanical equipment [13]. Because some industrial equipment is not allowed to stop or perform offline diagnosis, the localization technology can identify the fixed frequency of noise for noise spectrum analysis or noise feature identification, so as to realize online detection and real-time health monitoring.

(3) For large-scale meetings, intelligent robots, security monitoring, and other scenes. In large-scale audio and video conference scenes, sound source tracking and speech enhancement can achieve a better conference pickup [14]. In the field of intelligent mobile robots, localization technology can help robots obtain more external information and respond to the changes of the external environment [15]. In the field of intelligent security monitoring, When the visual monitoring equipment cannot normally work due to insufficient light or obstruction by obstacles, sound source localization can realize acoustic monitoring of the target area [16].

The taxonomy of localization system is visualized in Fig.1.2.

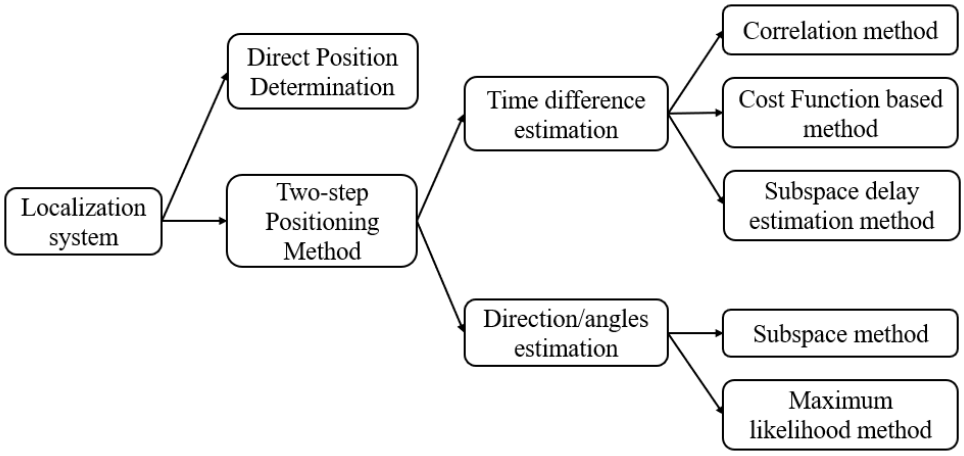

FIGURE 1.2: Localization system taxonomy

A large number of efforts have been made to improve the localization performance under various practical conditions. The location of the target signal can be realized by the Direct Position Determination (DPD) [17] or the Two-step Positioning Method (TPM) [18], in which the DPD is to directly solve the location of the target signal through the received signal. The TPM is to estimate the parameters first and then combine these parameters to solve the location effectively. Based on the Maximum Likelihood (ML) criterion, the direct location method directly estimates the location according to the received signal to avoid the loss of location information, and the localization performance is relatively better [19, 20]. However, compared with the DPD, the TMP has the obvious advantage of low computation and has more practical applications.

The well-known existing TPMs include the Time of Arrival (TOA) method [21], the Time Difference of Arrival (TDoA) method [22, 23], and the Angle of Arrival (AOA) method [24, 25]. they can be mainly divided into two categories: time delay estimation and direction estimation.

- **Time delay estimation**

Knapp and Carter [26] first proposed the generalized cross-correlation method, which marks the time delay estimation algorithm entering a new era. Soon, a large number of methods, such as cross-bispectrum delay estimation [27], high-order statistics delay estimation [28], and adaptive delay estimation [29], etc., have successively been proposed. Especially under multi-path conditions, the complexity of the localization system increases further. Generally speaking, time delay estimation can be divided into three categories: Cross-correlation method, Cost Function based method, and Subspace delay estimation method.

(1) Cross-correlation method

Cross-correlation methods, such as the classical basic correlation method and matched filtering method [30, 31], is to estimate the time delay by maximizing the correlation functions of the measured signal waves. However, these methods are easily limited by the influence of signal bandwidth and multi-path interference, and estimation performance degrades largely [32, 33]. In order to deal with the multi-path problem, Sun and Liu [34] introduced time refinement for delay estimation to reduce the influence of sidelobe in the correlation function by improving the resolution method. In addition, Ni et al. [35] used the phase correction factor to solve the fractional part of the delay, thereby suppressing multi-path interference by compensating the delay. The above methods have the advantages of low computational complexity and good real-time performance. However, in the severe multi-path environment, the delay estimation performance of these methods will decrease significantly. When the delay difference of multi-path components is tiny, they cannot even distinguish multi-path delay.

(2) Cost Function based method

Time delay estimation methods based on the cost function, such as the classic Least Squares (LS) method [36], ML method [37], etc. is to establish a cost function and use the minimum average cost as the criterion to optimate the time delay estimation by an iterative algorithm. These methods generally have no requirements for signal statistical characteristics. Under the multi-path condition, the estimation accuracy can reach the Cramér Rao Low Bound (CRLB) and realize super-resolution estimation of time delay. Therefore, the Expectation Maximization (EM) algorithm based on the ML criterion [38] and the Weighted Fourier Transform and RELAXation (WRELAX) algorithm based on the LS criterion [39] have been successively applied to engineering projects. Xie et al. [40] proposed a maximum likelihood delay estimation algorithm in a multipath wireless propagation channel. By sampling the frequency domain response of the multi-path channel, the joint probability density function of the multi-path channel was obtained, thereby estimating the time delay of different paths according to the ML criterion. Del Peral-Rosado et al. [41] combined the channel estimation model based on equispaced taps with time delay estimation to produce a low-complexity estimator. By introducing arbitrary taps with variable positions between the first two equispaced taps, this model is enhanced with a novel channel parameterization that can characterize close-in multipath. This new hybrid method is used in the Joint ML (JML) delay estimator to improve the ranging performance in the presence of short-delay multipath. However, these methods cannot avoid multi-dimensional optimization problems. The iterative algorithms converge to the global maximum at the cost of increased computational complexity, and their real-time performance is not strong.

(3) Subspace delay estimation method

Bruckstein et al. [42] first applied the MUltiple SIgnal Classification (MUSIC) [43] method to multipath delay estimation. Still, due to its special requirements for the array flow pattern, its estimation performance had not been greatly improved compared with the conventional correlation method. Saarnisaari [44] introduced the Estimating Signal Parameter via Rotational Invariance Techniques (ESPRIT) [45] method to estimate the time delay, and this method deconvolved the frequency domain model to construct an ESPRIT-like model to estimate the time delay by the total LS method. The subspace delay estimation methods are essentially the application of a spatial spectrum algorithm

with super-resolution characteristics in time delay estimation. Ge et al. [46] proposed a new super-resolution time delay estimation method under multi-path conditions. The received signal was first correlated and then transformed into the frequency domain, and by the MUSIC algorithm, the time delay was estimated. This method had better parameter estimation performance compared with the traditional MUSIC algorithm. Shin et al. [47] developed a super-resolution time delay estimation method based on ESPRIT for Real-Time Locating Systems (RTLS) and analyzed its performance in the multi-path environment. The above methods may produce large errors under the condition of narrow-band, especially at low Signal-to-Noise Ratio (SNR), and their performance still has a certain distance compared with the CRLB boundary.

- **Direction estimation**

In recent years, the Direction of Arrival (DoA) method for estimating the signal has become more perfect. The MUSIC method proposed by Schmidt [43] and the ESPRIT method proposed by Roy et al. [45] are the most famous. The MUSIC method breaks through the Rayleigh limit, marking that high-resolution direction-finding technology and subspace methods have entered a new era.

The basic idea of the subspace method is to extract useful low-rank information from the observation data of mixed noise. Usually, the eigenvalue decomposition of the covariance matrix of the observation data is used to estimate the angle parameters by constructing the signal or noise subspace method. ESPRIT method uses the rotation invariance of signal subspace to estimate the parameters of the closed-form solution, which avoids the spectral peak search required by the MUSIC method and greatly reduces the amount of computation [48]. On this basis, a large number of methods, such as the MUSIC method based on decoherence, Weighted ESPRIT method [49], and Weighted Subspace Fitting (WSF), ML method [50], have been proposed successively.

Jiang et al. [51] used a MUSIC algorithm for multiple signal classification in feature space based on forward-backward spatial smoothing. This algorithm first preprocessed the coherent signal and then applied the eigenspace MUSIC algorithm for accurate DOA estimation. Herzog and Habets [52] proposed a new Eigenbeam-ESPRIT method which

uses three recurrence relations and a joint-diagonalization procedure to estimate the unit-vectors pointing to the source DOAs. This method can estimate the source DOAs with higher accuracy, and the estimation accuracy does not depend on the source DOAs. Meng et al. [53] proposed a novel robust block sparse recovery algorithm by using the WSF to deal with the DOA problem under the condition of unknown mutual coupling.

1.2 Related Works

1.2.1 Identification methods

With the development of science and technology, the research in parameter identification has experienced from time-invariant systems to time-varying systems. Several categories of identification methods for time-varying systems have been developed. Some segmentation approaches separate a time-varying model into several local models by detecting the variation [54, 55] or following the variation information in some associated measurable variables of Linear Parameter Varying models (LPV) [56]. Some existing adaptive algorithms [57–59] may track the varying dynamics. Several methods explicitly approximate the parameter variation through the orthogonal basis functions.

These methods mainly consider two situations. The first case is that the change of time-varying parameters is relatively slow, or the output process is weakly non-stationary. Segmental identification using segmental time-invariant assumptions or adaptive tracking algorithms for online identification is used. The second case is that the signal has strong non-stationary characteristics. The model parameters are approximated by the weighted sum of some basis functions. They can help approximate dynamics at arbitrary rates when the signal has sufficient excitation. The following will summarize the above methods respectively.

(1) Segmentation method

The segmentation method separates a time-varying model into several local models by segmenting the observation data concerning the significant variation. Qin et al. [60]

proposed a local approach for the LPV identification of an actuated beam using the Frequency Response Functions (FRFs) of piezoelectric actuators and sensors and the spatially-varying characteristics of the FRFs at various input and output locations were explored. Steinbuch et al. [61] showed that an LPV model was derived by using measured FRFs at different positions, fitting a parametric model on each measurement, and combining these models by linking parameters via a fit as a function of the operating point. Lin et al. [62] developed an identification method based on short-time invariant assumption to identify timevarying system parameters for a multi-degreesoffreedom degrading structure. Yu [63] made steady processing of each segment of the response signal and used the local model to identify the structural parameters. The time segment length of this method determines the identification accuracy and time resolution. Too short a time segment will result in low identification accuracy, and too long a time segment will also result in poor time resolution. Therefore, this method can only be applied to problems with slowly varying parameters [64].

(2) Adaptive filtering method

In order to overcome the problems of low identification accuracy and selected time segment length in the local stationary model, Several types of adaptive filtering methods, such as the Recursive Least Squares (RLS) with a forgetting factor [65, 66], the Least Mean Square (LMS) or the Normalized Least Mean Square (NLMS) algorithms [67, 68], the Affine Projection algorithm (AP) [69], and Block Orthogonal Projection (BOP) [70], Kalman filter [71], wavelets [72] are used to analyze or track the varying dynamics for online identification.

- **Recursive Least Squares with a forgetting factor**

The forgetting factor can reduce the influence of past data on existing data. Like the time segment length in the segmentation method, the forgetting factor determines the accuracy of parameter identification and tracking ability. The smaller the forgetting factor, the faster the old data is forgotten, and the stronger the estimated tracking ability. However, estimation accuracy will decrease due to the increase of covariance matrix. Therefore, compared with the segmentation method, the accuracy of the adaptive

filtering method is improved to a certain extent. Still, it can only track slowly varying parameters and is sensitive to initial values in identification [73]. Kulhav [74] proposed a recursive identification method with an exponential forgetting factor for online real-time identification. Cooper [75] studied online versions of seven time-domain system identification algorithms and summarized the ability to track the time-varying frequency and damping parameters. Afterward, Cooper and Worden [76] presented an online parameter estimation scheme based on a physical model. Tracking of time-varying physical parameters was achieved by using a forgetting factor.

- **Least Mean Square algorithms**

LMS algorithm estimates gradient vectors with instantaneous values. Its main features include low computational complexity, easy convergence in the stationary environment, and unbiased convergence to the Wiener solution. The convergence rate of the LMS algorithm is inversely proportional to the step factor, and the steady-state error is proportional to the step factor. That is, the convergence rate of the fixed-step LMS algorithm and the steady-state error is contradictory [77, 78]. To overcome this problem, many improved LMS algorithms have been proposed by changing the step size [79, 80]. The idea of these algorithms is to initialize a larger step size so that the algorithm has a faster convergence speed and then gradually reduce the step size with the deepening of the convergence to reduce the steady-state error. However, when tracking the time-varying system, especially at the abrupt points, the tracking speed will become slower as the system parameters jump more frequently. As a result, the tracking performance of the algorithms is not satisfactory.

- **Affine Projection algorithm**

In order to overcome the limitations of the LMS and RLS algorithms, Ozeki and Umeda [81] first proposed the AP algorithm. AP algorithm improves the performance by reusing the past input signal, which can be regarded as a generalization of the NLMS algorithm [82]. AP algorithm is a method based on increasing dimensions. When the dimension of the input signal increases from a one-dimensional vector to a matrix, the

convergence speed of the weight coefficient vector is accelerated. But this method also comes with an increase in computational complexity and steady-state imbalance. Like other algorithms, the AP algorithm also suffers from a contradiction between the steady-state offset and the convergence speed [83].

(3) Basis function expansion methods

This method is to approximate the model parameters as the weighted sum of some functional series. The parameter estimation problem of the time-varying system will transform into the parameter estimation problem of the time-invariant system, and then the weight of the functional series of the system is estimated by the time-invariant method.

At present, a variety of basis functions, such as polynomial functions about time [84], Legendre polynomials [85], Fourier series [86, 87], Chebyshev polynomials [88], Jacobi polynomials [89], Walsh function [90], discrete oblate spheroid function [91], B-spline [92], various wavelet basis functions [93, 94],etc., have been applied to the approximation method based on Funcional Series. When using these methods to identify the modal parameters, it is necessary to deal with the problems such as the selection of model order, the solution of model coefficients, and the elimination of false modes. The quality of its processing will directly affect the reliability of the identification results [64].

Charbonnier [95] pointed out that the accuracy of model parameter estimation was affected by the type of basis functions. However, it was difficult to find a suitable criterion to select the type and dimension of the function family. Through numerical experiments, Zou et al. [90] pointed out that the Legendre polynomial was suitable for slowly varying time-varying coefficients, and the Walsh function was suitable for piecewise stationary time-varying coefficients. Asutkar et al. [96] pointed out that the Haar wavelet basis function had more advantages than the Fourier series and Legendre polynomial in dealing with step time-varying coefficients. In addition, different types of basis functions are combined to improve the tracking ability of basis functions for time-varying coefficients of different forms and speeds. For example, Chon et al. [97] proposed to use B-spline wavelet basis functions of various orders. Li et al. [98]

proposed to use a combination of smooth Legendre polynomials, and abrupt Walsh functions through Gram-Schmit orthogonalization. Walter and Shen [99] pointed out that as long as a sufficient number of basis functions were used, any basis functions can approximate any known curve with arbitrary precision.

1.2.2 Methods under insufficient information conditions

In the practical environment, observation data may suffer from insufficient information, the system is disturbed by a complicated noise. As a result, sufficient information on the model structure or parameter variation cannot be extracted from the observation data. Consequently, for conventional methods, the stability of numerical computation cannot be guaranteed [100], and large uncertainty remains in estimated models. The sensitivity to noise and identification accuracy of existing methods should be further improved.

Some methods for the problem of insufficient information have been developed. For example, some regularization terms [101–103] are introduced into the optimization algorithm to stabilize the numerical computation. Sparse modeling methods can efficiently recover high-dimensional unobserved signals from a limited number of measurements. Compensation methods are proposed to mitigate the influence of insufficient information. Output over-sampling scheme is applied to decrease the affection of the noise. In addition, due to the effectiveness and robustness of intelligence algorithms in coping with insufficient information and noise, some intelligence algorithms such as Genetic Algorithms (GA), Ant Colony Optimization (ACO) [104], Particle Swarm Optimization (PSO) [105], have been applied to the problem of system identification.

- **Regularization method**

Tarantola [106] added a Tikhonov regularization to the data-matching term in the objective function to be minimized. Chen [107] proposed an approach for detecting local damage in large-scale frame structures by utilizing regularization methods for ill-posed problems. Numerical examples for a building model structure showed that structural damage could be correctly identified at a detailed level using only limited

information on the measured noisy modal data for the damaged structure. Guo et al. [108] presented a novel sparse-regularized minimum constitutive relation error approach for structural damage identification with modal data in order to circumvent the ill-posedness of the inverse problem caused by the use of the possibly insufficient modal data and enhance the robustness of the identification process.

- **Sparse modeling method**

Mimasu et al. [109] utilized the optimal sensor groups decided by correlations between sensors to reconstruct sparse-like system matrix for system identification. The validity of the proposed approach was examined by utilizing the data both from simulations and field experiments on a steel girder bridge. Mohammadi et al. [110] pointed out Singularity Expansion Method (SEM) suffer from imposition of spurious poles on the expansion of signals due to the lack of apriori information about the number of true poles. Sparse Generalized Pencil-Of-Function (SGPOF) was proposed to address this problem. The proposed method excluded the spurious poles through sparsity-based regularization with ℓ_1-norm.

- **Compensation method**

Li and Jun [111] put forward the concept of compound inversion, and on this basis, they proposed representative compensation algorithms and statistical average algorithms. Wang et al. [112] reviewed structural identification with incomplete input information, and further studied the multiple inversion method based on the least square method. A new weighted average approach was proposed for the multiple inversion method based on the average statistical approach. Mayr et al. [113] studied optimal input design and bias-compensating parameter estimation methods for continuous-time models applied on a mechanical laboratory experiment in order to reduce the deviation caused by insufficient incentive information.

- **Output over-sampling scheme**

Sun et al. [114] applied an output over-sampling scheme to collect the experimental data, and then more information on cyclo-stationarity could be detected from the over-sampled data even under severe conditions. Sun et al. [115] applied the cyclo-stationarity to deal with the numerical problems. The model structure was determined by both the mean squared error and the cyclo-stationarity detection. The parameter estimation was performed by optimizing both the criteria in both the time domain and the cyclo-stationarity in the subspace. Sun et al. [116] introduced the output over-sampling scheme to collect the experimental input-output data and extracted the information in time and space domains to complement information criteria for numerical optimization (more details can be found in published papers).

- **Intelligent algorithm**

Na et al. [117] introduced a new damage evaluation method in order to overcome the problem of the lack of data provided by structural monitoring. The method identified the structural damage in a shear building based on a GA using the structural flexibility matrix with dynamic analyses. Tang et al. [118] proposed the Shuffled Complex Evolution (SCE) algorithm to identify the parameters of the structural system. Numerical examples, including incomplete output information, noise interference, and no prior parameter information, demonstrated the effectiveness of the SCE algorithm for structural system identification problems.

1.3 Goals of the Thesis

Considering the system modeling problems of fast variation or inadequate information, effective system modeling should work well under these complicated conditions to satisfy the practical requirements by extracting much information and applying it more efficiently. This thesis proposes new approaches based on information in time and frequency domains.

1.3.1 New recursive algorithm using time-varying model

The purpose is to implement the cosine series based approximation into recursion of parameter update for the rapid time-varying systems.

Through expanding the time-varying parameters into the virtual even periodic functions, the parameters can explicitly be approximated by the orthogonal cosine series. By making use of the orthogonality of the trigonometric functions, the parameter estimation problem becomes the estimation problem of the series coefficients with respect to each degree of the cosine harmonic term in the frequency domain in a recursive manner.

1.3.2 Extension of identification system

The purpose is to decrease the series degree without degrading the tracking performance of the identification method, promptly detect the rapid changing points, and further compensate for the fluctuation in parameter estimates in order to improve the approximation performance.

By introducing a weight factor to the output and time-varying parameters, the weighted parameters can be approximated by the cosine series with considerable low degree cosine series through virtually expanding them into the even periodic functions. Detection of abrupt variation points and parameter compensation are introduced into the recursive identification algorithm for the time-varying systems with rapidly changing, and more time-domain variation information can be obtained through parameter compensation. Moreover, a smoothing technique is also considered to reduce the influence of the noise term (Chapter 4).

1.3.3 Localization system for band-limited signal source

The purpose is to propose an information evaluation based genetic algorithm (IEGA) for time difference estimation to avoid ill-conditioned numerical optimization in order to tackle the challenge of insufficient frequency components caused by limited bandwidth.

The originality of the proposed algorithm has two folds. Firstly, to reduce the influence of noise outside the signal band, the fitness function defined by following the signal band limitation is designed. The spectral characteristics including phase information in frequency domain are used to analyze the characteristics of multiple paths. Secondly, to avoid the local optimum, a time-domain information evaluation through cross-evaluation within the multi-receivers is introduced in the selection operation (Chapter 5).

1.4 Challenges

1.4.1 Model structure selection problem

The basis function expansion method transforms the time-varying problem into a time-invariant problem by introducing an explicit basis function, and it is suitable for rapidly varying systems. By selecting an appropriate basis function, the identification accuracy can be improved. However, the accompanying problems are: How to choose the model structure, including basis function type and model order.

1.4.2 Online identification problem

With the continuous development of recursive algorithms, they have also been widely used in time-varying parameter identification. In addition to recursive subspace methods, adaptive filtering methods and segmentation methods can all be used in online identification. However, there are not many studies on the online identification of the basis function expansion methods. In order to make use of the high precision and the ability to track different change speeds based on the basis function expansion method, how to rewrite this method into a recursive form has become a focus issue.

1.4.3 Gibbs effect

Gibbs effects that occur at the rapidly changing points, such as abrupt variation or discontinuous points, cause the fluctuation in the parameter estimation. As a result, the tracking performance of identification will degrade severely. In the recursive identification algorithms based on the parameter approximation of basis function expansion, how to improve the efficiency and accuracy of the algorithm is a crucial issue.

1.4.4 Limited bandwidth

In the practical environment, the source signals, such as low-frequency seismograms, vibration signals, some signals in instrumentation systems, often have severe band limitation, while the frequency components outside the signal band will be dominated by noise. As a result, the band-limited signals often yield significant errors in space decomposition or parameter estimation, and hence deteriorated localization accuracy leads to extensive degradation of localization performance, whereas few effective methods can handle the problem with band-limited signals.

1.5 Thesis Outlines and Main Contributions

This thesis shows the cumulative works over my doctoral period through six chapters.

Chapter 1 lays the fundamental background that connects the whole thesis and shows an outline. **Chapter 2** gives some main preliminaries for the time-varying model and multi-path model. **Chapter 3** proposes a new recursive algorithm for the system with rapid variation but less variation information. **Chapter 4** proposes the extension of identification system using time-varying model. **Chapter 5** proposes a localization system using multi-path model for band-limited signal source. Finally, **Chapter 6** summarizes our findings and applications and discusses the future study. The outline of

this thesis is depicted in Fig.1.3, in which the indexes represent the published paper in Publication List.

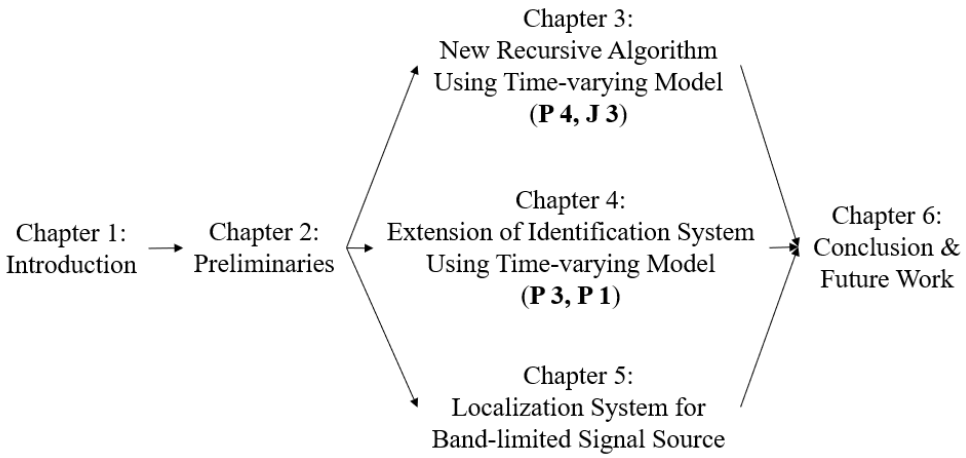

FIGURE 1.3: Outline of this thesis

Chapter 2 gives the description of time-varying and multi-path models and illustrates some main preliminaries for time-varying system and localization system.

Chapter 3 proposes a new recursive algorithm using time-varying model for insufficient variation information. The parameters can be approximated by the cosine series through virtually expanding into the even periodic functions. Then the parameter estimation can be realized by estimating the coefficients of the cosine series with respect to each degree of the cosine harmonic term in a recursive manner. Furthermore, in the virtual expansion of even periodic functions, the Gibbs effect at the window edges can be reduced largely.

The main contributions related to this chapter are shown as follows:

- This thesis builds a linear time-varying model for the rapid time-varying system.
- The parameters can be approximated by the cosine series by virtually expanding into the virtual even periodic functions.
- The virtual even periodic function can reduce the influence of the Gibbs effect at the window edges.
- The orthogonality of the trigonometric functions is applied to effectively implement the recursion of the cosine basis.

Chapter 4 proposes the extension of identification system based on time-varying model of **Chapter 3**. A weight factor imposed on the output and parameters is introduced into the recursive identification based on cosine series approximation to reduce the series degree. A smoothing technique is considered to reduce the influence of the noise term. Moreover, detection of abrupt variation points and parameter compensation is introduced into the recursive identification algorithm for the time-varying systems with rapidly changing to mitigate the fluctuation in the parameter estimation.

The main contributions related to this chapter are shown as follows:

- A weight factor is imposed on the output and parameters to decrease the degree of cosine series and suppress the rapid variation.
- A smoothing technique is introduced to reduce the influence of the noise term.
- Detection of abrupt variation and the parameter compensation is introduced to reduce the influence of the Gibbs effect.

Chapter 5 proposes a localization system using multi-path model for insufficient frequency information. The cross power spectral ratio method from the phase information is introduced to analyze multi-path characteristics. Moreover, weight functions determined by the envelope variation are introduced to extract the spectrum characteristics from the frequency domain, and the time difference is estimated by a genetic algorithm based on information evaluation with time-domain information.

The main contributions related to this chapter are shown as follows:

- This thesis proposes a localization algorithm using band-limited measured data under multi-path conditions.
- The information that relates to time difference can be extracted from the phase information in the frequency domain.
- Spectrum characteristics are extracted from the frequency domain through detecting the envelope variation to deal with band-limited signals.

- An information evaluation based genetic algorithm for time difference estimation is introduced to avoid the ill-conditioned numerical optimization.

Chapter 6 concludes the thesis and provides several suggestions for future research. In conclusion, this thesis shows the system models under insufficient information conditions and proposes new approaches based on both time and frequency information. In future works, some meaningful issues, for example, the accuracy improvement of changing points detection, implementation of the parameter compensation into recursion of parameter update, will be considered in the time-varying system. The algorithm for the more complex environment, such as multi-source or signal-dependent noise, will be investigated in the localization system.

Chapter 2

Preliminaries

2.1 Time-varying Model

In many signal processing areas such as digital communication and acoustics, the dynamics of a physical process are described by impulse response. Consider such a propagation channel in the mobile digital communication or the acoustic process. When it changes with time, it can be described by a time-varying FIR model as

$$y(k) = h_0^k u(k) + h_1^k u(k-1) + \cdots + h_n^k u(k-n) + e(k) = \phi^T(k)\mathbf{h}(k) + e(k), \tag{2.1}$$

where n is the model order, $u(k)$, $y(k)$ and $e(k)$ are the input signal, output signal and noise terms at an discrete time k, respectively, while the superscript and subscript of the parameter h_i^k indicate the lag time i, the normalized sampling instant k, respectively. $\phi(k) = [u(k), \cdots, u(k-n)]^T$, $\mathbf{h}(k) = [h_0^k, \cdots, h_n^k]^T$. $u(k)$ is assumed as a wide-sense stationary signal with persistent excitation for system identification, and is independent of the noise $e(k)$. It indicates that the model parameters h_i^k vary with time k in (2.1), and should be estimated promptly from the data of $u(k)$, $y(k)$.

This model is the model basis of recursive identification algorithm in **Chapter 3** and **Chapter 4**.

2.2 Variation Rate Decision

Analogous to [86], the variation rate of parameters is measured by

$$\kappa(k) = \sqrt{\frac{\mathrm{tr}\{E\{\phi(k)\}\mathrm{cov}\{\mathbf{h}(k)-\mathbf{h}(k-1)\}\}}{\sigma_e^2}}, \tag{2.2}$$

where σ_e^2 is the variance of the noise $e(k)$. $E\{\phi(k)\}/\sigma_e^2$ is the stationary part, and $\mathrm{cov}\{\mathbf{h}(k)-\mathbf{h}(k-1)\}$ corresponds to the varying part. It is indicated as fast variation when $\kappa(k) > 0.0005\sqrt{n}$ empirically, where n is model order, and the conventional methods may fail to sufficiently track the fast variation.

2.3 The Even Periodic Expansion

In the conventional method based on the Fourier series, for example, the parameters h_i^k within a window $[0, N]$ are expanded into the virtual periodic functions, as shown in Fig.2.1(a) where the period is the same as the window width N. It is noted that the discontinuity at the window edge $0, \pm N, \pm 2N, \cdots$ causes the Gibbs effect. If the series degree M is finite, the Gibbs effect on the series expansion often yields severe overshot and fluctuation, which distort the prediction error signal. As a result, all the parameter estimates at this point will be biased due to the distortion of the prediction error signal, i.e., the algorithm performance degrades seriously.

Through expanding the virtual even periodic functions, the virtual functions are continuous at the window edges. It implies that the parameter functions within the window $[0, N]$ are regarded as the right-half period of the expanded virtual even functions, as illustrated in Fig.2.1(b). As a result, the virtual functions are the periodic ones whose period is $2N$, and can be approximated by a finite degree of the sine or cosine series representation with a small bias.

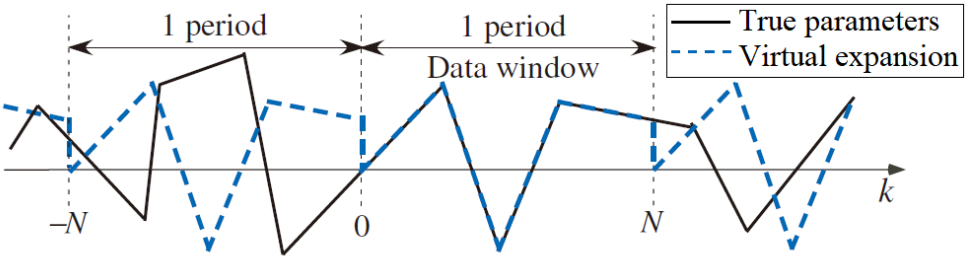

(a) Expansion of a virtual periodic function

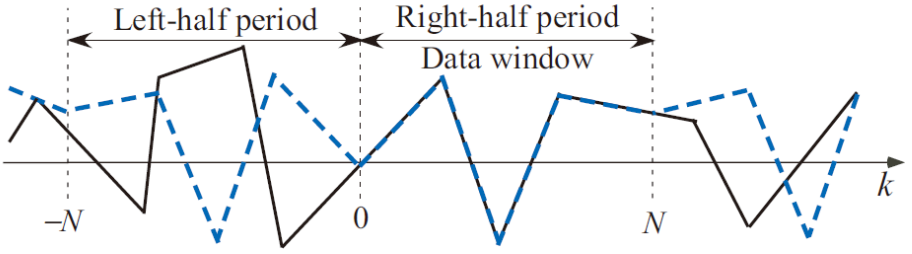

(b) Expansion of a virtual even periodic function

FIGURE 2.1: Illustration of the virtual expansion of time-varying parameters

2.4 Cosine Series Based Approximation

According to Section 2.3, It is seen that the even periodic functions can remove the discontinuity of the model parameters, so as not to cause the Gibbs effect at the time window edges.

Consider the parameters h_i^{k-N}, h_i^{k-N+1}, $\cdots$, h_i^k in the kth sliding time window $[k-N,k]$. If they are expanded into an even periodic functions with respect to $[k-2N,k-N]$ and $[k-N,k]$, then $h_i^{k_0+k_1}$ can be approximated by the cosine series with period $2N$ as follows.

$$h_i^{k_0+k_1} \approx \sum_{m=0}^{M} c_{i,m}^k \cos(m\omega k_1), \tag{2.3}$$

where $k_0 = k-N$ and k_1 are the left and right edges of time window, $0 \le k_1 \le N$, $\omega = \pi/N$, M is the degree of the series, and the virtual parameters for $-N \le k_1 \le 0$ can also be calculated from (2.3). Within cosine series of time window $[k-N,k]$, the coefficients $c_{i,m}^k$ can be treated as constants. Correspondingly, the identification problem of the time-varying model (2.1) becomes to the constant coefficients $c_{i,m}^k$ estimation problem within the sliding data window. Furthermore, in the virtual expansion of even periodic

functions, the virtual parameter $h_i^{k_0+k_1}$ for $k_1 = 2K$ equals to h_i^k at the window edges of virtual functions, the Gibbs effect occurs at the window edges can be reduced largely.

2.5 System Output

Within the window $[k_0, k]$, the input-output relation can be written as follows:

$$\begin{aligned}
&y(k_0+k_1) = y(k-N+k_1) \triangleq y^k(k_1) \\
&\approx \sum_{m=0}^{M} c_{0,m}^k \cos(m\Omega k_1) u(k_0+k_1) + \sum_{m=0}^{M} c_{1,m}^k \cos(m\Omega k_1) u(k_0+k_1-1) + \cdots \\
&+ \sum_{m=0}^{M} c_{n,m}^k \cos(m\Omega k_1) u(k_0+k_1-n) + e(k_0+k_1) \\
&= (\phi_{c,0}^k(k_1))^T \theta_{c,0}^k + (\phi_{c,1}^k(k_1))^T \theta_{c,1}^k + \cdots + (\phi_{c,M}^k(k_1))^T \theta_{c,M}^k + e(k_0+k_1) \\
&= (\phi_c^k(k_1))^T \theta_c^k + e(k_0+k_1),
\end{aligned} \tag{2.4}$$

2.6 Definitions of Data and Parameter Vectors

The main regressions are as follows:

$$\begin{aligned}
&\phi_c^k(k_1) = \begin{bmatrix} \phi_{c,0}^k(k_1) \\ \phi_{c,1}^k(k_1) \\ \vdots \\ \phi_{c,M}^k(k_1) \end{bmatrix}, \quad \phi_s^k(k_1) = \begin{bmatrix} \phi_{s,1}^k(k_1) \\ \vdots \\ \phi_{s,M}^k(k_1) \end{bmatrix}, \\
&\phi_{c,0}^k(k_1) = [u(k_0+k_1),\ u(k_0+k_1-1),\ \cdots,\ u(k_0+k_1-n)]^T \\
&\phi_{c,m}^k(k_1) = \mathbf{W}_{c,m}^{k_1} \phi_{c,0}^k(k_1), \quad \phi_{s,m}^k(k_1) = \mathbf{W}_{s,m}^{k_1} \phi_{c,0}^k(k_1), \\
&\mathbf{W}_{c,m}^{k_1} = \cos(m\omega k_1)\mathbf{I}, \quad \phi_{s,m}^k(k_1) = \sin(m\omega k_1)\mathbf{I},
\end{aligned} \tag{2.5}$$

while the coefficient vectors are

$$\begin{aligned}
&\theta_c^k = [(\theta_{c,0}^k)^T,\ (\theta_{c,1}^k)^T,\ \cdots,\ (\theta_{c,M}^k)^T]^T, \\
&\theta_{c,m}^k = \left[c_{0,m}^k,\ c_{1,m}^k,\ \cdots,\ c_{n,m}^k\right]^T.
\end{aligned} \tag{2.6}$$

Where $\mathbf{I}$ is the identity matrix with the appropriate dimension, $\mathbf{W}_{c,m}^{k_1}$ and $\mathbf{W}_{s,m}^{k_1}$ are the diagonal matrices whose diagonal elements are $\cos(\omega m k_1)$, $\sin(\omega m k_1)$, respectively.

The approximation in (2.3) and (2.4) implies that the variation of model parameters can be approximated by the linear combination of the known basis functions, whereas unknown coefficients θ_c^k become an important issue. Therefore, the parameter estimation problem of a time-varying model can be realized by estimating the coefficient vector θ_c^k instead of the direct estimation of the varying model parameters. θ_c^k can be estimated by minimizing the criterion function

$$\hat{\theta}_c^k = \arg\min_{\theta_c^k} \sum_{k_1=0}^{N} \left(y^k(k_1) - (\phi_c^k(k_1))^T \theta_c^k \right)^2. \tag{2.7}$$

The minimization problem can be solved by some optimization algorithms such as the LS algorithm

$$\hat{\theta}_c^k = \left(\sum_{k_1=0}^{N} \phi_c^k(k_1)(\phi_c^k(k_1))^T \right)^{-1} \left(\sum_{k_1=0}^{N} \phi_c^k(k_1) y^k(k_1) \right) = (\mathbf{\Phi}_{cc}^k)^{-1} \phi_{cy}^k \triangleq \mathbf{P}^k \phi_{cy}^k, \tag{2.8}$$

where $\mathbf{\Phi}_{cc}^k$ and $\mathbf{P}^k$ are the correlation matrix and its inverse, ϕ_{cy}^k is the correlation vector of the regression and the process output in the window $[k_0, k]$.(2.8) turns the estimation of varying parameter into the estimation problem of the series coefficients.

The window shifts forward to $[k_0+1, k+1]$ at the next instant $k+1$. Correspondingly, the updated regression in the new window is

$$\phi_{c,0}^{k+1}(k_1) = [u(k_0+k_1+1),\ u(k_0+k_1),\ \cdots,\ u(k_0+k_1+1-n)]^T = \phi_{c,0}^k(k_1+1), \tag{2.9}$$

and following $\mathbf{W}_{c,m}^{k_1} = \mathbf{W}_{c,m}^1 \mathbf{W}_{c,m}^{k_1+1} + \mathbf{W}_{s,m}^1 \mathbf{W}_{s,m}^{k_1+1}$, $\phi_{c,m}^{k+1}(k_1)$ can be expressed by

$$\phi_{c,m}^{k+1}(k_1) = \mathbf{W}_{c,m}^{k_1} \phi_{c,0}^{k+1}(k_1) = \begin{bmatrix} \mathbf{W}_{c,m}^1 & \mathbf{W}_{s,m}^1 \end{bmatrix} \begin{bmatrix} \phi_{c,m}^k(k_1+1) \\ \phi_{s,m}^k(k_1+1) \end{bmatrix} \tag{2.10}$$

It illustrates that besides the time-shift term $\mathbf{W}_{c,m}^{1}\phi_{c,m}^{k}(k_1+1)$, an extra term $\mathbf{W}_{s,m}^{1}\phi_{s,m}^{k}(k_1+1)$ also appears in (2.10). Then, the correlation matrix $\mathbf{\Phi}_{cc}^{k+1}$ is updated by

$$\begin{aligned}\mathbf{\Phi}_{cc}^{k+1} &= \sum_{k_1=0}^{N}\phi_c^{k+1}(k_1)(\phi_c^{k+1}(k_1))^T \\ &= [\ \mathbf{W}_c\ \mathbf{W}_s\ ]\left(\begin{bmatrix}\phi_c^k(N+1)\\ \mathbf{0}\end{bmatrix}[\ \phi_c^k(N+1)\ \mathbf{0}\ ]\right. \\ &\left.-\begin{bmatrix}\phi_c^k(0)\\ \mathbf{0}\end{bmatrix}[\ \phi_c^k(0)\ \mathbf{0}\ ]+\begin{bmatrix}\mathbf{\Phi}_{cc}^k & \mathbf{\Phi}_{cs}^k\\ \mathbf{\Phi}_{sc}^k & \mathbf{\Phi}_{ss}^k\end{bmatrix}\right)\begin{bmatrix}\mathbf{W}_c\\ \mathbf{W}_s\end{bmatrix}\end{aligned} \tag{2.11}$$

where $\mathbf{W}_{c,m}$ and $\mathbf{W}_{s,m}$ are the diagonal matrices with the diagonal blocks $\mathbf{W}_{c,m}^{1}$, $\mathbf{W}_{s,m}^{1}$, $m=0,1,\cdots,M$, respectively.

From (2.11), it is deduced that $\mathbf{\Phi}_{cc}^{k+1}$ consists of the innovative term, the term beyond the new window and the transition term. Let the inverse of $\mathbf{\Phi}_{cc}^{k+1}$ be denoted as $\mathbf{P}^{k+1}$, the coefficient vector can be obtained by $\hat{\theta}_c^{k+1}=\mathbf{P}^{k+1}\phi_{cy}^{k+1}$, where the computation of $\mathbf{P}^{k+1}$ suffers from the heavy computational load due to extra terms such as $\mathbf{\Phi}_{cs}^k$, $\mathbf{\Phi}_{sc}^k$ and $\mathbf{\Phi}_{ss}^k$ in (2.11).

2.7 Inversion of Correlation Matrix

In the time window, $u(k)$ is assumed as a stationary signal, the following property holds for the data vectors.

$$\begin{aligned}&\frac{1}{N}\left[\sum_{k_1=0}^{N}\phi_{c,m_1}^k(k_1)(\phi_{c,m_2}^k(k_1))^T\right]\\ &\approx E\left\{\phi_c^k(k_1)(\phi_c^k(k_1))^T\right\}\frac{1}{N}\sum_{k_1=0}^{N}\cos(m_1\omega k_1)\cos(m_2\omega k_1)\\ &\rightarrow\begin{cases}\neq 0 & (m_1=m_2)\\ 0 & (m_1\neq m_2)\end{cases}.\end{aligned} \tag{2.12}$$

By virtue of the stationarity assumption of $u(k)$, and the regression $\phi^k_{c,m}(k_1)$ does not contain the weight factor, in the correlation matrix $\frac{1}{N}\sum_{k=1}^{N}\phi^k_c(k_1)(\phi^k_c(k_1))^T$, the non-diagonal blocks are close to 0, while the diagonal blocks are positive definite matrices. It implies that the inverse of $(\mathbf{\Phi}^k_{cc})^{-1}$ can be realized through the inverse of the diagonal blocks.

2.8 Gibbs Effect

The trigonometric basis based approximation suffers from the Gibbs effect at the rapid changing points such as abrupt variation or discontinuous points. As shown in Fig.2.2, the parameter approximation has fluctuation caused by the Gibbs effect at a discontinuous point around $k = 700$, and the fluctuation yields about 14% approximation error with the data window for $M = 20$, whereas the approximation error yields a more considerable bias round such points in the identification procedure. Therefore, it is expected to promptly detect the rapid changing points and further compensate for the fluctuation in parameter estimates to improve the approximation performance. This thesis proposes a neural network based soft threshold function to be adaptive to the various changing characteristics in detail in **Chapter 4**.

2.9 Multi-path Model in Time Domain

The localization scenario of multi-path propagation is depicted in Fig. 2.3. The signal transmitted by the emitter is denoted as $s(t)$, which is reflected by M transponders and intercepted by L receivers. Denote the positions of emitter as $\mathbf{P}_e$, transponders as $\mathbf{P}_t$, receivers as $\mathbf{P}_r$, where

$$\begin{aligned}\mathbf{P}_t &= \left[\mathbf{P}_t^T(1), \mathbf{P}_t^T(2), \cdots, \mathbf{P}_t^T(M)\right],\\ \mathbf{P}_r &= \left[\mathbf{P}_r^T(1), \mathbf{P}_r^T(2), \cdots, \mathbf{P}_r^T(L)\right],\end{aligned} \tag{2.13}$$

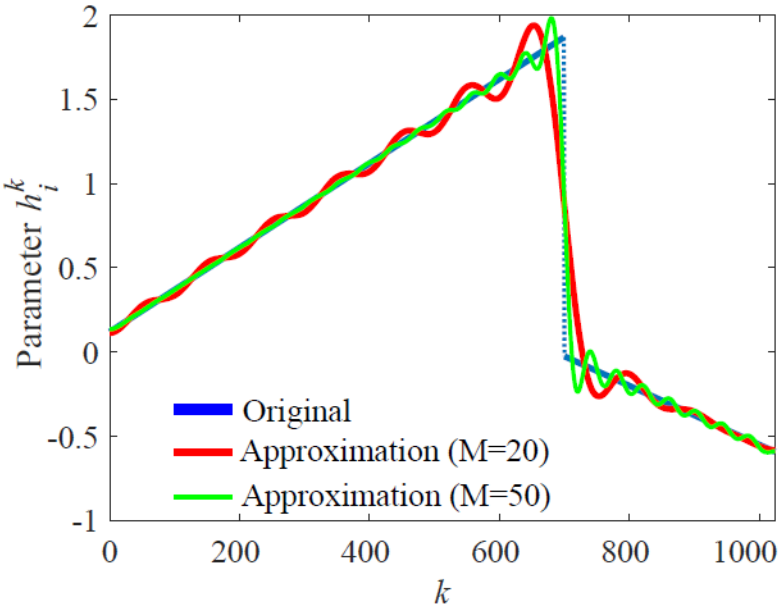

FIGURE 2.2: Illustration of Gibbs effect at discontinuous point

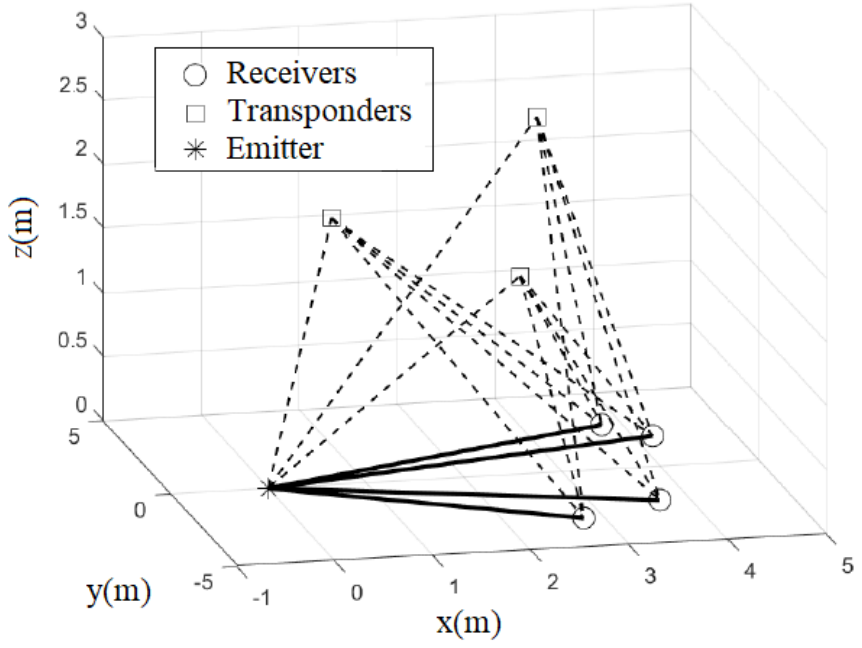

FIGURE 2.3: Multiple-path localization problem with the transponders and receivers

and $\mathbf{P}_t(m) = [P_t(m,x),\ P_t(m,y),\ P_t(m,z)]^T$, $\mathbf{P}_r(l) = [P_r(l,x),\ P_r(l,y),\ P_r(l,z)]^T$ are the position coordinates of the mth transponder, the lth receiver, respectively. Let the signal measured by the lth receiver be denoted as $r^{(l)}(t)$, which is contaminated with the noise term $v^{(l)}(t)$. Then, the relation of the received signal $a^{(l)}(t)$ and signal source $s(t)$ can be approximated by

$$\begin{aligned} & a^{(l)}(t) \\ = \ & h^{(l)} s(t-\tau^{(l)}) + \sum_{m=1}^{M} h_m^{(l)} s(t-\tau_m^{(l)}) + v^{(l)}(t), \end{aligned} \tag{2.14}$$

where $\tau^{(l)} = \frac{1}{C}\|\mathbf{P}_e - \mathbf{P}_r(l)\|_2$ denotes the delay time related with the distance of emitter and lth receiver, while $\tau_m^{(l)} = \frac{1}{C}\|\mathbf{P}_e - \mathbf{P}_t(m)\|_2 + \frac{1}{C}\|\mathbf{P}_t(m) - \mathbf{P}_r(l)\|_2$ denotes the denotes the delay time between emitter and lth receiver through mth transponder, and C is the propagation velocity of the signal wave. $h^{(l)}$ is the path attenuation coefficient from the emitter to lth receiver, while $h_m^{(l)}$ is the path attenuation coefficient via mth transponder. $v^{(l)}(t)$ is the noise term that is assumed as the zero-mean white Gaussian one independent of $s(t)$. Generally, the farther the receivers to each other are, the weaker the correlation of noise signals. Correspondingly, the noise correlation can be reduced by choosing the signals received by the receivers with far distance.

2.10 Time Difference Estimation in Time Domain

Let the Discrete Fourier Transform (DFT) of the measured signal in the ith time window $[t_i,\ t_i + N - 1]$ be denoted as

$$A_i^{(l)}(e^{jn\omega}) = \sum_{k=0}^{N-1} a^{(l)}(t_i + k) e^{-jnk\omega}, \tag{2.15}$$

where t_i is the time offset of the ith window, k indicates a normalized instant of kt_s, and t_s is the sampling interval to sample the measured signals, N is the window length, while ω is the frequency interval $2\pi/N$. If N is chosen as a power of 2, the DFT can be performed through Fast Fourier Transform (FFT) to reduce the computation load. Furthermore, let the average periodogram of $a^{(l_1)}(k)$ and $a^{(l_2)}(k)$ be given by shifting the

time window to $t_0, \cdots, t_{I-1}$,

$$\bar{A}^{(l_1,l_2)}(e^{jn\omega}) = \frac{1}{I}\sum_{i=0}^{I-1}\left(A_i^{(l_1)}(e^{jn\omega})\right)^* A_i^{(l_2)}(e^{jn\omega}), \tag{2.16}$$

where * indicates the complex conjugate.

Correspondingly, the correlation function defined in the time domain

$$R^{(l_1,l_2)}(\tau) = \frac{1}{K}\sum_{k=1}^{K} a^{(l_1)}(k_0+k)a^{(l_2)}(k_0+k+\tau) \tag{2.17}$$

can be approximated by

$$R^{(l_1,l_2)}(\tau) \approx \frac{1}{N}\sum_{n=0}^{N-1} \bar{A}^{(l_1,l_2)}(e^{jn\omega})e^{jn\tau\omega} \tag{2.18}$$

in the frequency domain. Then the initial time difference between $a^{(l_1)}(k)$ and $a^{(l_2)}(k)$ can be given by

$$\hat{\tau}^{(l_1,l_2)}_{\text{init},0} = \arg \max_{\tau} R^{(l_1,l_2)}(\tau) \tag{2.19}$$

from the periodogram as in (2.18). If the distortion caused by multi-path interferences can be neglected, the estimation in (2.19) might be a good estimation for $\tau^{(l_1,l_2)}_0 = \tau^{(l_2)}_0 - \tau^{(l_1)}_0$. Nevertheless, the distortion may shift position of main-lobe of the correlation functions so the estimation in (2.19) may have large errors, which should be reduced further to guarantee the effectiveness of source localization.

2.11 Multi-path Interference

In the multi-path environment, a signal wave from an emitter to a receiver, which is shown in Fig. 2.4, is generally described by a model that consists of the direct wave, early reflections, and late reverberations. The signal wave is simply modelled by two components, the main wave $h^{(l)}s(t-\tau^{(l)})$ and the sub-waves $\sum_{m=1}^{M} h_m^{(l)}s(t-\tau_m^{(l)})$ (Section 2.9), where the latter includes both the early reflections and the late reverberations.

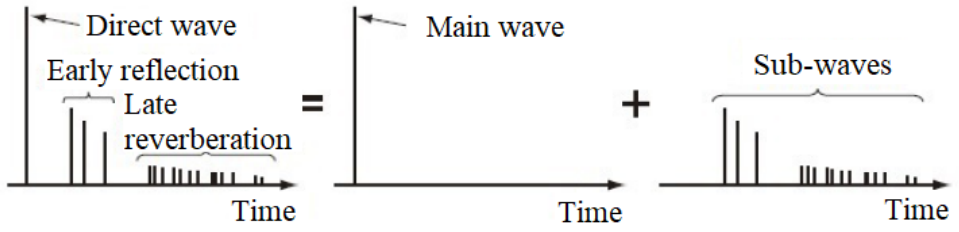

FIGURE 2.4: Signal from emitter to receiver in the multi-path environment

These sub-waves will alter the waveforms and affect the estimation of the source location. Moreover, in some practical applications such as low-frequency seismic analysis and vibration signal processing, $s(t)$ is a band-limited signal with no sufficient frequency components to estimate time difference or direction of arrivals. As a result, estimating the model parameters from the received data is not an easy task.

Many conventional methods attempt to estimate the time difference of the main wave between the signal measured by multiple receivers. The estimation can be performed through the correlation functions, the semblance of the signal waveforms, and the difformity of waveforms. However, in the multi-path environment, the sub-waves generate side lobes that primarily affect the main lobe's peak value in the correlation function, especially for band-limited signal [119]. The distortion of the main lobe caused by the side lobe leads to considerable estimation errors that may yield a significant mismatch of the source location. Consequently, the affection of the side lobe should be reduced, and the estimation errors of time difference are also required to be dealt with for high localization performance.

2.12 Multi-path Model in Frequency Domain

Let kth DFT coefficient of the lth receiver in the frequency-domain model be denoted as

$$
\begin{aligned}
& A^{(l)}(k) \\
= \; & h^{(l)} e^{-j\omega_k \tau^{(l)}} S(k) + \sum_{m=1}^{M} h_m^{(l)} e^{-j\omega_k \tau_m^{(l)}} S(k) + V^{(l)}(k) \\
= \; & \left[h^{(l)} e^{-j\omega_k \tau^{(l)}} + \sum_{m=1}^{M} h_m^{(l)} e^{-j\omega_k \tau_m^{(l)}} \right] S(k) + V^{(l)}(k) \\
= \; & H^{(l)}(k) S(k) + V^{(l)}(k),
\end{aligned} \tag{2.20}
$$

where $S(k)$ is the DFT coefficient of the signal source $s(t)$, $V^{(l)}(k)$ is the corresponding noise term, and is independent of $S(k)$. ω_k is the normalized frequency point $2k\pi/N$, while N is the window length. $h^{(l)}$ and $h_m^{(l)}$ are the path attenuation coefficients from the emitter to the lth receiver with regard to the direct wave and the reflection, respectively.

Chapter 3

New Recursive Algorithm

3.1 Background

Due to component aging, fast variation of the environment, the dynamic characteristics of a physical process vary with time. When the process varies slowly, some existing adaptive algorithms, such as the segmentation approach to separate a time-varying model into several local models [56, 120], the Recursive Least Square (RLS) with a forgetting factor [121], the Least Mean Square (LMS) or the Normalized Least Mean Square (NLMS) algorithms [122, 123], the Affine Projection algorithm (AP) and Block Orthogonal Projection (BOP) [124], may track the varying dynamics.

Identification of time-varying systems has been successfully applied in many practical applications. For example, the identification of the time-varying system is used to address the terminal control problem [125] in computer engineering and robotic manipulator, the adaptive equalization of rapidly fading communication channels for non-stationary signals [126], the linear parameter varying model in transportation systems such as flight projectile and car steering [127, 128], the identification-based fault diagnosis [129] and time-varying model for effective treatments for certain brain diseases in biomedical engineering [130].

Nevertheless, if the variation is too fast, most of the existing algorithms fail to follow the variation satisfactorily, unless the prior information of the variation is available

[86]. For the systems with less prior information, several methods use an explicit approximation of the parameter variation through some orthogonal basis functions such as the trigonometric or Legendre basis. They help to approximate the dynamics at an arbitrary rate when the signals have sufficient excitations, so that they have better tracking performance than other existing methods. Since the trigonometric functions have differentiability and computational stability, the varying parameters are often approximated by the Fourier series in the conventional basis function methods, where the parameters within a chosen time window are expanded into the virtual periodic functions whose right and left window edges correspond to the newest, the oldest information on the process variation, respectively. Nevertheless, the values of the virtual periodic functions are generally different at the right and left edges. As a result, the discontinuity causes the Gibbs effect in the series expansion and severely degrades the tracking performance at the window edges [131]. On the other hand, when expanding the varying parameters into the virtual even periodic functions that are approximated by the cosine series [132], the virtual functions are continuous at the window edges when the true parameters vary continuously.

On the other hand, it is expected to implement the algorithms recursively for the rapid time-varying systems in many applications, where the recursive computability of the basis functions is an essential issue in the recursive algorithms. Nevertheless, the recursion of cosine series is more complicated than the standard Fourier series when updating the data matrices, and their inversion, recursively, so most of the conventional cosine basis based algorithms work in batches rather than the recursive processing. A recursive identification algorithm with a forgetting factor for time-varying systems is proposed [133]. The forgetting factor makes the time window shift easily since the past data beyond the window decay to zero, and has high tracking performance in rapid varying system. However, it will weaken the orthogonality of the basis functions, as a result, the data matrix often has such large condition number that degrades the tracking performance for the basis series with high degree.

In order to improve the tracking performance, a new recursive identification algorithm based on the trigonometric functions is investigated for the rapid time-varying systems in this chapter. In the proposed algorithm, the orthogonality of the trigonometric

functions is applied to effectively implement the recursion of the cosine basis. In contrast with the conventional methods based on the Fourier series expansion, the new one holds the orthogonality for the high basis degree, and has less Gibbs effect at the window edges. Consequently, the proposed algorithm has high tracking performance even in the rapid varying processes.

The rest of the chapter is organized as follows. Section 3.2 shows the new recursive identification algorithm. Section 3.3 demonstrates some numerical simulation examples to show the effectiveness of the algorithm. Finally, the conclusions are given in Section 3.4.

3.2 New Recursive Identification Algorithm

Preliminaries as Section 2.1-Section 2.6. The mild assumptions in the proposed algorithm are summarized as follows: the input signal $u(k)$ has quasi-stationarity and ergodicity, and is independent of the noise $e(k)$; the window width $N > (n+1)(M+1)$; the varying parameters have at most a finite number of discontinuous points in the window. Then, following the expansion theorem of cosine series, the approximation in (2.3) is guaranteed for the parameter estimation if these assumptions hold.

3.2.1 Properties of data matrices

In order to illustrate the update of the matrices in the recursive algorithm, their properties are investigated. Let the matrices $\mathbf{\Phi}_1$, $\mathbf{\Phi}_2$ be denoted as

$$
\begin{aligned}
&\mathbf{\Phi}_1 = \phi_c^k(N+1)(\phi_c^k(N+1))^T - \phi_c^k(0)(\phi_c^k(0))^T + \mathbf{\Phi}_{cc}^k = \mathbf{\Psi}^{k+1} + \mathbf{\Phi}_{cc}^k, \\
&\mathbf{\Phi}_2 = \mathbf{W}_{cs}^{-1}\mathbf{\Phi}_{sc}^k + \mathbf{\Phi}_{cs}^k\mathbf{W}_{cs}^{-1} + \mathbf{W}_{cs}^{-1}\mathbf{\Phi}_{ss}^k\mathbf{W}_{cs}^{-1}, \\
&\psi^{k+1} = \begin{bmatrix} \phi_c^k(N+1), & \phi_c^k(0) \end{bmatrix}, \ \bar{\psi}^{k+1} = \begin{bmatrix} \phi_c^k(N+1), & -\phi_c^k(0) \end{bmatrix}, \\
&\bar{\mathbf{y}}^{k+1} = \begin{bmatrix} y^k(N+1), & -y^k(0) \end{bmatrix}^T,
\end{aligned}
\tag{3.1}
$$

where $\mathbf{W}_{cs}^{-1} = \mathbf{W}_c^{-1}\mathbf{W}_s$ then $\mathbf{\Phi}_{cc}^{k+1}$ in (2.11) can be expressed by

$$\mathbf{\Phi}_{cc}^{k+1} = \mathbf{W}_c(\mathbf{\Phi}_1 + \mathbf{\Phi}_2)\mathbf{W}_c. \tag{3.2}$$

It is seen that the extra matrices in $\mathbf{\Phi}_2$ make the inverse of $\mathbf{\Phi}_{cc}^{k+1}$ be very complicated. The matrix inverse will be simplified by using the properties of data matrices in the new recursive algorithm.

According to the properties of quasi-stationarity and orthogonality, $\|\mathbf{\Phi}_1\| \gg \|\mathbf{\Phi}_2\|$ holds for $N \gg M$, and $\left\|{\mathbf{\Phi}_1}^{-1}\mathbf{\Phi}_2\right\| \ll 1$. Consequently, the following inversion can be approximated by

$$(\mathbf{I} + \mathbf{\Phi}_1^{-1}\mathbf{\Phi}_2)^{-1} = \mathbf{I} - \mathbf{\Phi}_1^{-1}\mathbf{\Phi}_2 + (\mathbf{\Phi}_1^{-1}\mathbf{\Phi}_2)^2 - \cdots \approx \mathbf{I} - \mathbf{\Phi}_1^{-1}\mathbf{\Phi}_2, \tag{3.3}$$

and it yields the approximation of inverse of $\mathbf{P}^{k+1}$, i.e., the inverse of $\mathbf{\Phi}_{cc}^{k+1}$ as follows

$$\mathbf{P}^{k+1} = (\mathbf{\Phi}_{cc}^{k+1})^{-1} = \mathbf{W}_c^{-1}(\mathbf{\Phi}_1 + \mathbf{\Phi}_2)^{-1}\mathbf{W}_c^{-1} \approx \mathbf{W}_c^{-1}(\mathbf{I} - \mathbf{\Phi}_1^{-1}\mathbf{\Phi}_2)\mathbf{\Phi}_1^{-1}\mathbf{W}_c^{-1}, \tag{3.4}$$

where $\mathbf{\Phi}_1^{-1}$ can be updated following matrix inversion lemma

$$\mathbf{\Phi}_1^{-1} = (\mathbf{I} - \mathbf{g}^{k+1}(\bar{\psi}^{k+1})^T)\mathbf{P}^k, \tag{3.5}$$

whereas $\mathbf{g}^{k+1}$ is a gain vector given by

$$\mathbf{g}^{k+1} = \mathbf{P}^k\psi^{k+1}(\mathbf{I}_2 + (\bar{\psi}^{k+1})^T\mathbf{P}^k\psi^{k+1})^{-1}. \tag{3.6}$$

In (3.6), $\mathbf{I}_2$ is a (2×2) identity matrix, so the calculation of $(\mathbf{I}_2 + (\bar{\psi}^{k+1})^T\mathbf{P}^k\psi^{k+1})^{-1}$ is very easy in the recursive algorithm.

Similarly as $\mathbf{\Phi}_{cc}^{k+1}$, the correlation vectors ϕ_{cy}^{k+1} and ϕ_{sy}^{k+1} can be updated by

$$\begin{aligned}
\phi_{cy}^{k+1} &= \mathbf{W}_c(\psi^{k+1}\bar{\mathbf{y}}^{k+1} + \phi_{cy}^k + \mathbf{W}_{cs}^{-1}\phi_{sy}^k), \\
\phi_{sy}^{k+1} &= -\mathbf{W}_s(\psi^{k+1}\bar{\mathbf{y}}^{k+1} + \phi_{cy}^k) + \mathbf{W}_c\phi_{sy}^k.
\end{aligned} \tag{3.7}$$

From (3.7), the extra term ϕ_{sy}^k can be expressed by the past data

$$\phi_{sy}^k = -\mathbf{W}_s(\psi^k \bar{\mathbf{y}}^k + \phi_{cy}^{k-1}) + \mathbf{W}_c \phi_{sy}^{k-1}, \tag{3.8}$$

Since the matrices $\mathbf{W}_c$,$\mathbf{W}_s$ and $\mathbf{W}_{cs}^{-1}$ are diagonal, ϕ_{sy}^k can be rewritten as

$$\phi_{sy}^k = \mathbf{W}_c(\mathbf{I} + \mathbf{W}_{cs}^{-2})\phi_{sy}^{k-1} - \mathbf{W}_{cs}^{-1}\phi_{cy}^k. \tag{3.9}$$

3.2.2 Update of parameter estimation

Now substitute the approximated formulae of $\mathbf{P}^{k+1}$ and ϕ_{cy}^{k+1} to deduce the recursive estimation $\hat{\theta}_c^{k+1} = \mathbf{P}^{k+1}\phi_c^{k+1}$ in the new window $[k_0+1, k+1]$, where ϕ_{cy}^{k+1} in (3.7) is split into two parts: $\mathbf{W}_c(\psi^{k+1}\bar{\mathbf{y}}^{k+1} + \phi_{cy}^k)$ and $\mathbf{W}_s\phi_{sy}^k$.

Multiplying $\mathbf{\Phi}_1^{-1}\mathbf{W}_c^{-1}$ by the first part of ϕ_{cy}^{k+1} yields that

$$\mathbf{\Phi}_1^{-1}\mathbf{W}_c^{-1}\mathbf{W}_c\left(\psi^{k+1}\bar{\mathbf{y}}^{k+1} + \phi_{cy}^k\right) = \left(\psi^{k+1}(\bar{\psi}^{k+1})^T + \mathbf{\Phi}_{cc}^k\right)^{-1}\left(\psi^{k+1}\bar{\mathbf{y}}^{k+1} + \phi_{cy}^k\right). \tag{3.10}$$

Similarly as the standard recursive formula in [134], (3.10) can be compactly rewritten as

$$\mathbf{P}^k\phi_{cy}^k + \mathbf{g}^{k+1}\varepsilon^{k+1} = \hat{\theta}_c^k + \mathbf{g}^{k+1}\varepsilon^{k+1}, \tag{3.11}$$

where the prediction error ε^{k+1} is defined by

$$\varepsilon^{k+1} = \bar{\mathbf{y}}^{k+1} - (\bar{\psi}^{k+1})^T\hat{\theta}_c^k. \tag{3.12}$$

For the second part of ϕ_{cy}^{k+1}, substituting (3.8) into the multiplication of $\mathbf{P}^{k+1}$ and $\mathbf{W}_s\phi_{sy}^k$ yields that

$$\mathbf{\Phi}_1^{-1}\mathbf{W}_c^{-1}\mathbf{W}_s\phi_{sy}^k \approx (\mathbf{I} - \mathbf{g}^{k+1}(\bar{\psi}^{k+1})^T)(\mathbf{I} + \mathbf{W}_{cs}^{-2})\bar{\theta}_s^k - (\mathbf{I} - \mathbf{g}^{k+1}(\bar{\psi}^{k+1})^T)\mathbf{W}_{cs}^{-2})\bar{\theta}_c^k. \tag{3.13}$$

Now, we complement the rest terms in the update of $\mathbf{P}^{k+1}$ and $\hat{\theta}_c^{k+1}$. Denote the following gain matrices to simplify the recursive formulae

$$\begin{aligned}
&\mathbf{\Omega}^k = \mathbf{P}^k(\mathbf{W}_{cs}^{-1}\phi_{cs}^k + (\phi_{cs}^k)^T\mathbf{W}_{cs}^{-1} + \mathbf{W}_{cs}^{-1}\phi_{ss}^k\mathbf{W}_{cs}^{-1}),\\
&\mathbf{G}^{k+1} = \mathbf{W}_c^{-1}(\mathbf{I} - (\mathbf{I} - \mathbf{g}^{k+1}(\bar{\psi}^{k+1})^T)\mathbf{\Omega}^k), \quad \mathbf{G}_s^{k+1} = \mathbf{G}^{k+1}(\mathbf{I} - \mathbf{g}^{k+1}(\bar{\psi}^{k+1})^T).
\end{aligned} \tag{3.14}$$

Then, by combining (3.11) with (3.13), the new parameter vector and the inverse of the correlation matrix can be concluded as follows:

$$\hat{\theta}_c^{k+1} = \mathbf{P}^{k+1}\phi_{cy}^{k+1} = \mathbf{G}^{k+1}(\hat{\theta}_c^k + \mathbf{g}^{k+1}\varepsilon^{k+1}) + \hat{\theta}_s^{k+1}, \tag{3.15}$$

$$\mathbf{P}^{k+1} = \mathbf{G}^{k+1}\mathbf{\Phi}_1^{-1}\mathbf{W}_c^{-1} = \mathbf{G}^{k+1}(\mathbf{I} - \mathbf{g}^{k+1}(\bar{\psi}^k)^T)\mathbf{P}^k\mathbf{W}_c^{-1}. \tag{3.16}$$

The estimate in (3.15) is composed of 2 parts: the first part projects the term $\hat{\theta}_c^k + \mathbf{g}^{k+1}\varepsilon^{k+1}$ onto the cosine basis in the new window, while the second part $\hat{\theta}_s^{k+1}$ corresponds to transition effect on the sliding window with respect to the extra terms ϕ_s^k, ϕ_{sy}^k appeared in the update of ϕ_c^{k+1} and ϕ_{cy}^{k+1}.

Moreover, the correlation matrix and vector are updated as follows:

$$\begin{bmatrix} \mathbf{\Phi}_{cc}^{k+1} & \mathbf{\Phi}_{cs}^{k+1} \\ \mathbf{\Phi}_{sc}^{k+1} & \mathbf{\Phi}_{ss}^{k+1} \end{bmatrix} = \begin{bmatrix} \mathbf{W}_c & \mathbf{W}_s \\ -\mathbf{W}_s & \mathbf{W}_c \end{bmatrix} \begin{bmatrix} \mathbf{\Phi}_{cc}^k + \mathbf{\Psi}^{k+1} & \mathbf{\Phi}_{cs}^k \\ \mathbf{\Phi}_{sc}^k & \mathbf{\Phi}_{ss}^k \end{bmatrix} \begin{bmatrix} \mathbf{W}_c & -\mathbf{W}_s \\ \mathbf{W}_s & \mathbf{W}_c \end{bmatrix}. \tag{3.17}$$

3.3 Numerical Examples

A time-varying digital communication channel is considered in the numerical examples. Assume that the true channel model is described by (2.1) where $u(k)$ and $y(k)$ are the transmitted training signal, received signal, respectively, $e(k)$ is a white additive noise that is independent of $u(k)$, the parameter h_i^k varies with the instant k, and the variation rate in (2.2) is $\kappa(k) > 0.1 >> 0.0005\sqrt{n}$, where n is model order. So the processes are the fast time-varying ones and their parameter estimation is not an easy task.

3.3.1 Estimation of time-varying channel

Let the model order $n = 5$ and the time varying parameters of the channel model be the time functions. The following are the examples of h_0^k and h_2^k given by:

$$
\begin{aligned}
h_0^k &= \begin{cases} -1, \ \text{for} \ \ k \in [1, 1204], \text{ or } [3072, 3372], \\ 0.35 \sin\Big(\dfrac{k\pi}{150} + \dfrac{\pi}{6}\Big), \ \text{for } k \in [2561, 2880], \\ 1 + 0.35 \sin\Big(\dfrac{k\pi}{150} + \dfrac{\pi}{6}\Big), \ \text{otherwise}, \end{cases} \\
h_2^k &= \begin{cases} -0.75, \ \text{for} \ \ k \in [1, 1204], \text{ or } [3072, 3372], \\ -\dfrac{1}{4}\Big(1 - \sin\Big(\dfrac{k\pi}{100} + \dfrac{\pi}{3}\Big)\Big), \ \text{for } k \in [2561, 2880], \\ 0.5 + 0.25 \sin\Big(\dfrac{k\pi}{100} + \dfrac{\pi}{3}\Big), \ \text{otherwise}. \end{cases}
\end{aligned}
\tag{3.18}
$$

As shown in Figure 3.1, it is seen that there are significant jump points at $k = 2561, 2880$, 3072, 3372. Assume that the SNR is 10dB.

Generally, the more rapid variations arise in the time window, the higher series degree is necessary. On the other hand, the approximation with high series degree is easily influenced by the noise, and a long time window is often required to reduce the noise influence. Therefore, both the parameter variation velocity and the noise level should be considered when choosing the time window length N and series degree M. In the simulation, the window width is chosen as $N = 1024$, and the series degree $M = 3$. The mean values of the estimated parameters $\hat{h}_{0,k}$ and $\hat{h}_{2,k}$ for 50 simulation runs are plotted in Figure 3.1. As a comparison, the results of RLS with the forgetting factor 0.95, and NLMS with the updating step size 0.15 are also shown in the figure. It illustrates that the proposed algorithm tracks the variation more promptly than RLS and NLMS, especially at the sharp jump points.

Define the Mean Square Error (MSE) σ^2 of the estimated parameters as follows:

$$
\sigma^2 = \frac{1}{LK} \sum_{l=1}^{L} \sum_{k_1=1}^{K} \Big(\sum_{i=0}^{n} (\hat{h}_i^{k_0+k_1} - h_i^{k_0+k_1})^2 \Big) \tag{3.19}
$$

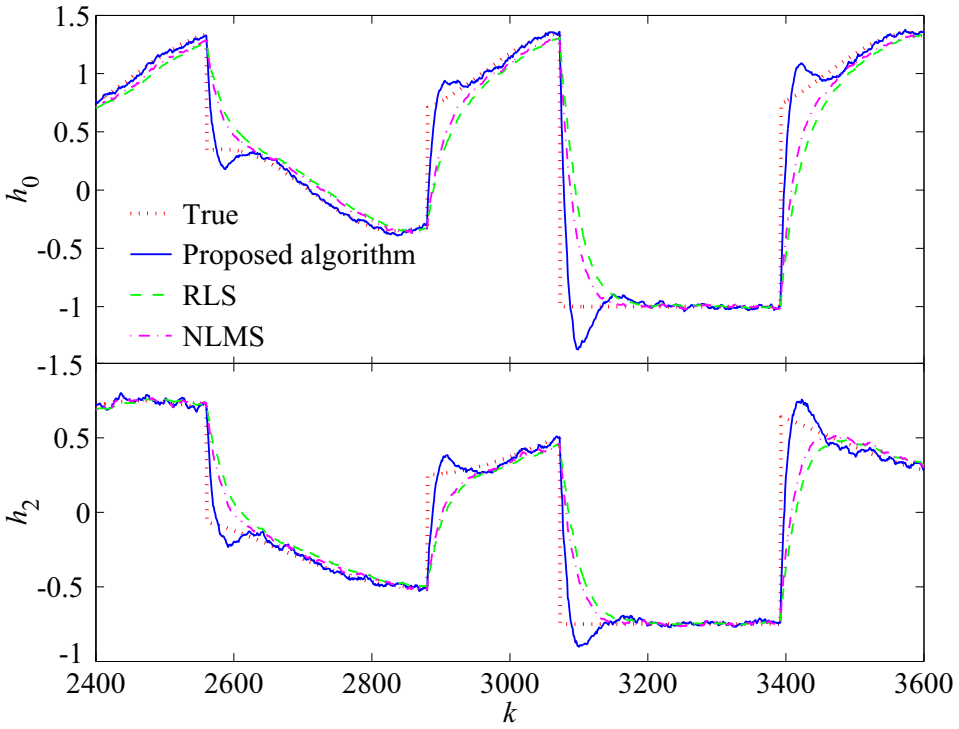

FIGURE 3.1: Estimation of time-varying channel

where L and K are the number of simulation runs, the number of recursions, respectively. The values of σ^2 for $k \in [2400, 3600]$ in the proposed algorithm, the standard RLS and NLMS algorithms are 0.0844, 0.1584, 0.1475, respectively. It is seen that the proposed algorithm has a smaller mean square error than the other two methods under the same simulation conditions, especially around the rapid varying points, due to the high degree cosine series approximation.

3.3.2 Estimation errors versus series degree

Let the series degree M be chosen from 1 to 6. The values of σ^2 under various noise environments are shown in Figure 3.2. It is seen that σ^2 decreases with increasing M under the low noise environment, whereas it becomes large for the high degree M under the strong noise environment due to the fluctuation in the estimation of $\theta_{c,m}^{k+1}$. These results imply that the optimal identification performance can be obtained through selecting an appropriate M with respect to the noise level and the variation velocity of

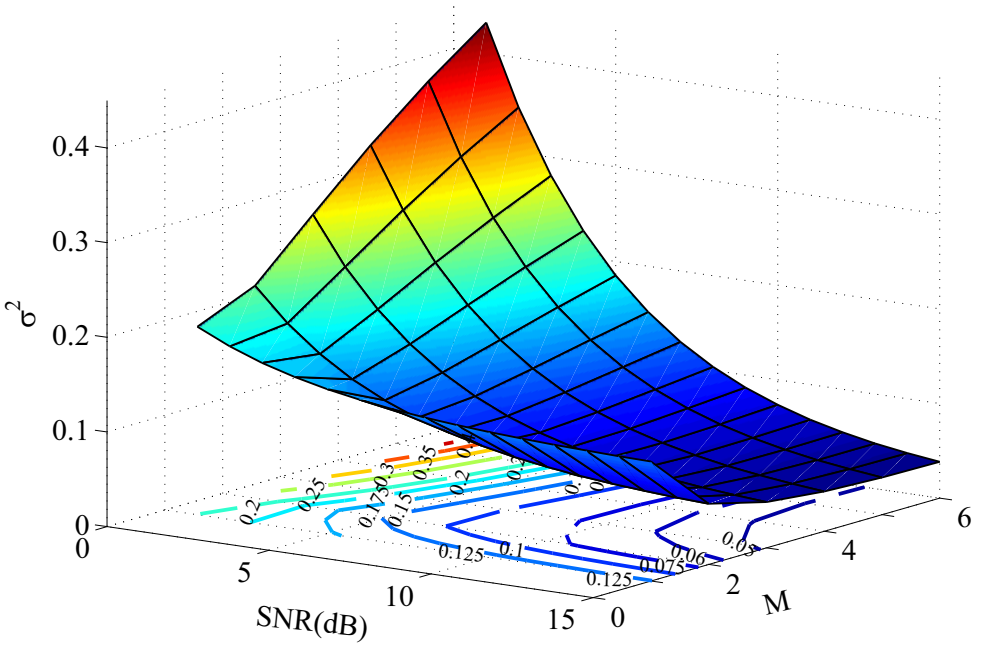

FIGURE 3.2: Estimation errors vs. series degree M and SNR

the model parameters at the present instant, which may be detected by combining the algorithm with some detection methods for the rapid variations.

3.3.3 Comparison of estimation performance

Consider the channel model has long lag time of $n = 60$. The window width and the series degree are chosen as $N = 3072$, $M = 30$, respectively. The value of σ^2 is 0.1237, and the estimates' mean values of $\hat{h}_{0,k}$ and $\hat{h}_{2,k}$ are plotted in Figure 3.3. As a comparison, the parameters are also estimated by AP, BOP, RLS and NLMS, and the values of σ^2 are 0.2498, 0.2748, 0.2751, 0.2778, respectively, which are more than 2 times of that in the proposed algorithm. Though the orthogonal projection of input data can improve the convergence performance when the input signal is colored, the AP and BOP methods also have lower convergence rate than the proposed algorithm since they do not use the explicit projection of the parameter variation. Moreover, the estimation error σ^2 of the algorithm [133] where the forgetting factor is chosen as 0.96 is 0.1934,

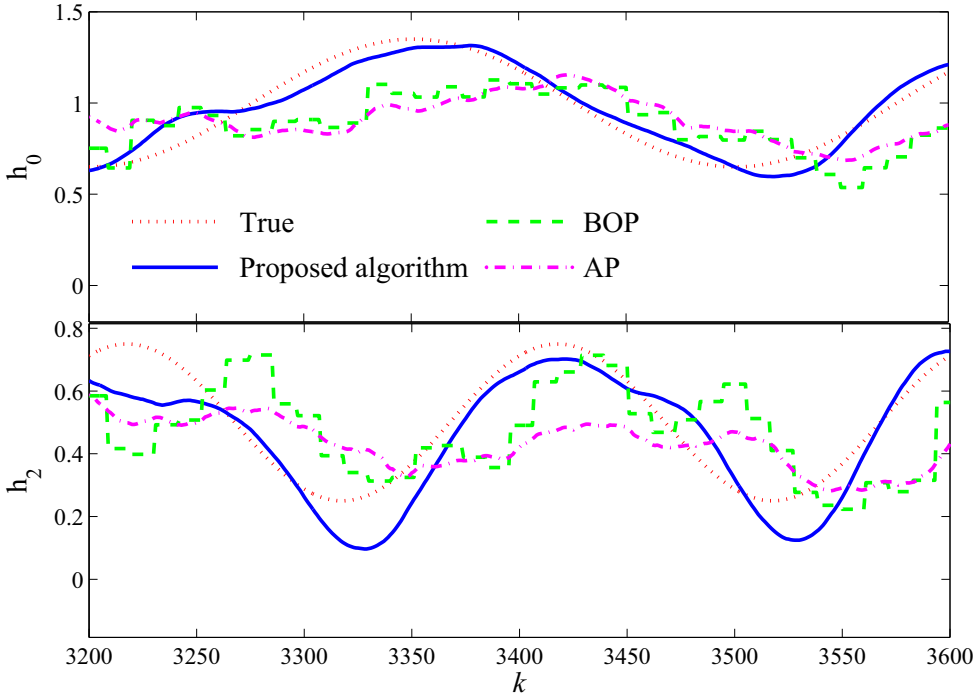

FIGURE 3.3: Estimation of h_0 and h_2 in Example 4

which is larger than that of the proposed algorithm since the noise influences become relatively large for high degree M.

3.4 Summary

The recursive identification algorithm based on the trigonometric functions has been developed for the linear time-varying systems. When the parameters of the process model have at most finite discontinuous points in the data window, they can be approximated by the cosine series through virtually expanding them into the even periodic functions, and then the parameter estimation can be obtained through estimating the coefficients of the cosine series. By making use of the orthogonality of the basis functions, the recursive identification algorithm has been proposed. The simulation results demonstrate that the proposed algorithm has a higher convergence rate than the conventional methods.

Chapter 4

Extension of Identification System Using Time-varying Model

4.1 Background

Due to the aging of components, variation of environment, fault or malfunction in the system operation, the dynamic process characteristics of a physical system often vary with time. The time-varying system examples can be found in many industrial applications, where the practical process manipulation often depends on the operating point and the workload [125, 130], the rapidly fading communication channels in remote sensing or mobile communication systems [126], the robotic manipulator and car steering in automatic driving [127, 128], and the applications in fault detection and diagnosis [129], etc. When the influence on the operating performance caused by such variation cannot be ignored, the system characteristics must be described by time-varying models and should be identified in real-time through some adaptive algorithms.

Several categories of identification methods for time-varying systems have been developed. (1) The Linear Parameter Varying model (LPV) detects the variation information from some special measurable variables that determine the process characteristics [56]. (2) The segmentation methods separate a time-varying model into several local models by segmenting the observation data with respect to the large variation [120, 135]. (3)

Several types of adaptive algorithms, such as the Recursive Least Square (RLS) with a forgetting factor [121, 134], the least mean square(LMS) or the Normalized Least Mean Square (NLMS) algorithms [122, 123], the Affine Projection algorithm (AP) and Block Orthogonal Projection (BOP) [124], Kalman filter, wavelets are used to analyze or track the varying dynamics [131]. (4) The explicit approximation of the parameter variation through the orthogonal basis functions such as the trigonometric or Legendre functions [86, 132, 136]. It has been illustrated that the approximation based on orthogonal basis help to approximate the dynamics at an arbitrary rate if the series have sufficiently high degree, consequently, the approximation may have better-tracking performance than the conventional adaptive algorithms or the segmentation approaches under the situation with rapid variation but less variation information [137].

Commonly, high approximation rate requires high series degree. Nevertheless, the estimation of the series coefficients for the high degree series becomes fragile to the noise term and the numerical conditions may become very poor in numerical computations. As a result, the estimation error easily occurs in the coefficient estimation of high degree cosine terms in the cosine series, and deteriorates the tracking performance. Correspondingly, it is expected to decrease the series degree without degrading the tracking performance of the identification method. Moreover, in the low degree of approximation, Gibbs effects that occur at the discontinuous points or the abrupt variation may cause the fluctuation in parameter estimates and deteriorate the identification performance. Cosine series based (CS) approximation is considered in the Recursive identification based on CS approximation (RCS) to remove the discontinuity at the data window edges [137]. However, at the discontinuous points or abrupt changing points inside the data window, Gibbs effects still influence the identification performance, and should be detected and compensated in order to guarantee the identification performance for rapidly varying systems.

In order to decrease the series degree and suppress the approximation error, a recursive identification algorithm with output Weighted Cosine Series (WCS) is investigated for the time-varying systems in this chapter. The weighted parameters effectively implement the recursion of the cosine basis, and some efficient approximation is used by the orthogonality of the trigonometric functions to decrease the computational

complexity, which is different from the ordinary forgetting factor imposed on the input and output regressions in RLS, the weight factor is imposed on the output and the time-varying parameters. And, a smoothing technique is considered to further reduce the influence of the noise term. Moreover, in order to reduce the influence of Gibbs effect, a soft threshold determined by neural network is also considered to detect the abrupt variation. In contrast with the conventional methods based on the Fourier series expansion, the new one effectively reduces the series degree and Gibbs effect, and it has high tracking performance with considerable low degree trigonometric series even in the rapid varying processes.

The rest of the chapter is organized as follows. In Section 4.2, the recursive algorithm of RCS with output weight factor is discussed. Then some simplifications and a smoothing technique are given in Section 4.3 and Section 4.4, respectively. The neural network based approach to detect the abrupt variation, and the compensation approach to reduce the Gibbs effect are investigated in Section 4.5. Section 4.6 illustrates the numerical example. Finally, the conclusions are given in Section 4.7.

4.2 Recursive Identification

4.2.1 Output weight factor

Preliminaries as Section 2.1-Section 2.4. In order to reduce the series degree M, a weight factor $\lambda, 0 < \lambda < 1$ is introduced into the system output $y(k-K), \cdots, y(k)$, then multiplying a weight factor λ^{K-k_1} to the output in the time window $[k-K, k]$ yields that

$$\begin{aligned} & \lambda^{K-k_1} y(k_0+k_1) \\ = \; & (\lambda^{K-k_1} h_0^{k_0+k_1}) u(k_0+k_1) + (\lambda^{K-k_1} h_1^{k_0+k_1}) u(k_0+k_1-1) + \cdots \\ & + (\lambda^{K-k_1} h_n^{k_0+k_1}) u(k_0+k_1-n) + \lambda^{K-k_1} e(k_0+k_1) \\ = \; & \overline{h}_0^{k_0+k_1} u(k_0+k_1) + \overline{h}_1^{k_0+k_1} u(k_0+k_1-1) + \cdots \\ & \overline{h}_n^{k_0+k_1} u(k_0+k_1-n) + \overline{e}(k_0+k_1) \end{aligned} \tag{4.1}$$

Unlike the weight factor or the forgetting factor imposed on the input-output data, as shown in (4.1), the weight factor is imposed on the output and the time-varying parameters. Fig. 4.1 illustrates the weighted parameters in time window $[0, 4096]$. It shows that even the original parameters $h_i^{k_0+k_1}$ vary largely at the past time, eg. $0 \le k_1 < 3000$, the weighted ones $\overline{h}_i^{k_0+k_1}$ are close to 0. Consequently, the high frequency components are reduced in weighted parameters.

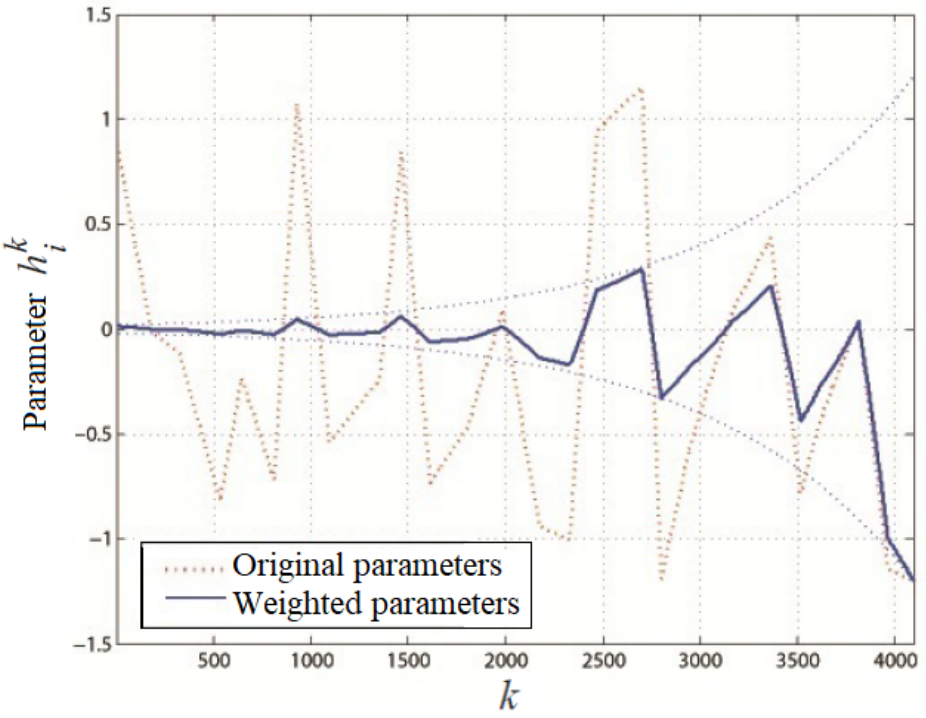

FIGURE 4.1: Example of a weighted parameter

Commonly it is expected to identify the time-varying models from the observation data recursively.

4.2.2 Definition of data matrices and vectors

Let the regression vectors and trigonometric function matrices be defined as preliminaries in Section 2.6. Then the model in (4.1) can be approximated as a compact formula

$$\lambda^{K-k_1} y(k_0+k_1) = (\phi_c^k(k_1))^T \theta_c^k + \overline{e}(k_0+k_1) \tag{4.2}$$

Furthermore, define the correlation vector, correlation matrix and its inverse as

$$\phi_{cy}^k = \sum_{k_1=0}^{K} \lambda^{K-k_1} \phi_c^k(k_1) y^k(k_1),$$
$$\mathbf{\Phi}_{cc}^k = \sum_{k_1=0}^{K} \phi_c^k(k_1)(\phi_c^k(k_1))^T, \mathbf{P}^k = (\mathbf{\Phi}_{cc}^k)^{-1}.$$

Then the estimation of the coefficient vector θ_c^k of the CS approximation can be given by

$$\hat{\theta}_c^k = (\mathbf{\Phi}_{cc}^k)^{-1} \phi_{cy}^k = \mathbf{P}^k \phi_{cy}^k \tag{4.3}$$

4.2.3 Update of data matrices and vectors

It is desired to implement (4.3) recursively. When the sliding data window shifts from $[k-K,k]$ forward to $[k+1-K,k+1]$ at thenext instant $k+1$, the updated correlation matrix $\mathbf{\Phi}_{cc}^{k+1}$ in the new data window is

$$\begin{aligned}
\mathbf{\Phi}_{cc}^{k+1} &= \sum_{k_1=0}^{K} \phi_c^{k+1}(k_1)(\phi_c^{k+1}(k_1))^T \\
&= [\mathbf{W}_c \quad \mathbf{W}_s]\Bigg(\begin{bmatrix} \mathbf{W}_c^{-1}\phi_c^k(K+1) \\ \mathbf{0} \end{bmatrix} [(\phi_c^k(K+1)^T \mathbf{W}_c^{-1} \quad \mathbf{0}^T)] \\
&\quad - \begin{bmatrix} \phi_c^k(0) \\ \mathbf{0} \end{bmatrix} [(\phi_c^k(0))^T \quad \mathbf{0}^T] + \begin{bmatrix} \mathbf{\Phi}_{cc}^k & \mathbf{\Phi}_{cs}^k \\ \mathbf{\Phi}_{sc}^k & \mathbf{\Phi}_{ss}^k \end{bmatrix}\Bigg) \begin{bmatrix} \mathbf{W}_c \\ \mathbf{W}_s \end{bmatrix}
\end{aligned} \tag{4.4}$$

where $\mathbf{W}_c$ and $\mathbf{W}_s$ are the diagonal matrices with the diagonal blocks $\mathbf{W}_{c,m}^1, \mathbf{W}_{s,m}^1$ for $m = 0, 1, \cdots$ respectively.

From (4.4), the inverse of $\mathbf{\Phi}_{cc}^{k+1}$ is difficult to be updated due to extra terms such as $\mathbf{\Phi}_{cs}^k, \mathbf{\Phi}_{sc}^k$ and $\mathbf{\Phi}_{ss}^k$. Therefore, The updating should be simplified in the recursion to guarantee the recursive computability. Let the matrices $\mathbf{\Phi}_1, \mathbf{\Phi}_2$ be denoted as

$$\begin{aligned}
&\mathbf{\Phi}_1 = \mathbf{W}_c^{-1}\phi_c^k(K+1)(\phi_c^k(K+1))^T\mathbf{W}_c^{-1} - \phi_c^k(0)(\phi_c^k(0))^T + \mathbf{\Phi}_{cc}^k = \psi^{k+1} + \mathbf{\Phi}_{cc}^k, \\
&\mathbf{\Phi}_2 = \mathbf{W}_{cs}^{-1}\mathbf{\Phi}_{sc}^k + \mathbf{\Phi}_{sc}^k\mathbf{W}_{cs}^{-1} + \mathbf{W}_{cs}^{-1}\mathbf{\Phi}_{ss}^k\mathbf{W}_{cs}^{-1}, \\
&\psi^{k+1} = \begin{bmatrix} \mathbf{W}_c^{-1}\phi_c^k(K+1), & \phi_c^k(0) \end{bmatrix}, \ \bar{\psi}^{k+1} = \begin{bmatrix} \mathbf{W}_c^{-1}\phi_c^k(K+1), & -\phi_c^k(0) \end{bmatrix}, \\
&\bar{\mathbf{y}}^{k+1} = \begin{bmatrix} y^k(K+1), & -\lambda^{K+1}y^k(0) \end{bmatrix}^T,
\end{aligned} \tag{4.5}$$

where $\mathbf{W}_{cs}^{-1} = \mathbf{W}_c^{-1}\mathbf{W}_s$, then $\mathbf{\Phi}_{cc}^{k+1}$ in (4.4) can be expressed by $\mathbf{\Phi}_{cc}^{k+1} = \mathbf{W}_c(\mathbf{\Phi}_1 + \mathbf{\Phi}_2)\mathbf{W}_c$. It implies that the extra matrices in $\mathbf{\Phi}_2$ make the inverse of $\mathbf{\Phi}_{cc}^{k+1}$ be very complicated. On the other hand, generally $\|\mathbf{\Phi}_1\| >> \|\mathbf{\Phi}_2\|$ holds when the data window length K is much larger than the series degree M, and the entries of $\mathbf{\Phi}_1^{-1}\mathbf{\Phi}_2$ are much smaller than 1. Consequently, the following inversion can be approximated by

$$(I + \mathbf{\Phi}_1^{-1}\mathbf{\Phi}_2)^{-1} = I - \mathbf{\Phi}_1^{-1}\mathbf{\Phi}_2 + (\mathbf{\Phi}_1^{-1}\mathbf{\Phi}_2)^2 - \cdots \approx I - \mathbf{\Phi}_1^{-1}\mathbf{\Phi}_2 \tag{4.6}$$

and it yields the approximation of inverse of $\mathbf{P}^{k+1}$, i.e., the inverse of $\mathbf{\Phi}_{cc}^{k+1}$ cc as follows

$$\begin{aligned} \mathbf{P}^{k+1} &= (\mathbf{\Phi}_{cc}^{k+1})^{k-1} \\ &= \mathbf{W}_c^{-1}(\mathbf{\Phi}_1 + \mathbf{\Phi}_2)^{-1}\mathbf{W}_c^{-1} \\ &\approx \mathbf{W}_c^{-1}(1 - \mathbf{\Phi}_1^{-1}\mathbf{\Phi}_2)\mathbf{\Phi}_1^{-1}\mathbf{W}_c^{-1} \end{aligned} \tag{4.7}$$

where $\mathbf{\Phi}_1^{-1}$ can be updated following matrix inversion lemma [11]

$$\mathbf{\Phi}_1^{-1} = (\mathbf{I} - \mathbf{g}^{k+1}(\overline{\psi}^{k+1})^T)\mathbf{P}^k \tag{4.8}$$

where $\mathbf{g}^{k+1}$ is a gain vector given by

$$\mathbf{g}^{k+1} = \mathbf{P}^k\psi^{k+1}(\mathbf{I}_2 + (\overline{\psi}^{k+1})^T\mathbf{P}^k\psi^{k+1})^{-1} \tag{4.9}$$

In (4.9), $\mathbf{I}_2$ is a (2×2) identity matrix, so the calculation of $(\mathbf{I}_2 + (\overline{\psi}^{k+1})^T\mathbf{P}^k\psi^{k+1})^{-1}$ is very easy in the recursive algorithm.

Similarly as $\mathbf{\Phi}_{cc}^{k+1}$, the correlation vectors ϕ_{cy}^{k+1} and ϕ_{sy}^{k+1} can be updated by

$$\begin{aligned} \phi_{cy}^{k+1} &= \mathbf{W}_c(\psi^{k+1}\overline{y}^{k+1} + \lambda\phi_{cy}^k + \mathbf{W}_{cs}^{-1}\lambda\phi_{sy}^k), \\ \phi_{sy}^{k+1} &= -\mathbf{W}_s(\psi^{k+1}\overline{y}^{k+1} + \lambda\phi_{cy}^k) + \mathbf{W}_c\lambda\phi_{sy}^k. \end{aligned} \tag{4.10}$$

From (4.10), the extra term ϕ_{sy}^k can be expressed by the past data

$$\phi_{sy}^k = -\mathbf{W}_s(\psi^k\overline{y}^k + \lambda\phi_{cy}^{k-1}) + \mathbf{W}_c\lambda\phi_{cy}^{k-1} \tag{4.11}$$

Since Since the matrices $\mathbf{W}_c, \mathbf{W}_s$ and $\mathbf{W}_{cs}^{-1}$ are diagonal, ϕ_{sy}^k can be rewritten as

$$\phi_{sy}^k = \mathbf{W}_c(\mathbf{I} + \mathbf{W}_{cs}^{-2})\lambda\phi_{cy}^{k-1} - \mathbf{W}_{cs}^{-1}\lambda\phi_{cy}^k \tag{4.12}$$

4.2.4 Update of parameter estimation

Now substitute the approximated formulae of $\mathbf{P}^{k+1}$ and ϕ_{cy}^{k+1} to deduce the recursive estimation $\hat{\theta}_c^{k+1} = \mathbf{P}^{k+1}\phi_c^{k+1}$ in the new window $[k+1-K, k+1]$, where ϕ_{cy}^{k+1} in (4.10) is split into two parts: $\mathbf{W}_c(\psi^{k+1}\overline{y}^{k+1} + \lambda\phi_{cy}^k)$ and $\mathbf{W}_s\lambda\phi_{sy}^k$. Multiplying $\mathbf{\Phi}_1^{-1}\mathbf{W}_c^{-1}$ by the first part of ϕ_{cy}^{k+1} yields that

$$\begin{aligned} & \mathbf{\Phi}_1^{-1}\mathbf{W}_c^{-1}\mathbf{W}_c(\psi^{k+1}\overline{y}^{k+1} + \lambda\phi_{cy}^k) \\ = \quad & (\psi^{k+1}(\overline{\psi}^{k+1})^T + \mathbf{\Phi}_{\mathbf{cc}}^{\mathbf{k}})^{-1}(\psi^{k+1}\overline{y}^{k+1} + \lambda\phi_{cy}^k) \end{aligned} \tag{4.13}$$

Similarly as the standard recursive formula in [134], (4.13) can be compactly rewritten as

$$\lambda\mathbf{P}^k\phi_{cy}^k + \mathbf{g}^{k+1}\varepsilon^{k+1} = \lambda\hat{\theta}_c^k + \mathbf{g}^{k+1}\varepsilon^{k+1} \tag{4.14}$$

where the prediction error ε^{k+1} is defined by

$$\varepsilon^{k+1} = \overline{y}^{k+1} - (\overline{\psi}^{k+1})^T\lambda\hat{\theta}_c^k \tag{4.15}$$

For the second part of ϕ_{cy}^{k+1}, substituting (4.11) into the multiplication of $\mathbf{P}^{k+1}$ and $\mathbf{W}_s\lambda\phi_{sy}^k$ yields that

$$\begin{aligned} & \mathbf{\Phi}_1^{-1}\mathbf{W}_c^{-1}\mathbf{W}_s\lambda\phi_{cy}^k \approx \\ & (\mathbf{I} - \mathbf{g}^{k+1}(\overline{\psi}^{k+1})^T)(\mathbf{I} + \mathbf{W}_{cs}^{-2})\lambda\overline{\theta}_s^k - (\mathbf{I} - \mathbf{g}^{k+1}(\overline{\psi}^{k+1})^T)\mathbf{W}_{cs}^{-2}\lambda\overline{\theta}_c^k \end{aligned} \tag{4.16}$$

Furthermore, the rest terms in the update of $\mathbf{P}^{k+1}$ and $\hat{\theta}_c^{k+1}$ are defined. Denote the following gain matrices to simplify the recursive formulae

$$\Omega^k \quad = \mathbf{P}^k(\mathbf{W}_{cs}^{-1}\phi_{cs}^k + (\phi_{cs}^k)^T\mathbf{W}_{cs}^{-1} + \mathbf{W}_{cs}^{-1}\phi_{ss}^k\mathbf{W}_{cs}^{-1}),$$

$$\begin{aligned} G^{k+1} &= \mathbf{W}_c^{-1}(\mathbf{I} - (\mathbf{I} - \mathbf{g}^{k+1}(\overline{\psi}^{k+1})^T)\Omega^k), \\ G_s^{k+1} &= G^{k+1}(\mathbf{I} - \mathbf{g}^{k+1}(\overline{\psi}^{k+1})^T). \end{aligned} \tag{4.17}$$

Then, by combining (4.14) with (4.16), the new parameter vector and the inverse of the correlation matrix can be concluded as follows

$$\hat{\theta}_c^{k+1} = \mathbf{P}^{k+1}\phi_{cy}^{k+1} = G^{k+1}(\lambda\hat{\theta}_c^k + \mathbf{g}^{k+1}\varepsilon^{k+1}) + \hat{\theta}_s^{k+1} \tag{4.18}$$

$$\mathbf{P}^{k+1} = G^{k+1}\mathbf{\Phi}_1^{-1}\mathbf{W}_c^{-1} = G^{k+1}(\mathbf{I} - \mathbf{g}^{k+1}(\overline{\psi}^k)^T)\mathbf{P}^k\mathbf{W}_c^{-1}. \tag{4.19}$$

The estimate in (4.18) is composed of two parts: the first part projects the term $\lambda\hat{\theta}_c^k + \mathbf{g}^{k+1}\varepsilon^{k+1}$ onto the cosine basis in the new window, while the second part $\hat{\theta}_s^{k+1}$ corresponds to transition effect on the sliding window with respect to the extra terms ϕ_s^k, ϕ_{sy}^k appeared in the update of ϕ_c^{k+1} and ϕ_{cy}^{k+1}.

Moreover, the correlation matrix and vector are updated as follows:

$$\begin{bmatrix} \mathbf{\Phi}_{cc}^{k+1} & \mathbf{\Phi}_{cs}^{k+1} \\ \mathbf{\Phi}_{sc}^{k+1} & \mathbf{\Phi}_{ss}^{k+1} \end{bmatrix} = \begin{bmatrix} \mathbf{W}_c & \mathbf{W}_s \\ -\mathbf{W}_s & \mathbf{W}_c \end{bmatrix} \begin{bmatrix} \mathbf{\Phi}_{cc}^k + \mathbf{\Psi}^{k+1} & \mathbf{\Phi}_{cs}^k \\ \mathbf{\Phi}_{sc}^k & \mathbf{\Phi}_{ss}^k \end{bmatrix} \begin{bmatrix} \mathbf{W}_c & -\mathbf{W}_s \\ \mathbf{W}_s & \mathbf{W}_c \end{bmatrix} \tag{4.20}$$

4.3 Simplification of Recursive Computation

It is seen that in (4.18) the matrix size $(M+1)(n+1)$ makes the computation of matrix multiplication complicated for the high order model approximated by the high degree cosine series. In order to reduce the computational complexity, the implementation of the parameters and matrices' update is divided into $(M+1)$ sub-blocks for each of the basis function $\cos(m\omega k_1)$, with respect to the orthogonality of the trigonometric functions.

Preliminaries as Section 2.7. Therefore, following the structure of $\phi_{c,m}^k(k_1)$ and $\phi_c^k(k_1)$ defined in (2.5), it is seen that $\mathbf{\Phi}_{cc}^k$ is composed of the following sub-blocks

$$\mathbf{\Phi}_{cc,m_1m_2}^k = \sum_{k_1=0}^{N} \phi_{c,m_1}^k(k_1)(\phi_{c,m_2}^k(k_1))^T. \tag{4.21}$$

Similar definitions are given for the blocks of $\mathbf{\Phi}^k_{cs,m_1m_2}$, $\mathbf{\Phi}^k_{sc,m_1m_2}$ and $\mathbf{\Phi}^k_{ss,m_1m_2}$. For the simplicity of notation, the blocks for $m_1 = m_2 = m$ are abbreviated as $\mathbf{\Phi}^k_{cc,m}$, $\mathbf{\Phi}^k_{ss,m}$.

The updates are just given by replacing the counterparts with the sub-blocks corresponding to mth degree of the basis function. For example, the gain vector $\mathbf{g}^{k+1}_m$ is calculated as follows:

$$\mathbf{g}^{k+1}_m = \mathbf{P}^k_m \, \psi^{k+1}_m (\mathbf{I}_2 + (\bar{\psi}^{k+1}_m)^T \mathbf{P}^k_m \psi^{k+1}_m)^{-1}. \tag{4.22}$$

Furthermore, the matrices $\mathbf{G}^{k+1}_m$, $\mathbf{G}^{k+1}_{s,m}$ are given by

$$\mathbf{G}^{k+1}_m = \mathbf{W}^{-1}_{c,m}(\mathbf{I} - (\mathbf{I} - \mathbf{g}^{k+1}_m (\bar{\phi}^{k+1}_m)^T)\mathbf{\Omega}^k_m), \tag{4.23}$$

$$\mathbf{G}^{k+1}_{s,m} = \mathbf{G}^{k+1}_m (\mathbf{I} - \mathbf{g}^{k+1}_m (\bar{\phi}^{k+1}_m)^T). \tag{4.24}$$

Then $\hat{\theta}^{k+1}_{s,m}$ and $\hat{\theta}^{k+1}_{c,m}$ can be given by

$$\varepsilon^{k+1}_m = \bar{\mathbf{y}}^{k+1}_m - (\bar{\psi}^{k+1}_m)^T \lambda \hat{\theta}^k_{c,m}, \tag{4.25}$$

$$\hat{\theta}^{k+1}_{s,m} = \mathbf{G}^{k+1}_{s,m}((\mathbf{I} + \mathbf{W}^{-2}_{cs,m})\lambda \bar{\theta}^k_{s,m} - \mathbf{W}^{-2}_{cs,m} \lambda \bar{\theta}^k_{c,m}), \tag{4.26}$$

$$\hat{\theta}^{k+1}_{c,m} = \mathbf{G}^{k+1}_m (\lambda \bar{\theta}^k_{c,m} + \mathbf{g}^{k+1}_m \varepsilon^{k+1}_m) + \bar{\theta}^{k+1}_{s,m}. \tag{4.27}$$

Moreover, the correlation matrix and its inverse are updated as follows:

$$\mathbf{P}^{k+1}_m = \mathbf{G}^{k+1}_m (\mathbf{P}^k_m - \mathbf{g}^{k+1}_m (\bar{\psi}^{k+1}_m)^T \mathbf{P}^k_m) \mathbf{W}^{-1}_{c,m}, \tag{4.28}$$

$$\begin{bmatrix} \mathbf{\Phi}^{k+1}_{cc,m} & \mathbf{\Phi}^{k+1}_{cs,m} \\ \mathbf{\Phi}^{k+1}_{sc,m} & \mathbf{\Phi}^{k+1}_{ss,m} \end{bmatrix} = \begin{bmatrix} \mathbf{W}_{c,m} & \mathbf{W}_{s,m} \\ -\mathbf{W}_{s,m} & \mathbf{W}_{c,m} \end{bmatrix} \begin{bmatrix} \mathbf{\Phi}^k_{cc,m} + \mathbf{\Psi}^{k+1}_m & \mathbf{\Phi}^k_{cs,m} \\ \mathbf{\Phi}^k_{sc,m} & \mathbf{\Phi}^k_{ss,m} \end{bmatrix} \begin{bmatrix} \mathbf{W}_{c,m} & -\mathbf{W}_{s,m} \\ \mathbf{W}_{s,m} & \mathbf{W}_{c,m} \end{bmatrix}. \tag{4.29}$$

It is obvious that $\mathbf{W}_{c,0}$ is an identity matrix, and all the elements of $\mathbf{W}_{s,0}$, $\phi_{s,0}(k_1)$ are zero, then $\mathbf{\Omega}^k_0 = 0$, $\theta^k_{s,0} = \theta^{k+1}_{s,0} = 0$. Therefore, the update for $m = 0$ is almost the same as the standard RLS algorithm. The simplified algorithm can be regarded as an extension of RLS algorithm into the high degree of the basis series to track the rapid variations.

4.4 Smoothing of Parameter Estimates

In the time window $[k-N,k]$, not only the parameters $\overline{h}_i^k$ defined in (4.1) can be calculated from the cosine series, but the past weighted parameters $\overline{h}_i^{k_0+k_1}$, $0 \le k_1 < N$, can also be given by the same series. With the time window sliding to the next one, the weighted parameters $\overline{h}_i^{k_0+k_1+1}$ are estimated in the new window, and the redundant estimates overlap with the adjacent time windows. Consequently, the simple smoothing way is to smooth the estimated parameters by using the overlapped parameters. For example, the parameters of $\hat{h}_i^{k_0+k_1}$ can be smoothed by using the cosine expansion with $\hat{\theta}_{c,m}^{k_0+1},\cdots,\hat{\theta}_{c,m}^{k+1}$ at point k_0+k_1 as follows:

$$\hat{h}_i^{k_0+k_1} = \frac{\sum_{n_1=0}^{n_0}\left(\sum_{m=0}^{M}\hat{c}_{i,m}^{k_0+k_1+n_1}\cos(m\omega(k_1-n_1))\right)}{\sum_{n_1=0}^{n_0}\lambda^{n_1}}. \tag{4.30}$$

Moreover, by using some methods to estimate the jump points [135], the Gibbs effect inside the window can be further mitigated at the discontinuous points, and can improve the approximation accuracy of the cosine series.

4.5 Detection of Rapid Changing Points

Preliminaries as Section 2.8. In order to reduce the influence of Gibbs effect, the detection of abrupt variation is considered. Using the estimated parameters $\hat{h}_i^k$ and the prediction errors ε^k within a sliding parameter window $[k-K_p,k]$, soft thresholds $\Delta^0,\cdots,\Delta^{k-K_p}$ at the instants $k,k-1,\cdots,k-K_p$ are determined by neural network.

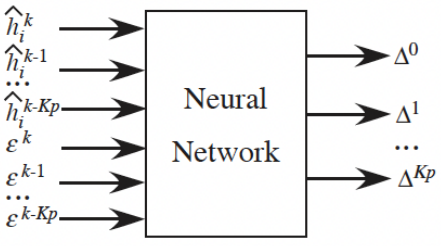

FIGURE 4.2: Detection of abrupt variation point

As illustrated in Figure 4.2, the input data to the neural network are the estimated parameters $\hat{h}_i^k, \cdots, \hat{h}_i^{k-K_p}$ for $i = 0, \cdots, n$, the prediction error $\varepsilon^k, \cdots, \varepsilon^{k-K_p}$, and the neural network can be trained by using the simulation data.

When the neural network detects the rapid changing at point k_2, a compensation function $\eta_i^k(k_1)$

$$\eta_i^k(k_1) = \begin{cases} \hat{\Delta}_i e^{-\alpha(k_2-k_1)}, & k_1 < k_2 \\ \hat{\Delta}_i e^{-\alpha(k_1-k_2)}, & k_1 \geq k_2 \end{cases} \tag{4.31}$$

is used to compensate $\overline{h}_i^{k_0+k_1} - \eta_i^k(k_1)$ to mitigate the variation of parameters, where α and β are positive constants and $\alpha > \beta$, and the estimates $\hat{h}_i^{k_0+k_1}$ is calculated by the sum of estimated CS approximation and $\eta_i^k(k_1)$.

4.6 Numerical Examples

A digital communication system with time-varying fading channel is considered in the numerical examples. It is assumed that the dominant dynamic properties are described as the model in (2.1), where $u(k)$ and $y(k)$ are the transmitted training signal, received signal, respectively, $e(k)$ is a white additive noise that is independent of $u(k)$ and the signal to noise rate (SNR) is $15dB$. In the examples, the channel has rapid variation, whose variation index is much larger than the common rapid varying index given in [136], so it is difficult to promptly track the fast variation by the conventional methods.

4.6.1 Errors versus series degree

The longest lag time of the channel model is $n = 40$. The time window length is chosen as $N = 3072$. The approximation accuracy is investigated in the simulation first. The true model parameters are approximated by an M-degree cosine series within one time window and the squares error are calculated. Fig. 4.3 shows the parameters approximated by a 30-degree cosine series. It can be seen that the approximation errors arise explicitly around $k = 1700$, 2200 and $k = 2600$. After introducing a output weight

$\lambda = 0.998$, the approximation error is decreased largely by the cosine series with the same degree of $M = 30$.

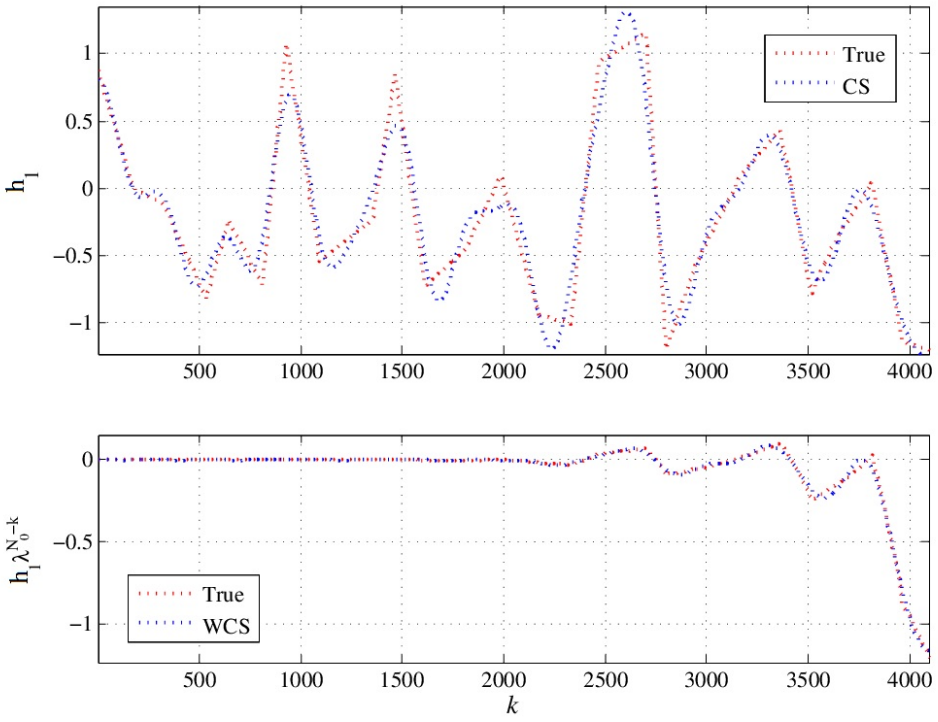

FIGURE 4.3: Approximation of weighted parameter

The illustration of approximation errors vs. series degree is plotted in Fig. 4.4. It is obvious that the approximation with output weight has less error than the conventional cosine series with considerable low series degree.

4.6.2 Cosine series versus weighted cosine series

Select the series degree $M = 20$. The mean square error (MSE) σ^2 of the estimated parameters is defined in (3.19).

Let the simulation conditions be the same as example 1. The estimates' mean values of $\hat{h}_0^k$ and $\hat{h}_2^k$ obtained by the proposed WCS algorithm and the CS algorithm [138] without weight factor are illustrated in Fig. 4.5. The estimation error σ^2 of WCS and CS is 0.0928, 0.1887 respectively. The MSE σ^2 of WCS is smaller than that of CS since the weight factor reduces the components for high degree M.

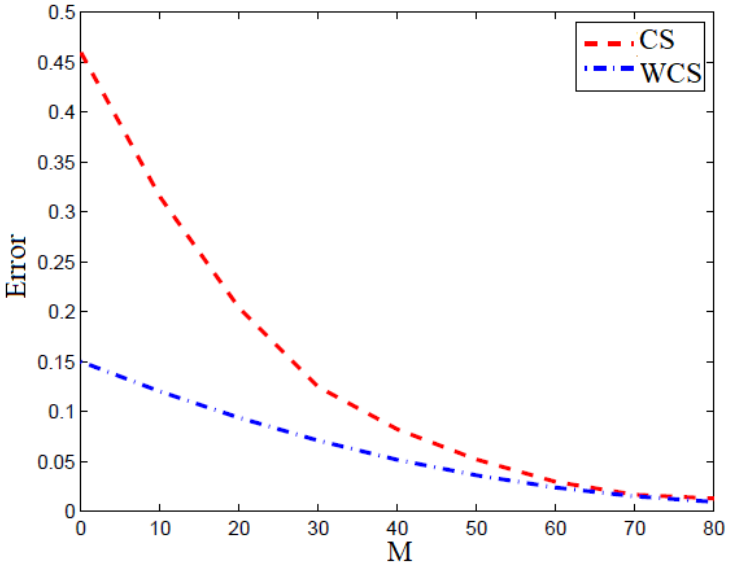

FIGURE 4.4: Errors vs. series degree M

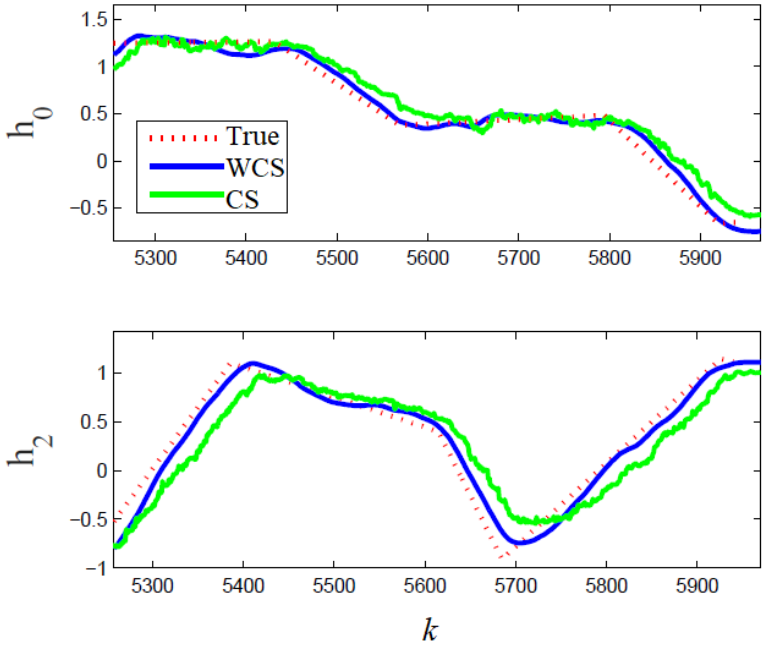

FIGURE 4.5: Estimation of h_0 and h_2

4.6.3 Comparison of estimation performance

The simulation conditions are the same as Example 1.The estimates' mean values of $\hat{h}_0^k$ and $\hat{h}_2^k$ are plotted in Fig. 4.6. The value of σ^2 for $k \in [5300, 5900]$ is 0.0718 in the proposed algorithm, as a comparison, the parameters are also estimated by RLS, NLMS,

BOP and AP, and the values of σ^2 are 0.2331, 0.2924, 0.3273, 0.3767, respectively, It is seen that the proposed algorithm (WCS) has better tracking performance than the conventional methods.

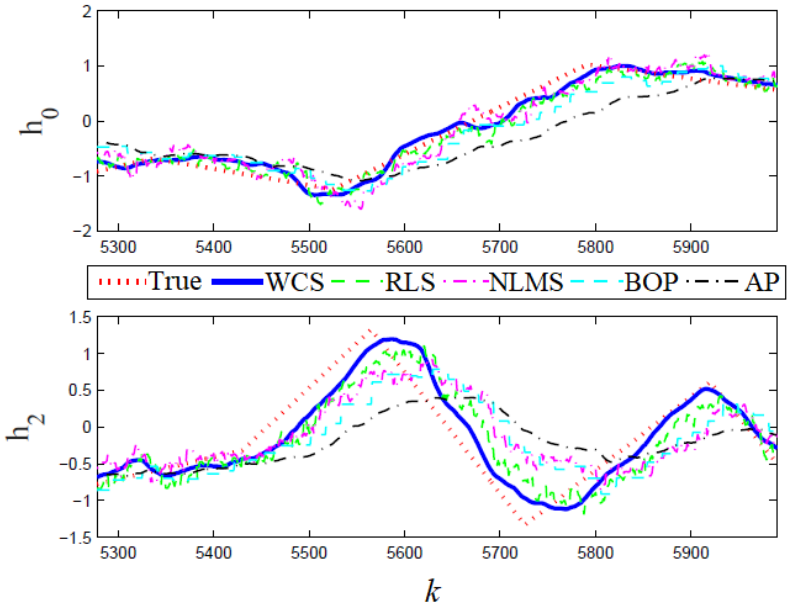

FIGURE 4.6: Estimation of h_0 and h_2

4.6.4 Performance of parameter estimation

Let SNR be from 0dB to 15dB. The other simulation conditions are the same as example 1. The mean squares errors σ^2 obtained by estimating with 5 points, 10 points in 50 simulation runs are shown in Figure 4.7. It is shown that the MSE can be decreased by applying the smoothing technique.

4.6.5 Detection and compensation

A simple 3rd order linear model is considered in the numerical example, where the model parameters vary with time and there are 2 abrupt variation points. The CS approximation with $M = 50$ is used for the time-varying parameters. The identification result of h_2^k around one discontinuous point is shown in the left of Figure 4.8, while

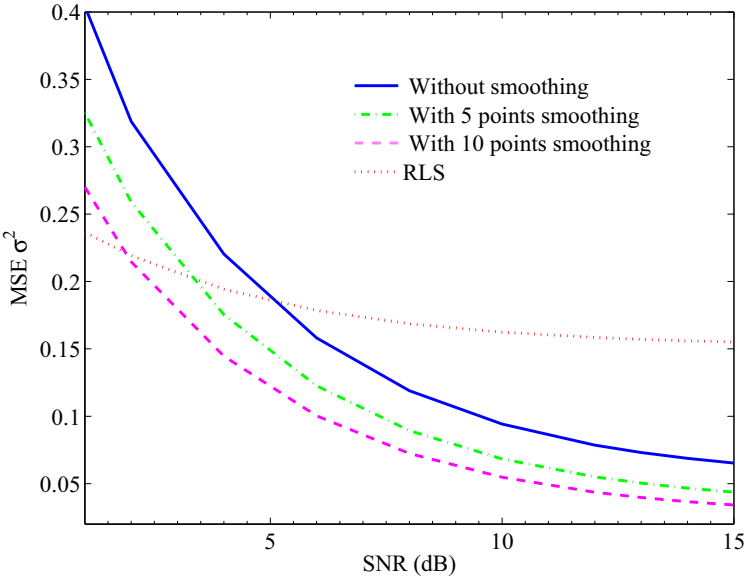

FIGURE 4.7: Performance of parameter estimation

the estimate obtained by the proposed RCS algorithm tracks the true time-varying parameters faster than RLS, but there is fluctuation around the discontinuous point.

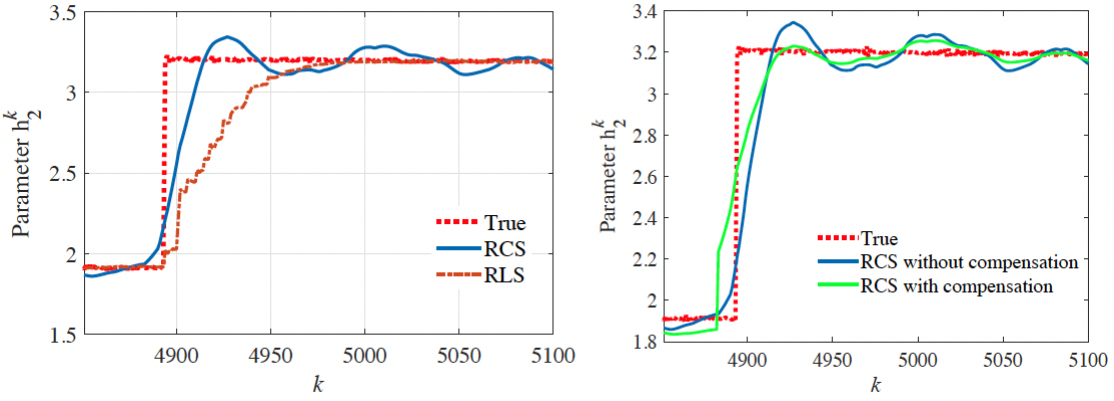

FIGURE 4.8: Example of identification result for h_2^k

By using the detection of abrupt variation point shown in Figure 4.9, the parameter estimation is compensated and the fluctuation is mitigated, as shown in the right of Figure 4.8.

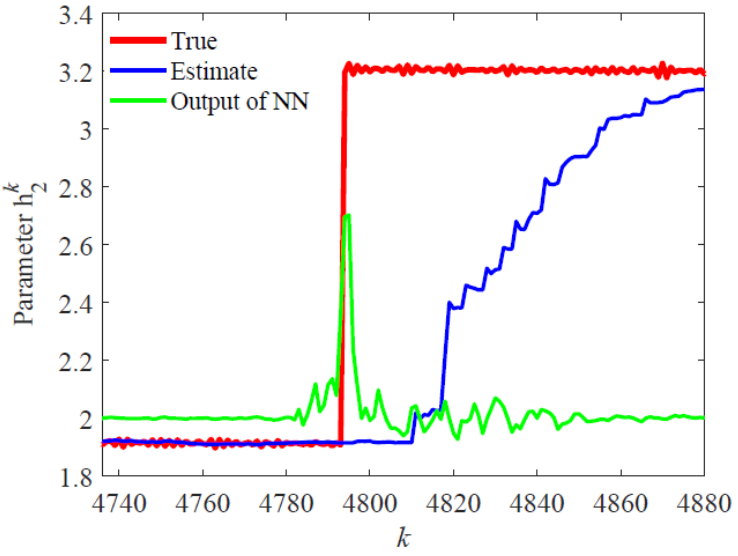

FIGURE 4.9: Detection example of abrupt variation

4.7 Summary

The recursive identification algorithm is presented for rapid time-varying systems using the cosine series approximation. The weight factor on the system output and detecting rapid changing are introduced in the proposed algorithm. By using the orthogonality of the basis functions, the recursive identification algorithm has been proposed where recursive computability is guaranteed. The compensation of the parameter estimates through detecting the rapid changing can mitigate the fluctuation in the parameter estimates. Therefore, the identification performance can be improved for the rapidly changing systems. The simulation results demonstrate that the proposed algorithm has a tracking performance than the conventional methods.

Chapter 5

Localization System for Band-limited Signal Source

5.1 Background

Localization has been utilized in many applications to exploit target's location information, such as the radar or ultrasonic wave recognition through combining sensory information to identify appropriate navigation paths or obstacles in the instrumentation unit of autonomous vehicles, autonomous robots [139–141], the location information of the epicenter in seismic analysis and early warning system [142–145], and the fault detection to pinpoint the fault type and location for system monitoring [146]. Moreover, plenty of efforts have been made to improve the localization performance under various practical conditions.

The well-known existing methods deal with the localization problem through estimating the Time Difference of Arrival (TDoA), Received Signal Strength (RSS), and Direction of Arrival (DoA) of the signal wave gathered by multiple receivers [147–150]. The time difference can be obtained by maximizing the correlation functions of the measured signal waves, or the distances are detected through analyzing the energy of signal waves, or the arrival angles are estimated through some subspace-based algorithms and the Maximum Likelihood (ML) algorithms based on array signal

processing techniques [151, 152]. The common subspace-based algorithms involve the estimation of the covariance matrix and eigendecomposition, such as MUltiple SIgnal Classification (MUSIC) algorithm [153], Estimating Signal Parameter via Rotational Invariance Techniques (ESPRIT) algorithm [154] and Weighted Subspace Fitting (WSF) algorithm [155]. They decompose the observation space into signal subspace and noise subspace by optimizing the projection of the array manifold vectors onto the subspace to achieve the optimal emitter position estimations. On the other hand, localization based on the ML algorithms [156, 157], including the Alternation Projection Maximum Likelihood (AP-ML) [158] and the Refined Maximum Likelihood (RML) algorithms [159], which establish a likelihood function of the received signals determined by emitter position, and then obtain the position's maximum likelihood estimate.

The existing methods work well when the signal waves propagate to the receivers through a single path directly. For multi-path interference in buildings, canyons, and urban areas, some instinctive characteristics such as space diversity, principal component analysis are used to reduce the affection of multi-path [160]. However, if the emitted source signals, such as low-frequency seismograms, vibration signals, some signals in instrumentation systems, often have severe band limitations. In that case, the noise will largely influence the property of the received signal outside the signal band. For subspace-based algorithms, it is difficult to separate the signal subspace from the space, especially at a low SNR, regularization becomes an ill-conditioned problem [161]. The localization performance of these algorithms that depend on spectral decomposition of the covariance matrix degrades severely in the case of few snapshots caused by limited observation time or large noise eigenvalues spread [162], and even fails to work due to the rank deficiency [163]. For ML algorithms, the Hessian matrix is very likely ill-conditioned, so the algorithm cannot guarantee convergence to the global optimal solution. Furthermore, a direct implementation of the ML criterion requires a multi-dimensional search which may be impractical since its complexity increases exponentially with the number of unknown parameters. As a result, the multi-path signals often yield large errors in space decomposition or parameter estimation, and hence deteriorated localization accuracy leads to extensive degradation of localization

performance, whereas few effective methods can handle the problem with band-limited signals. Due to insufficient frequency components of the band-limited signal, gradient-based search [164] will be greatly affected by noise, and the parameters are hard to be optimized by gradient-based search in the neural network. Therefore, numerical optimization through gradient-based search or neural network is very likely an ill-conditioned problem and cannot even guarantee convergence. In contrast, the update of Genetic Algorithm (GA) depends on the genetic operations rather than gradient-based search, and conventional GA can handle constraints well. However, for band-limited signals, the insufficient frequency components will lead to no explicit difference in the main lobe and side lobes in the fitness function, so conventional GA is difficult to distinguish between good individuals and those that are not good enough. How to deal with the localization problem under severe conditions is a challenging task.

In this chapter, we investigate the effective techniques to work for band-limited signals in the multi-path environment using the insufficient frequency data measured by the multiple receivers. For the multi-path problem, an explicit approximation of cross power spectral ratio is introduced in the new algorithm to analyze the characteristics of the different propagation paths from the emitter to the receivers; For limited bandwidth problem, weight functions determined by the spectral property of signal are considered for the optimization of the time difference, and the time difference is estimated through a new Information Evaluation based Genetic Algorithm (IEGA) under multi-path conditions. It combines the floating-point coding on a binary-coded basis. In the operation of selection, the information of estimation error evaluated through cross-evaluation within the multiple receivers is utilized to refine the fitness function. Besides, it introduces the mutation of individual bits to avoid local optimum. In contrast with the conventional GA, the new one has high accuracy for the time difference estimation. The performance of the proposed algorithm is analyzed and evaluated by numerical simulations. Root Mean Square Errors (RMSE) for different SNR and time differences in the multi-path environment are shown to approximate the Cramér Rao Bounds (CRB). The proposed estimators perform better than the existing state-of-the-art algorithms such as the MUSIC algorithm [165] and correlation approach [166].

The remainder of this chapter is organized as follows. In Section 5.2, the characteristics of the receivers through the cross power spectral ratio method are investigated, and the information fusion through IEGA and the nonlinear optimization to localize the signal source is illustrated. Section 5.3 demonstrates some numerical simulation examples. Finally, the conclusion and the future research work are given in 5.4.

5.2 Estimation of Time Difference

Preliminaries as Section 2.1 and Section 2.9-Section 2.12. Most of the conventional methods [147, 149] confront the accuracy degradation in estimating the time difference if the source signals have severe band limitation [167]. The information that relates to time difference can be extracted from the phase information in frequency analysis so that the frequency method is considered to estimate the time difference. To ensure accuracy, this chapter assumes that at least one receiver is far from the other two receivers. The situation that the receivers are very close to each other will be discussed in the future work.

5.2.1 Cross power spectral ratio method

To guarantee effective localization, the signals are pre-processed to reduce the affection of noise term $V^{(l)}(k)$ before using the estimation of time difference to localize the signal source. Let the cross power spectral ratio of l_1th and l_2th received signals be defined as follows:

$$Y^{(l_1,l_2)}(k) = \frac{E\left\{A^{(l)}(k)^* A^{(l_2)}(k)\right\}}{E\left\{A^{(l)}(k)^* A^{(l_1)}(k)\right\}}, \tag{5.1}$$

Choose such a receiver that is far away from both the l_1th and l_2th receivers to make the correlation between $V^{(l)}(k)$ and $V^{(l_1)}(k)$, $V^{(l)}(k)$ and $V^{(l_2)}(k)$ be very low. Therefore, the time average of the cross-spectral density in the different time windows in (5.1) can reduce the influence of noise outside the signal band. If the noise term and numerical

distortion are reduced, the cross power spectral ratio can be approximated as follow:

$$\begin{aligned} & Y^{(l_1,l_2)}(k) \\ & h^{(l_2)}e^{-j\omega_k(\tau^{(l_2)}-\tau^{(l_1)})} + \sum_{m=1}^{M} h_m^{(l_2)}e^{-j\omega_k(\tau_m^{(l_2)}-\tau^{(l_1)})} \\ \approx & \frac{}{h^{(l_1)} + \sum_{m=1}^{M} h_m^{(l_1)}e^{-j\omega_k(\tau_m^{(l_1)}-\tau^{(l_1)})}}, \end{aligned} \tag{5.2}$$

where $h^{(l_1)}$ is fixed as 1, the time difference $\tau^{(l_2)}-\tau^{(l_1)}$, $\tau_m^{(l_2)}-\tau^{(l_1)}$, $\tau_m^{(l_1)}-\tau^{(l_1)}$ can only be estimated with respect with to the reference $\tau^{(l_1)}$. It is seen that the cross power spectral ratio of two signals can reflect the characteristics between the paths.

Consequently, the estimation of the time difference between the l_1th and l_2th receivers can be given by

$$\hat{\tau}^{(l_1,l_2)} = \tau^{(l_2)} - \tau^{(l_1)}. \tag{5.3}$$

Due to the insufficient frequency components in the band-limited signals, the spectrum is mutually verified before using the estimation parameter to localize the signal source. Consequently, the output of the beamformer is represented by

$$G^{(l_1,l_2)}(k) \quad = \quad w^{(l_1,l_2)}(k)Y^{(l_1,l_2)}(k), \tag{5.4}$$

where $w^{(l_1,l_2)}(k)$ is the weight coefficient concerning the spectrum characteristics, it is determined by the envelope variation of signals, which is given by the Hilbert transform. Spectrum characteristics are extracted from the frequency domain, and a normalization module for normalizing the modulus of extracted features into [0, 1], a good set of weight coefficients of the signal can be obtained from the kurtosis of envelope spectrum.

5.2.2 Path estimation using IEGA

When the bandwidth of the signal is limited, the optimization through gradient-based search or neural network is an ill-conditioned problem, where the insufficient frequency components of band-limited signals will lead to ambiguities. In addition,

the numerical computation of the gradient also becomes complicated because the optimization function involves several constrained conditions. IEGA is considered for estimating time differences to solve the location problem of signals with limited bandwidth in the multi-path environment. The fitness function can easily involve the evaluation and constraints for every individual in the population. The update depends on the genetic operations rather than gradient-based search, which is largely influenced by the signal bandwidth.

5.2.3 Coding scheme

In the present binary-coded GA, binary strings represent the parameter variables in the genetic population. The length of the binary string needs to solve the problem according to the accuracy and complexity of the problem. Binary-coded GA has a Hamming distance problem, which sometimes may cause difficulties in the case of coding continuous variables. Moreover, binary strings will be very long while performing multi-parameter optimization. A lengthy binary string always occupies memory, resulting in inefficient use of computer memory. In order to accelerate convergence and perform better in genetic operations, floating-point coding is used in IEGA. Each individual is coded as a vector of floating-point numbers with the same length as the number of parameters.

5.2.4 Refinement of fitness function

The following fitness function is applied to evaluate the individual quality

$$f = \sum_{l_1,l_2=1}^{L} \frac{\alpha}{\sum_{k=0}^{N-1} \left(\Delta_G^{(l_1,l_2)}(k)^* \cdot \Delta_G^{(l_1,l_2)}(k) \right)}$$

$$\alpha = \begin{cases} 1, if \quad \hat{h}^{(l)} > \hat{h}_m^{(l)} \; m = 1, 2, \cdots, M; \\ \qquad \hat{\tau}^{(l)} < \hat{\tau}_m^{(l)} \; l = l_1, l_2 \\ 0.01, the\ other \end{cases}, \tag{5.5}$$

where

$$\Delta_G^{(l_1,l_2)}(k) = G^{(l_1,l_2)}(k) - \hat{G}^{(l_1,l_2)}(k). \tag{5.6}$$

while * indicates the complex conjugate, $G^{(l_1,l_2)}(k)$ is given by the measured data in (5.1), while $\hat{G}^{(l_1,l_2)}(k)$ is the estimate given by substituting the parameter estimates $\hat{\tau}_m^{(l_1)} - \hat{\tau}^{(l_1)}$, $\hat{\tau}^{(l_2)} - \hat{\tau}^{(l_1)}$, $\hat{\tau}_m^{(l_2)} - \hat{\tau}^{(l_1)}$, $\hat{h}_m^{(l_1)}$, $\hat{h}^{(l_2)}$, $\hat{h}_m^{(l_2)}$ into (5.4).

In order to reduce the probability of local optimum, the estimation error of $\hat{\tau}^{(l_1,l_2)}$ is evaluated by verifying the difference between $\hat{\tau}^{(l_1,l_2)}$ and $\hat{\tau}^{(l,l_2)} - \hat{\tau}^{(l,l_1)}$, where $\hat{\tau}^{(l,l_2)}$ and $\hat{\tau}^{(l,l_1)}$ are estimated respectively by (5.5), and the information of estimation error is used in the operation of selection. Thus, the refinement of fitness function is as follows:

$$F = e^{\frac{min(\varepsilon^{(l_1,l_2)})}{\varepsilon^{(l_1,l_2)}}} f \tag{5.7}$$

where

$$\varepsilon^{(l_1,l_2)} = \sum_{l \neq l_1,l_2} \left\| \hat{\tau}^{(l_1,l_2)} - \left(\hat{\tau}^{(l,l_2)} - \hat{\tau}^{(l,l_1)} \right) \right\|_2, \tag{5.8}$$

while $\varepsilon^{(l_1,l_2)}$ is the estimation error index for $\hat{\tau}^{(l_1,l_2)}$. It is seen that the larger $\varepsilon^{(l_1,l_2)}$ is, the more errors exist in $\hat{\tau}^{(l_1,l_2)}$, the less probability to be selected for fitness with relative to the minimum estimation error. Moreover, the matrix, whose (l_1,l_2)th element is $\varepsilon^{(l_1,l_2)}$, can be considered as indices of all the estimated time difference, it can be used to determine the weight coefficients in the estimation of the emitter location.

Similarly as $\varepsilon^{(l_1,l_2)}$, the estimation error $\varepsilon_m^{(l_1,l_2)}$ in multi-path paths can be given by

$$\varepsilon_m^{(l_1,l_2)} = \sum_{l \neq l_1,l_2} \left\| \hat{\tau}_m^{(l_1,l_2)} - \left(\hat{\tau}_m^{(l,l_2)} - \hat{\tau}_m^{(l,l_1)} \right) \right\|_2, \tag{5.9}$$

where

$$\hat{\tau}_m^{(l_1,l_2)} = \tau_m^{(l_2)} - \tau_m^{(l_1)}. \tag{5.10}$$

5.2.5 Genetic space and operation

Assume that GA has a population of γ individual chromosomes. The encoding of difference in time, amplitude to the reference point is connected to form the chromosome of each individual according to the above coding scheme. The population evolves successively from the previous population by employing genetic operators of selection, crossover, and mutation. GA initiates the search for the optimal solution with an initial population at the 0th generation.

First, the chromosomes are evaluated and sorted based on the refinement of the fitness function in (5.7). In selection, better-performing chromosomes with a lower error are selected by the roulette wheel method. The probability of each individual in the population is as follows:

$$I_s = \frac{F_i}{\sum_{i=1}^{\gamma} F_i}, \tag{5.11}$$

F_i represents the fitness of the ith individual. Then the child individuals are generated by crossover operations, where the chromosome bits of the selected parents for crossover are determined by a crossover probability I_c. Since there are many time and amplitude parameters in the chromosome corresponding to the reference point, a multi-point crossover is adopted, and each part of time and amplitude has more than one crossover point in the crossover. In IEGA, two mutation operations are considered. Besides the general mutation at probability I_m, the mutation of individual bits at a low probability I_i is introduced to avoid the local optimum and sustain the performance of convergence. GA iteratively replaces the previous population with a new population. Finally, path characteristics can be estimated by decoding the chromosomes of the optimal candidate with the largest fitness in the individuals. The detailed steps of the proposed method are as follows:

Step1: Acquire the signal $a^{(l)}(t)$ by the lth receiver.

Step2: Transform $a^{(l)}(t)$ to frequency domain by fast Fourier transform and obtain weight coefficients $w^{(l_1,l_2)}(k)$ from kurtosis of envelope spectrum by the Hilbert transform.

Step3: Calculate the cross power spectral ratio $Y^{(l_1,l_2)}(k)$ and let $G^{(l_1,l_2)}(k)$ be given by $w^{(l_1,l_2)}(k)Y^{(l_1,l_2)}(k)$.

Step4: Set the number of iterations to 0 and initialize the population by floating-point coding for design requirements of parameter tuning.

Step5: Decode the chromosomes of γ individuals.

Step6: Evaluate the fitness of each individual based on information of estimation error and find the individual with the highest fitness value by (5.7).

Step7: Generate intermediate generation by selection operator based on a rule determined by individual fitness according to (5.11).

Step8: Select individuals according to crossover probability I_c for crossover operation.

Step9: Mutation operation of individual reproductive individuals according to general mutation probability I_m, and copy several bits from the most optimal candidate to a selected individual in the current generation according to new mutation probability I_i.

Step10: Go to Step5 for the next iteration until the iteration number exceeds the maximal iteration number. Otherwise, stop the iteration.

5.2.6 Estimation of emitter location

In order to acquire high accuracy, the coefficient $\lambda \in (0, 1)$ is introduced to complement the information of location. Using the estimation of $\hat{\tau}_m^{(l_1,l_2)}$, the emitter location can be estimated by solving the following optimization problem

$$\arg \min_{P_e(x),P_e(y),P_e(z)} (J_e + \lambda J_t), \tag{5.12}$$

where

$$J_e = \sum_{l_1,l_2=1}^{L} W^{(l_1,l_2)} \left(\Delta_e^{(l_1,l_2)} - c\hat{\tau}^{(l_1,l_2)}\right)^2,$$

$$J_t = \sum_{m=1}^{M} \sum_{l_1,l_2=1}^{L} W_m^{(l_1,l_2)} \left(\Delta_t^{(l_1,l_2)} - c\hat{\tau}_m^{(l_1,l_2)} \right)^2, \tag{5.13}$$

while $P_e(x), P_e(y), P_e(z)$ are the coordinates of emitter position, $W^{(l_1,l_2)}$ and $W_m^{(l_1,l_2)}$ are the weight coefficients with respect to the estimation error $\varepsilon^{(l_1,l_2)}$ and $\varepsilon_m^{(l_1,l_2)}$, respectively. Here the weight coefficients $W^{(l_1,l_2)}$ and $W_m^{(l_1,l_2)}$ are determined by

$$W^{(l_1,l_2)} = e^{\frac{1-\varepsilon^{(l_1,l_2)}}{d}}, W_m^{(l_1,l_2)} = e^{\frac{1-\varepsilon_m^{(l_1,l_2)}}{d_m}}, \tag{5.14}$$

where d and d_m are positive numbers to ensure the large weight for estimates with low error. $\Delta^{(l_1,l_2)}$ is the distance difference between the distance from the l_2th receiver, and the distance from the l_1th receiver to the source location as follows:

$$\begin{aligned} \Delta_e^{(l_1,l_2)} = & \left\| \begin{bmatrix} P_e(x) \\ P_e(y) \\ P_e(z) \end{bmatrix} - \begin{bmatrix} P_r(l_2,x) \\ P_r(l_2,y) \\ P_r(l_2,z) \end{bmatrix} \right\|_2 \\ & - \left\| \begin{bmatrix} P_e(x) \\ P_e(y) \\ P_e(z) \end{bmatrix} - \begin{bmatrix} P_r(l_1,x) \\ P_r(l_1,y) \\ P_r(l_1,z) \end{bmatrix} \right\|_2 \end{aligned} \tag{5.15}$$

Similarly as $\Delta_e^{(l_1,l_2)}$, the distance difference $\Delta_t^{(l_1,l_2)}$ between the mth transponder and the l_1th, l_2th receivers can be given by

$$\begin{aligned} \Delta_t^{(l_1,l_2)} = & \left\| \begin{bmatrix} P_t(m,x) \\ P_t(m,y) \\ P_t(m,z) \end{bmatrix} - \begin{bmatrix} P_r(l_2,x) \\ P_r(l_2,y) \\ P_r(l_2,z) \end{bmatrix} \right\|_2 \\ & - \left\| \begin{bmatrix} P_t(m,x) \\ P_t(m,y) \\ P_t(m,z) \end{bmatrix} - \begin{bmatrix} P_r(l_1,x) \\ P_r(l_1,y) \\ P_r(l_1,z) \end{bmatrix} \right\|_2 \end{aligned} \tag{5.16}$$

5.3 Numerical Examples

Some numerical examples are presented in this section to test the performances of the proposed algorithm. The simulation scenarios in this chapter follow from Fig. 2.3. The band-limited signals in low-frequency vibration signals are considered. The emitter is located at $[-60;-35;20]$, and six receivers are located at $[0;0;0]$, $[10;0;0]$, $[0;10;0]$, $[-10;0;0]$, $[0;-10;0]$ and $[0;0;10]$. Assume that three transponders are located at $[-20;30;0]$, $[25;15;-20]$ and $[30;-10;20]$ to transmit the signals. The unit of values is m. The measured signals $r^{(l)}(t)$ are sampled at the sampling rate of 4 kHz, the records within a time window of 10 s are used for the data analysis. The SNR is set as 10 dB, and the path attenuation coefficients remain constant during the observation time interval. The estimation performance of the parameters is evaluated in terms of RMSE, which is defined by

$$RMSE = \sqrt{\frac{\sum_{i=1}^{N_s} \|x - \hat{x}\|_2}{N_s}} \tag{5.17}$$

where N_s is the number of Monte-Carlo runs, which is set as 200, x is the real value, and $\hat{x}$ is the estimated value.

In IEGA, let the population size of one generation be $\gamma = 100$, and the probabilities of crossover, mutation be $I_c = 0.618$, $I_m = 0.0625$, $I_i = 0.005$, respectively.

5.3.1 Estimation with known spectral envelope

If the spectrum characteristics of the measured signals are known, the weight coefficient $w^{(l)}(k)$ is directly given according to the spectrum characteristics. The localization performance of the proposed algorithm is illustrated in Fig. 5.1, it is seen that the localization system still has high localization accuracy when the bandwidth of signals is up to 30 Hz.

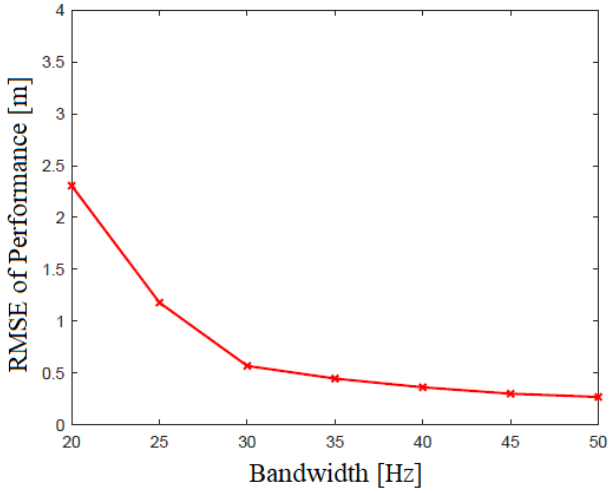

FIGURE 5.1: Performance and bandwidth of signals with known spectral information (SNR=10 dB)

5.3.2 Estimation with unknown spectral envelope

For signals with unknown spectral information, the weight coefficient $w^{(l)}(k)$ is determined by the envelope variation of signals. The weight function is illustrated in Fig. 5.2, it is seen that the frequency components are concentrated within a limited bandwidth. Therefore, the propagation path parameters are not estimated easily by the neural network or gradient-based search. The localization performance of the proposed

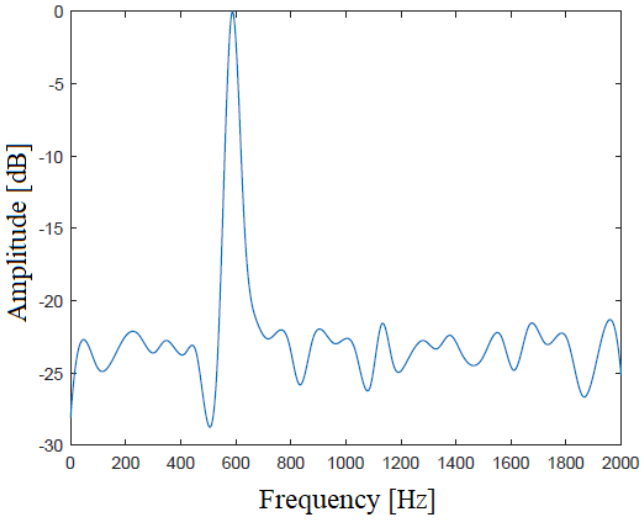

FIGURE 5.2: Weight function of signals with unknown spectral information

algorithm is shown in Fig. 5.3, it is seen that the localization system still has high localization accuracy when the bandwidth of signals is up to 40 Hz.

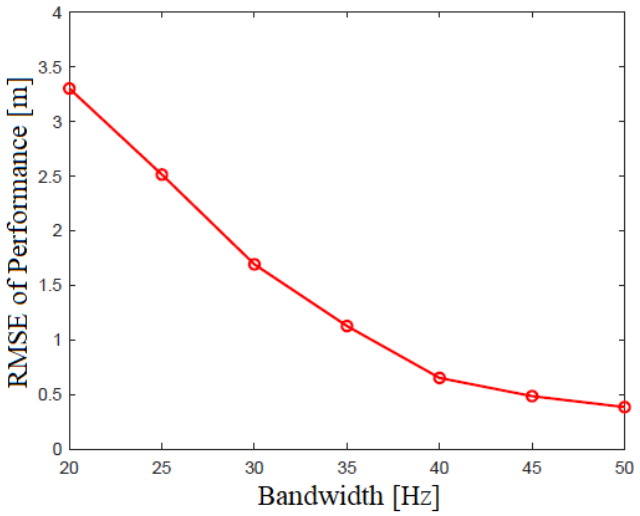

FIGURE 5.3: Performance and bandwidth of signals with unknown spectral information (SNR=10 dB)

5.3.3 Performance versus SNR

Let the snapshot be the same, and the bandwidth be 40 Hz. The comparison of the proposed algorithm versus the MUSIC algorithm [165] and correlation approach [166] is shown in Fig. 5.4. Few snapshots will significantly affect the performance of the MUSIC algorithm and correlation approach. In contrast, the proposed algorithm can avoid the local optimum by the information evaluation scheme. It can work well under the same snapshot condition and almost approaches the corresponding CRB under the multi-path environment, especially for band-limited signals.

5.3.4 Performance versus number of transponders

When emitter and receiving stations are fixed, the fewer transponders, the higher positioning accuracy. 30 Hz bandwidth signals with known spectral information and

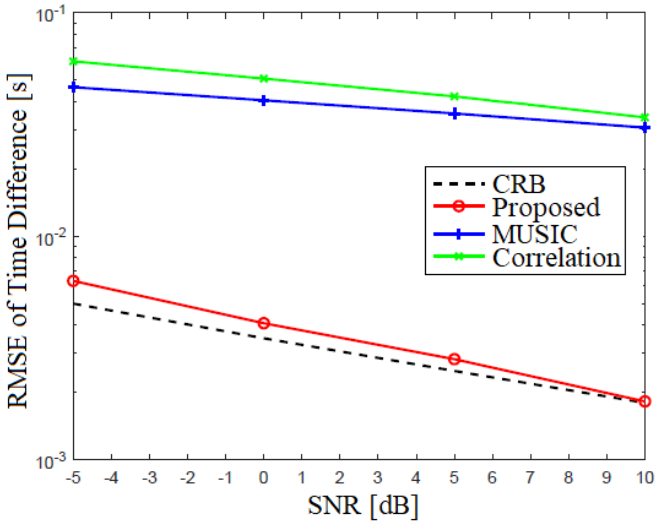

FIGURE 5.4: CRB and RMSE of time difference estimation versus SNR

40 Hz bandwidth signals with unknown spectral information are considered in Fig. 5.5, which shows the localization performance in the different number of transponders.

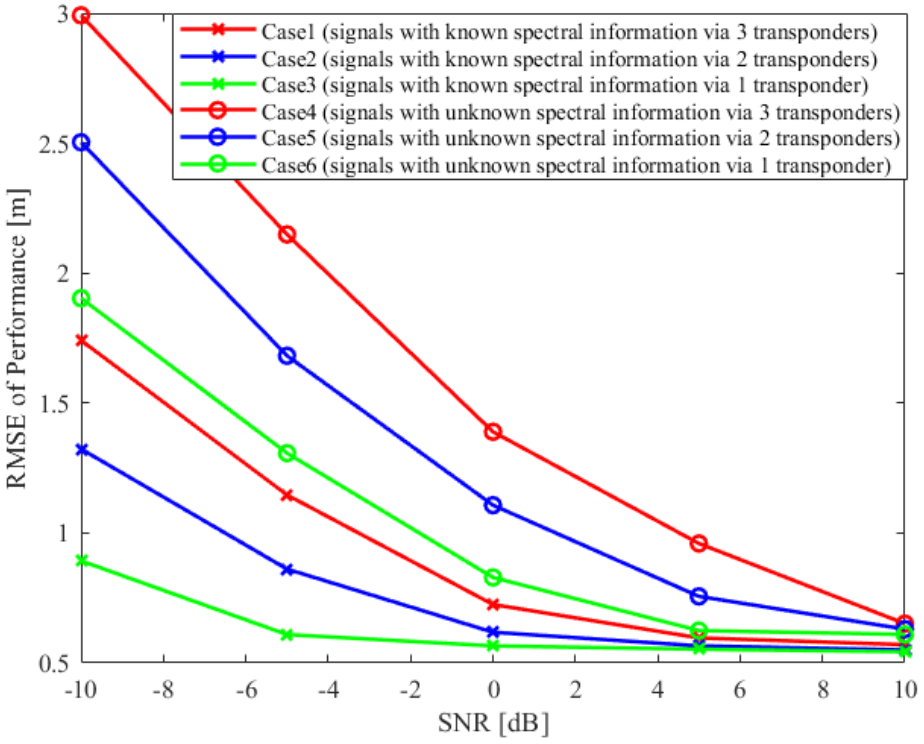

FIGURE 5.5: Performance versus the number of transponders

5.3.5 Estimation performance against noise

Consider the performance of the proposed IEGA against the noises and band-limited interferences. Let the iteration be the same, and the bandwidth varies from 20 Hz to 40 Hz. Ten simulation runs have been executed. The relative error of the estimated distance from the reference point to the emitter versus the true one is summarized in Table 1. For the comparison, it illustrates the relative errors in the conventional algorithms and IEGA. It is seen that IEGA can work well even for limited bandwidth in the multi-path environment.

TABLE 5.1: Comparison of IEGA versus conventional algorithms on relative errors (%) (Noise with the bandwidth of 20 Hz and SNR of 10 dB)

Algorithm \ Bandwidth	20	25	30	35	40
Correlation	39.25	24.89	17.62	13.79	11.25
MUSIC	14.23	13.86	13.58	13.3	12.88
GA	14.98	13.66	12.47	11.19	9.48
IEGA	4.56	3.52	2.05	1.31	0.67

5.4 Summary

The localization problem of signal sources has been investigated through multiple receivers. It has been shown that by introducing weight functions to extract the effective signals and introducing the cross power spectral ratio method for time difference estimation through IEGA into the nonlinear optimization problem, the proposed algorithm can work for band-limited signals under the multi-path environment. The analysis of band-limited radar signals has demonstrated the effectiveness of the algorithm.

Chapter 6

Conclusions

6.1 Summary

This thesis shows the system models under insufficient information conditions and proposes new approaches based on information in both time and frequency domains. 1) a new recursive algorithm for the system with rapid variation but less variation information. 2) extension of identification system using time-varying model. 3) localization system using multi-path model for band-limited signal source.

Chapter 3 proposes a new recursive algorithm for the system with rapid variation but less variation information. The recursive identification based on cosine series based approximation is introduced to remove the discontinuity of the model parameters by expanding the varying parameters into even periodic functions in order not to cause the Gibbs effect at the time window edges. The parameter estimation can be obtained by estimating the coefficients of the cosine series in frequency domain.

Chapter 4 proposes the extension of identification system based on time-varying model of **Chapter 3**. A weight factor is imposed on the output and parameters to decrease the degree of cosine series and suppress the approximation error. And a smoothing technique is considered to reduce the influence of the noise term. Moreover, in order to mitigate the fluctuation caused by Gibbs effect in the parameter estimation, detection

of abrupt variation points is introduced into the rapid time-varying system, and more time-domain variation information can be complemented by parameter compensation.

Chapter 5 proposes a localization algorithm using multi-path model for insufficient frequency information. The spectral characteristics including phase information in frequency domain are used to analyze the characteristics of multiple paths. Moreover, a time-domain information evaluation based genetic algorithm is considered for the time difference estimation.

6.2 Topics for Future Research

They still have many works to continue from very different perspectives. A few possible extensions are listed here.

- Noise has always been an unavoidable problem in signal processing. Therefore, the study on reducing estimation error under the strong noise environment is necessary for the time-varying and localization systems.
- Based on **Chapter 3**, **Chapter 4** adds abrupt changing point detection, the identification of a fast time-varying system with high accuracy is realized in two steps. The implementation of the parameter compensation into the recursion of parameter updates will be considered in future work.
- **Chapter 5** assumes that at least one receiver is far from the other two receivers. As a result, the noise correlation can be reduced by choosing the signals received by the receivers with far distances. However, if the receivers are very close to each other, the correlation of noise signals will become stronger, the cyclostationarity characteristics of the received signals can be utilized to reduce the influence of correlated noise. Solving such a problem of signal-dependent noise is a direction of future work in the localization system.

Bibliography

[1] F. Ding, L. Xu, and Q. Zhu, "Performance analysis of the generalised projection identification for time-varying systems," *IET Control Theory & Applications*, vol. 10, no. 18, pp. 2506–2514, 2016.

[2] C. Bao, H. Hong, Z. Li, and X. Zhu, "Time-varying system identification using a newly improved HHT algorithm," *Computers & Structures*, vol. 87, no. 23-24, pp. 1611–1623, 2009.

[3] L. Shang, J. Liu, and Y. Zhang, "Recursive fault detection and identification for time-varying processes," *Ind.eng.chem.res*, 2016.

[4] S. Zhang, S. Lu, Q. He, and F. Kong, "Time-varying singular value decomposition for periodic transient identification in bearing fault diagnosis," *Journal of Sound and Vibration*, vol. 379, pp. 213–231, 2016.

[5] M. Zhong, T. Xue, and S. Ding, "A survey on model-based fault diagnosis for linear discrete time-varying systems," *Neurocomputing*, vol. 306, 2018.

[6] Y. Gu, H. Wei, R. J. Boynton, S. N. Walker, and M. A. Balikhin, "System identification and data-driven forecasting of AE index and prediction uncertainty analysis using a new cloud-NARX model," *Journal of Geophysical Research: Space Physics*, vol. 124, no. 1, pp. 248–263, 2019.

[7] X. Li, J. Wen, and E. Bai, "Building energy forecasting using system identification based on system characteristics test," in *2015 Workshop on Modeling and Simulation of Cyber-Physical Energy Systems (MSCPES)*, 2015, pp. 1–6.

[8] Y. Li, X. Wang, S. Sun, X. Ma, and G. Lu, "Forecasting short-term subway passenger flow under special events scenarios using multiscale radial basis function networks - ScienceDirect," *Transportation Research Part C: Emerging Technologies*, vol. 77, pp. 306–328, 2017.

[9] D. Arifianto, "Crack detection of propeller shaft on board marine ship using microphone array," *Journal of Physics Conference*, vol. 1075, no. 1, p. 012086, 2018.

[10] D. Sun, H. Li, C. Zheng, and X. Li, "Sound velocity correction based on effective sound velocity for underwater acoustic positioning systems," *Applied Acoustics*, vol. 151, pp. 55–62, 2019.

[11] L. David, W. Olof, G. Fredrik, and H. Hans, "Shooter localization in wireless microphone networks," *Eurasip Journal on Advances in Signal Processing*, 2010.

[12] W. A. Ahroon, A. Houtsma, and B. E. Acker-Mills, "Speech intelligibility in noise using throat and acoustic microphones," *Aviation Space and Environmental Medicine*, vol. 77, no. 1, pp. 26–31, 2006.

[13] R. Wang and S. Bei, "Optimization of fixed microphone array in high speed train noises identification based on far-field acoustic holography," *Advances in Acoustics and Vibration,2017,(2017-02-1)*, vol. 2017, pp. 1–11, 2017.

[14] L. Alsteris and K. Paliwal, "Further intelligibility results from human listening tests using the short-time phase spectrum," *Speech Communication*, vol. 48, no. 6, pp. 727–736, 2006.

[15] J. M. Valin, F. Michaud, J. Rouat, and D. Létourneau, "Robust sound source localization using a microphone array on a mobile robot," *IEEE*, 2016.

[16] X. Du, F. Lao, and G. Teng, "A sound source localisation analytical method for monitoring the abnormal night vocalisations of poultry," *Sensors*, vol. 18, no. 9, 2018.

[17] A. J. Weiss, "Direct position determination of narrowband radio frequency transmitters," *IEEE Signal Processing Letters*, vol. 11, no. 5, pp. 513–516, 2004.

[18] J. Caffery, "Wireless location in CDMA cellular radio systems," Ph.D. dissertation, Kluwer academic publishers, 1998.

[19] A. Eshkevari and S. M. S. Sadough, "An improved method for localization of wireless capsule endoscope using direct position determination," *IEEE Access*, vol. 9, pp. 154 563–154 577, 2021.

[20] Z. Lu, J. Wang, B. Ba, and D. Wang, "A novel direct position determination algorithm for orthogonal frequency division multiplexing signals based on the time and angle of arrival," *IEEE Access*, vol. 5, pp. 25 312–25 321, 2017.

[21] Y. T. Chan, W. Y. Tsui, H. C. So, and P. C. Ching, "Time-of-arrival based localization under NLOS conditions," *IEEE Transactions on Vehicular Technology*, vol. 55, no. 1, pp. 17–24, 2006.

[22] F. Gustafsson and F. Gunnarsson, "Positioning using time-difference of arrival measurements," in *2003 IEEE International Conference on Acoustics, Speech, and Signal Processing, 2003. Proceedings. (ICASSP '03).*, vol. 6, 2003, pp. VI–553.

[23] J. D. Bard and F. M. Ham, "Time difference of arrival dilution of precision and applications," *IEEE Transactions on Signal Processing*, vol. 47, no. 2, pp. 521–523, 1999.

[24] R. Peng and M. L. Sichitiu, "Angle of arrival localization for wireless sensor networks," in *2006 3rd Annual IEEE Communications Society on Sensor and Ad Hoc Communications and Networks*, vol. 1, 2006, pp. 374–382.

[25] P. Kulakowski, J. Vales-Alonso, E. Egea-López, W. Ludwin, and J. García-Haro, "Angle-of-arrival localization based on antenna arrays for wireless sensor networks," *Computers & Electrical Engineering*, vol. 36, no. 6, pp. 1181–1186, 2010.

[26] C. Knapp and G. Carter, "The generalized correlation method for estimation of time delay," *IEEE Transactions on Acoustics, Speech, and Signal Processing*, vol. 24, no. 4, pp. 320–327, 1976.

[27] K. Sasaki, T. Sato, and Y. Nakamura, "Holographic passive sonar," *Research Laboratory of Precision Machinery and Electronics*, pp. 43–53, 1976.

[28] J. K. Tugnait, "On time delay estimation with unknown spatially correlated gaussian noise using fourth-order cumulants and cross cumulants," *IEEE Transactions on Signal Processing*, vol. 39, no. 6, pp. 1258–1267, 1991.

[29] H. H. Chiang and C. L. Nikias, "A new method for adaptive time delay estimation for non-gaussian signals," *IEEE Transactions on Acoustics, Speech, and Signal Processing*, vol. 38, no. 2, pp. 209–219, 1990.

[30] B. Bell and T. Ewart, "Separating multipaths by global optimization of a multidimensional matched filter," *IEEE transactions on acoustics, speech, and signal processing*, vol. 34, no. 5, pp. 1029–1037, 1986.

[31] S. Wu, Q. Zhang, R. Fan, and N. Zhang, "Match-filtering based TOA estimation for IR-UWB ranging systems," in *2008 International Wireless Communications and Mobile Computing Conference*. IEEE, 2008, pp. 1099–1105.

[32] B. R. Townsend, P. C. Fenton, K. J. V. Dierendonck, and D. J. R. V. Nee, "Performance evaluation of the multipath estimating delay lock loop," *Navigation*, vol. 42, no. 3, p. 502514, 1995.

[33] R. S. Istepanian and M. Stojanovic, *Underwater acoustic digital signal processing and communication systems*. Springer, 2002.

[34] L. Sun and X. Liu, "Algorithm of signal source localization via sensor networks," *ICIC Express Letters*, vol. 12, no. 5, pp. 441–447, 2018.

[35] H. Ni, G. Ren, and Y. Chang, "A TDOA location scheme in OFDM based WLANs," *IEEE Transactions Consumer Electronics*, vol. 54, no. 3, pp. 1017–1021, 2008.

[36] T. G. Manickam and R. J. Vaccaro, "A least-squares algorithm for multipath time-delay estimation," *Signal Processing IEEE Transactions on*, vol. 42, no. 11, pp. 3229–3233, 1994.

[37] B. Champagne, M. Eizenman, and S. Pasupathy, "Exact maximum likelihood time delay estimation," in *International Conference on Acoustics, Speech, and Signal Processing,*. IEEE, 1989, pp. 2633–2636.

[38] M. Feder and E. Weinstein, "Parameter estimation of superimposed signals using the EM (estimate maximize) algorithm," 1988.

[39] J. Li and R. Wu, "An efficient algorithm for time delay estimation," *Signal Processing, IEEE Transactions on*, vol. 46, no. 8, pp. 2231–2235, 1998.

[40] S. Xie, A. Hu, and Y. Huang, "Time-delay estimation in the multi-path channel based on maximum likelihood criterion," *KSII Transactions on Internet and Information Systems (TIIS)*, vol. 6, no. 4, pp. 1063–1075, 2012.

[41] J. A. del Peral-Rosado, J. A. López-Salcedo, G. Seco-Granados, F. Zanier, and M. Crisci, "Joint maximum likelihood time-delay estimation for LTE positioning in multipath channels," *EURASIP Journal on Advances in Signal Processing*, vol. 2014, no. 1, pp. 1–13, 2014.

[42] A. Bruckstein, T. J. Shan, and T. Kailath, "The resolution of overlapping echos," *IEEE Transactions on Acoustics, Speech, and Signal Processing*, vol. 33, no. 6, pp. 1357–1367, 1985.

[43] R. Schmidt, "Multiple emitter location and signal parameter estimation," *IEEE Transactions on Antennas and Propagation*, vol. 34, no. 3, pp. 276–280, 1986.

[44] H. Saarnisaari, "TLS-ESPRIT in a time delay estimation," in *1997 IEEE 47th Vehicular Technology Conference. Technology in Motion*, vol. 3, 1997, pp. 1619–1623.

[45] R. Roy, A. Paulraj, and T. Kailath, "ESPRIT–A subspace rotation approach to estimation of parameters of cisoids in noise," *Acoustics, Speech and Signal Processing, IEEE Transactions on*, 1986.

[46] F. Ge, D. Shen, Y. Peng, and V. O. Li, "Super-resolution time delay estimation in multipath environments," *IEEE Transactions on Circuits and Systems I: Regular Papers*, vol. 54, no. 9, pp. 1977–1986, 2007.

[47] J. H. Shin, H. R. Park, and E. Y. Chang, "An ESPRIT-based super-resolution time delay estimation algorithm for real-time locating systems," *The Journal of Korean Institute of Communications and Information Sciences*, vol. 38, no. 4, pp. 310–317, 2013.

[48] D. Zhang, Y. Zhang, G. Zheng, C. Feng, and T. Tang, "Improved DOA estimation algorithm for co-prime linear arrays using root-MUSIC algorithm," *Electronics Letters*, vol. 53, no. 18, pp. 1277–1279, 2017.

[49] B. D. Rao and K. V. S. Hari, "Weighted subspace methods and spatial smoothing: analysis and comparison," *IEEE Transactions on Signal Processing*, vol. 41, no. 2, pp. 788–803, 1993.

[50] B. Ottersten, M. Viberg, P. Stoica, and A. Nehorai, "Exact and large sample maximum likelihood techniques for parameter estimation and detection in array processing," in *Radar Array Processing*. Springer, 1993, pp. 99–151.

[51] X. Jiang and S. Qian, "DOA estimation of coherent signals based on modified music algorithm," in *2021 IEEE 3rd International Conference on Civil Aviation Safety and Information Technology (ICCASIT)*. IEEE, 2021, pp. 918–921.

[52] A. Herzog and E. A. Habets, "Eigenbeam-esprit for DOA-vector estimation," *IEEE Signal Processing Letters*, vol. 26, no. 4, pp. 572–576, 2019.

[53] D. Meng, X. Wang, M. Huang, L. Wan, and B. Zhang, "Robust weighted subspace fitting for DOA estimation via block sparse recovery," *IEEE Communications Letters*, vol. 24, no. 3, pp. 563–567, 2019.

[54] G. Doretto, D. Cremers, P. Favaro, and S. Soatto, "Dynamic texture segmentation," in *Computer Vision, IEEE International Conference on*, vol. 3. IEEE Computer Society, 2003, pp. 1236–1236.

[55] M. Boussé, O. Debals, and L. Lathauwer, "Tensor-based large-scale blind system identification using segmentation," *IEEE Transactions on Signal Processing*, vol. 65, no. 21, pp. 5770–5784, 2017.

[56] Q. Zhang and L. Ljung, "From structurally independent local LTI models to LPV model," *Automatica A Journal of IFAC the International Federation of Automatic Control*, pp. 232–235, 2017.

[57] W. J. Ko and C. F. Hung, "Extraction of structural system matrices from an identified state-space system using the combined measurement of dva," *Journal of Sound & Vibration*, vol. 249, no. 5, pp. 955–970, 2002.

[58] J. N. Yang and S. Lin, "Identification of parametric variations of structures based on least squares estimation and adaptive tracking technique," *Journal of Engineering Mechanics*, vol. 131, no. 3, pp. 290–298, 2005.

[59] J. W. Lin and R. Betti, "On-line identification and damage detection in non-linear structural systems using a variable forgetting factor approach," *Earthquake Engineering & Structural Dynamics*, vol. 33, no. 4, pp. 419–444, 2004.

[60] L. Qin, J. Gross, S. Pfeiffer, and H. Werner, "A local approach for the LPV identification of an actuated beam using piezoelectric actuators and sensors," *Mechatronics*, vol. 24, no. 4, pp. 289–297, 2014.

[61] M. Steinbuch, D. Van, and D. Van, "Experimental modelling and LPV control of a motion system," in *American Control Conference*, 2003.

[62] C. C. Lin, T. T. Soong, and H. G. Natke, "Real-time system identification of degrading structures," *Journal of Engineering Mechanics*, vol. 116, no. 10, pp. 2258–2274, 1990.

[63] K. Yu, "Study on time-varying structural dynamics numerical algorithm and modal parameter identification method," *Harbin Institute of Technology, Harbin, China*, 2000.

[64] A. G. Poulimenos and S. D. Fassois, "Parametric time-domain methods for non-stationary random vibration modelling and analysis - A critical survey and comparison," *Mechanical Systems & Signal Processing*, vol. 20, no. 4, pp. 763–816, 2006.

[65] C. Paleologu, J. Benesty, and S. Ciochina, "A robust variable forgetting factor recursive least-squares algorithm for system identification," *IEEE Signal Processing Letters*, vol. 15, pp. 597–600, 2008.

[66] C. Paleologu and J. Benesty and S. Ciochina, "A practical variable forgetting factor recursive least-squares algorithm," in *2014 11th International Symposium on Electronics and Telecommunications (ISETC)*, 2014, pp. 1–4.

[67] M. O. B. Saeed, A. Zerguine, and S. A. Zummo, "Variable step-size least mean square algorithms over adaptive networks," in *10th International Conference on Information Science, Signal Processing and their Applications (ISSPA 2010)*, 2010, pp. 381–384.

[68] I. Song and P. Park, "A normalized least-mean-square algorithm based on variable-step-size recursion with innovative input data," *IEEE Signal Processing Letters*, vol. 19, no. 12, pp. 817–820, 2012.

[69] H. C. Shin, A. H. Sayed, and W. J. Song, "Variable step-size NLMS and affine projection algorithms," *IEEE Signal Processing Letters*, vol. 11, no. 2, pp. 132–135, 2004.

[70] A. Huang, G. Guan, Q. Wan, and A. Mehbodniya, "A block orthogonal matching pursuit algorithm based on sensing dictionary," *International Journal of Physical Sciences*, vol. 6, no. 5, pp. 992–999, 2011.

[71] M. Majji, J. N. Juang, and J. L. Junkins, "Observer/kalman-filter time-varying system identification," *Journal of Guidance, Control, and Dynamics*, vol. 33, no. 3, pp. 887–900, 2010.

[72] K. Andrzej and U. Tadeusz, "Identification of modal parameters of non-stationary systems with the use of wavelet based adaptive filtering," *Mechanical Systems and Signal Processing*, vol. 47, no. 1-2, pp. 21–34, 2014.

[73] C. S. Huang, S. L. Hung, W. C. Su, and C. L. Wu, "Identification of time-variant modal parameters using time-varying autoregressive with exogenous input

and low-order polynomial function," *Computer-Aided Civil and Infrastructure Engineering*, 2009.

[74] R. Kulhav, "Restricted exponential forgetting in real-time identification," *Automatica*, vol. 23, no. 5, pp. 589–600, 1987.

[75] J. E. Cooper, "Identification of time varying modal parameters," *Aeronautical Journal*, vol. 94, no. 938, pp. 271–278, 1990.

[76] J. E. Cooper and K. Worden, "On-line physical parameter estimation with adaptive forgetting factors," *Mechanical Systems and Signal Processing*, vol. 14, no. 5, pp. 705–730, 2000.

[77] S. Haykin, *Adaptive Filter Theory*, 4th ed. Upper Saddle River, NJ: Prentice Hall, 2002.

[78] S. B. Gelfand, Y. Wei, and J. V. Krogmeier, "The stability of variable step-size LMS algorithms," *Signal Processing, IEEE Transactions on*, vol. 47, no. 12, pp. 3277–3288, 1999.

[79] A. Tyseer and K. Mayyas, "A robust variable step-size LMS-type algorithm: Analysis," *IEEE Transactions on Signal Processing*, 1997.

[80] P. D. Anderson and M. A. Ingram, "The performance of the least mean squares algorithm combined with spatial smoothing," *Signal Processing IEEE Transactions on*, vol. 45, no. 4, pp. 1005–1012, 1997.

[81] K. Ozeki and T. Umeda, "An adaptive filtering algorithm using an orthogonal projection to an affine subspace and its properties," *Electronics and Communications in Japan (Part I: Communications)*, vol. 67, no. 5, pp. 19–27, 1984.

[82] B. Farhang-Boroujeny, *Adaptive Filters: Theory and Applications*. John Wiley & Sons, 2013.

[83] H. C. Shin and A. H. Sayed, "Mean-square performance of a family of affine projection algorithms," *IEEE Transactions on Signal Processing*, vol. 52, no. 1, pp. 90–102, 2004.

[84] L. A. Liporace, "Linear estimation of nonstationary signals," *Journal of the Acoustical Society of America*, vol. 58, no. 6, pp. 1288–1296, 1975.

[85] M. Niedzwiecki, "Functional series modeling approach to identification of nonstationary stochastic systems," *Automatic Control IEEE Transactions on*, vol. 33, no. 10, pp. 955–961, 1987.

[86] M. Niedzwiecki, *Identification of Time-varying Processes*, 2000.

[87] G. H. Mark, V. O. Alan, and S. Alan, "Time-varying parametric modeling of speech," *Signal Processing*, 1983.

[88] R. B. Mrad, S. D. Fassois, and J. A. Levitt, "Nonstationary signal estimation using time-varying ARMA models," in *Time-Frequency and Time-Scale Analysis, 1994., Proceedings of the IEEE-SP International Symposium on*, 1994.

[89] A. G. Poulimenos and S. D. Fassois, "Estimation and identification of non-stationary functional series TARMA models," *IFAC Proceedings Volumes*, vol. 36, no. 16, pp. 157–162, 2003.

[90] R. Zou, H. Wang, and K. H. Chon, "A robust time-varying identification algorithm using basis functions," *Annals of Biomedical Engineering*, vol. 31, no. 7, pp. 840–853, 2003.

[91] D. Slepian, "Prolate spheroidal wave functions, Fourier analysis, and uncertainty-V: The discrete case," *Bell System Technical Journal*, vol. 57, no. 5, 1978.

[92] M. J. Flaherty, "Application of polynomial splines to a time-varying autoregressive model of speech," *Acoustics, Speech, and Signal Processing, 1988. ICASSP-88., 1988 International Conference on*, 1988.

[93] J. R. Sato, P. A. Morettin, P. R. Arantes, and E. Amaro, "Wavelet based time-varying vector autoregressive modelling," *Computational Statistics & Data Analysis*, vol. 51, 2007.

[94] W. Weijtjens, J. Lataire, C. Devriendt, and P. Guillaume, "Dealing with periodical loads and harmonics in operational modal analysis using time-varying transmissibility functions," *Mechanical Systems and Signal Processing*, 2014.

[95] R. Charbonnier, M. Barlaud, G. Alengrin, and J. Menez, "Results on AR-modelling of nonstationary signals," *Signal Processing*, vol. 12, no. 2, pp. 143–151, 1987.

[96] V. G. Asutkar, B. M. Patre, and T. K. Basu, "Identification of linear time-varying systems using haar basis functions," *International Journal of Information and Systems Sciences*, vol. 6, no. 3, pp. 333–44, 2010.

[97] K. H. Chon, H. Zhao, R. Zou, and K. Ju, "Multiple time-varying dynamic analysis using multiple sets of basis functions," *IEEE Transactions on Biomedical Engineering*, vol. 52, no. 5, pp. 956–960, 2005.

[98] Y. Li, H. L. Wei, and S. A. Billings, "Identification of time-varying systems using multi-wavelet basis functions," *Control Systems Technology, IEEE Transactions on*, vol. 19, no. 3, pp. 656–663, 2011.

[99] G. G. Walter and X. Shen, *Wavelets and other orthogonal systems*. CRC press, 2000.

[100] J. Wang, T. Chen, and B. Huang, "Closed-loop identification via output fast sampling," *Journal of Process Control*, vol. 14, no. 5, pp. 555–570, 2004.

[101] G. Pillonetto, "System identification using kernel-based regularization: New insights on stability and consistency issues," *Automatica: A journal of IFAC the International Federation of Automatic Control*, pp. 321–332, 2018.

[102] O. Nelles, *Nonlinear System Identification*. Springer Berlin Heidelberg, 2001.

[103] T. Chen, "On kernel design for regularized LTI system identification," *Automatica*, vol. 90, pp. 109–122, 2018.

[104] S. H. Tsai and Y. W. Chen, "A novel fuzzy identification method based on ant colony optimization algorithm," *IEEE Access*, vol. 4, pp. 3747–3756, 2016.

[105] A. Alfi and H. Modares, "System identification and control using adaptive particle swarm optimization," *Applied Mathematical Modelling*, vol. 35, no. 3, pp. 1210–1221, 2011.

[106] A. Tarantola, *Inverse problem theory and methods for model parameter estimation*. SIAM, 2005.

[107] H. Chen, "Application of regularization methods to damage detection in large scale plane frame structures using incomplete noisy modal data," *Engineering Structures*, vol. 30, no. 11, pp. 3219–3227, 2008.

[108] J. Guo, L. Wang, and I. Takewaki, "Modal-based structural damage identification by minimum constitutive relation error and sparse regularization," *Structural Control and Health Monitoring*, vol. 25, no. 12, p. e2255, 2018.

[109] T. Mimasu, C. W. Kim, and Y. Goi, "Structural health monitoring of a steel girder bridge utilizing reconstructed sparse-like system matrix," in *The 6th International Symposium on Life-Cycle Civil Engineering*, 2018, pp. 28–31.

[110] R. Mohammadi-Ghazi and O. Büyüköztürk, "Sparse generalized pencil of function and its application to system identification and structural health monitoring," in *Health Monitoring of Structural and Biological Systems 2016*, vol. 9805. International Society for Optics and Photonics, 2016, p. 98050B.

[111] L. Jie and C. Jun, "Study on identification of structural dynamic parameters with unknown input information," *Chinese Journal of Computational Mechanics*, vol. 1, 1999.

[112] J. Wang, J. Huang, J. Chen, and J. Liu, "Study on mixed correction identification method with incomplete input information," *Journal of Vibration and Shock*, 2007.

[113] S. Mayr, G. Grabmair, and J. Reger, "Input design and online system identification based on poisson moment functions for system outputs with quantization noise," in *2017 25th Mediterranean Conference on Control and Automation (MED)*. IEEE, 2017, pp. 23–29.

[114] L. Sun, X. Liu, and J. Liu, "Determination of model structure via cyclo-stationarity based neural network," *International Journal of Innovative Computing, Information and Control*, vol. 16, no. 2, pp. 585–595, 2020.

[115] L. Sun, X. Liu, and A. Sano, "Model structure identification and parameter estimation for unstable process in closed-loop," *ICIC Express Letters*, vol. 13, no. 7, pp. 625–633, 2019.

[116] L. Sun, R. Uto, X. Liu, and A. Sano, "Multi-point search based identification under severe numerical conditions," in *IFAC-PapersOnLine*, 2020, pp. 468–473.

[117] C. Na, S. P. Kim, and H. G. Kwak, "Structural damage evaluation using genetic algorithm," *Journal of Sound and Vibration*, vol. 330, no. 12, pp. 2772–2783, 2011.

[118] H. Tang, P. Li, and C. Fan, "Structural system identification based on SCE algorithm," *Journal of Vibration Engineering*, vol. 23, no. 3, pp. 243–248, 2010.

[119] K. Mahata, "A subspace algorithm for wideband source localization without narrowband filtering," *IEEE Transactions on Signal Processing*, vol. 59, no. 7, pp. 3470–3475, 2011.

[120] M. Basseville and I. Nikiforov, *Detection of Abrupt Changes: Theory and Application*. prentice Hall Englewood Cliffs, 1993.

[121] S. V. Vaerenbergh, I. Santamaria, and M. Lazaro-Gredilla, "Estimation of the forgetting factor in kernel recursive least squares," in *IEEE International Workshop on Machine Learning for Signal Processing*, 2012.

[122] Z. H. Zhang and D. J. Zhang, "New variable step size LMS adaptive filtering algorithm and its performance analysis," *Systems Engineering and Electronics*, vol. 31, no. 9, pp. 2238–2241, 2009.

[123] N. Li, Y. Zhang, Y. Hao, and J. A. Chambers, "A new variable step-size NLMS algorithm designed for applications with exponential decay impulse responses," *Signal Processing*, vol. 88, no. 9, pp. 2346–2349, 2008.

[124] K. Ikeda, "Convergence analysis of block orthogonal projection and affine projection algorithms," *Signal Processing*, vol. 82, no. 3, pp. 491–496, 2002.

[125] W. B. J. Hakvoort, R. G. K. M. Aarts, J. V. Dijk, and J. B. Jonker, "A computationally efficient algorithm of iterative learning control for discrete-time linear time-varying systems," *Automatica*, vol. 45, no. 12, pp. 2925–2929, 2009.

[126] M. K. Tsatsanis and G. B. Giannakis, "Modelling and equalization of rapidly fading channels," *International Journal of Adaptive Control and Signal Processing*, 1996.

[127] G. Rödönyi, P. Körös, P. Dániel, A. Soumelidis, Z. Szabo, and J. Bokor, "Structure selection and LPV model identification of a car steering dynamics," 2018.

[128] D. Machala, S. Dobre, M. Albisser, F. Collin, and M. Gilson, "Quasi-LPV modelling of a projectile's behaviour in flight - ScienceDirect," *IFAC-PapersOnLine*, vol. 51, no. 15, pp. 1080–1085, 2018.

[129] S. Simani and R. J. Patton, "Fault diagnosis of an industrial gas turbine prototype using a system identification approach," *Control Engineering Practice*, vol. 16, no. 7, pp. 769–786, 2008.

[130] H. Wang, L. Bai, J. Xu, and W. Fei, "EEG recognition through time-varying vector autoregressive model," in *2015 12th International Conference on Fuzzy Systems and Knowledge Discovery (FSKD)*, 2016.

[131] S. A. Broughton and K. Bryan, "Discrete Fourier analysis and wavelets," *Journal of Applied Statistics*, vol. 37, 2011.

[132] M. D. Spiridonakos and S. D. Fassois, "Non-stationary random vibration modelling and analysis via functional series time-dependent ARMA (FS-TARMA) models A critical survey," *Mechanical Systems & Signal Processing*, vol. 47, no. 1-2, pp. 175–224, 2014.

[133] L. Sun and L. Li, "New recursive identification algorithm for time-varying systems," in *2009 ICCAS-SICE*. IEEE, 2009, pp. 4917–4922.

[134] L. Ljung, *System Identification Theory for the User*. 2nd Edition, Prentice Hall, Englewood Cliffs NJ, 1999.

[135] L. Blackmore, S. Rajamanoharan, and B. C. Williams, "Active estimation for jump markov linear systems," *IEEE Transactions on Automatic Control*, vol. 53, no. 10, pp. 2223–2236, 2008.

[136] M. Niedzwiecki, "Recursive functional series modeling estimators for identification of time-varying plants-more bad news than good?" *IEEE Transactions on Automatic Control*, vol. 35, no. 5, pp. 610–616, 1990.

[137] X. Liu and L. Sun, "Recursive identification algorithm based on cosine basis for rapid time-varying systems," *Int. Journal of Innovative Computing, Information and Control*, vol. 15, no. 2, pp. 617–628, 2019.

[138] X. Liu and L. Sun, "Recursive identification algorithm based on basis functions for time-varying system," in *13th International Conference on Innovative Computing, Information and Control*, 2018.

[139] S. Kamijo, Y. Gu, and L. Hsu, "Autonomous vehicle technologies: Localization and mapping," *IEICE Fundam. Rev.*, vol. 9, no. 2, pp. 131–141, 2015.

[140] M. Kloock, P. Scheffe, I. Tülleners, J. Maczijewski, B. Alrifaee, and S. Kowalewski, "Vision-based real-time indoor positioning system for multiple vehicles," *IFAC-PapersOnLine*, vol. 53, no. 2, pp. 15 446–15 453, 2020.

[141] A. Folkers, M. Rick, and C. Büskens, "Controlling an autonomous vehicle with deep reinforcement learning," in *2019 IEEE Intelligent Vehicles Symposium (IV)*. IEEE, 2019, pp. 2025–2031.

[142] K. Obara, "Nonvolcanic deep tremor associated with subduction in southwest japan," *Science*, vol. 296, no. 5573, pp. 1679–1681, 2002.

[143] H. Hirose and K. Obara, "Repeating short- and long-term slow slip events with deep tremor activity around the bungo channel region, southwest japan," *Earth Planets & Space*, vol. 57, no. 10, pp. 961–972, 2005.

[144] *Committee for Examining Earthquake Prediction, Seismological Society of Japan: Science of Earthquake Prediction*. The University of Tokyo Press, 2007.

[145] S. Saha, D. Mukherjee, and S. Mukhopadhyay, "Online detection and location estimation of earthquake events using continuous wavelet transform," in *2016 IEEE First International Conference on Control, Measurement and Instrumentation (CMI)*, 2016, pp. 77–82.

[146] R. Abreu, P. Zoeteweij, and A. J. van Gemund, "Spectrum-based multiple fault localization," in *2009 IEEE/ACM International Conference on Automated Software Engineering*. IEEE, 2009, pp. 88–99.

[147] P. Wu, S. Su, Z. Zuo, X. Guo, B. Sun, and X. Wen, "Time difference of arrival (TDoA) localization combining weighted least squares and firefly algorithm," *Sensors*, vol. 19, no. 11, pp. 2554–2567, 2019.

[148] T. K. Le and N. Ono, "Closed-form and near closed-form solutions for TDoA-based joint source and sensor localization," *IEEE Transactions on Signal Processing: A publication of the IEEE Signal Processing Society*, vol. 65, no. 5, pp. 1207–1221, 2017.

[149] X. Zhang, L. Xu, L. Xu, and D. Xu, "Direction of departure (DOD) and direction of arrival (DOA) estimation in MIMO radar with reduced-dimension MUSIC," *Communications Letters, IEEE*, vol. 14, no. 12, pp. 1161–1163, 2010.

[150] C. Feng, W. S. A. Au, S. Valaee, and Z. Tan, "Received-signal-strength-based indoor positioning using compressive sensing," *IEEE Transactions on Mobile Computing*, vol. 11, no. 12, pp. 1983–1993, 2012.

[151] N. Neidell and M. Taner, "Semblance and other coherency measures for multichannel data," *Geophysics*, vol. 36, no. 3, pp. 482–497, 1970.

[152] Y. Asano, K. Obara, and Y. Ito, "Spatiotemporal distribution of very-low frequency earthquakes in tokachi-oki near the junction of the kuril and japan trenches revealed by using array signal processing," *Earth Planets & Space*, vol. 60, no. 8, pp. 871–875, 2008.

[153] S. H. Jeong, Y. S. Won, and D. Shin, "Fast DOA estimation method based on MUSIC algorithm combined newton method for FMCW radar," in *2019*

IEEE MTT-S International Conference on Microwaves for Intelligent Mobility (ICMIM), 2019.

[154] S. Zhang, Y. Shi, R. Zhang, F. Yan, Y. Wu, W. X, and L. Shen, *Vehicle Localization Using Joint DOA/TOA Estimation Based on TLS-ESPRIT Algorithm*. Computational Stem Cell Biology, 2019.

[155] D. Meng, X. Wang, M. Huang, L. Wan, and B. Zhang, "Robust weighted subspace fitting for DOA estimation via block sparse recovery," *IEEE Communications Letters*, vol. 24, no. 3, pp. 563–567, 2020.

[156] N. Vankayalapati, S. Kay, and Q. Ding, "TDOA based direct positioning maximum likelihood estimator and the Cramer-Rao bound," *Aerospace & Electronic Systems IEEE Transactions on*, vol. 50, no. 3, pp. 1616–1635, 2014.

[157] R. B. B. Marxim and A. R. Mohanty, "Time delay estimation in reverberant and low SNR environment by EMD based maximum likelihood method," *Measurement*, vol. 137, pp. 655–663, 2019.

[158] B. Tang, J. Tang, Y. Zhang, and Z. Zheng, "Maximum likelihood estimation of DOD and DOA for bistatic MIMO radar," *Signal Processing*, vol. 93, no. 5, pp. 1349–1357, 2013.

[159] Y. Zhu, Y. Zhao, and P. Shui, "Low-angle target tracking using frequency-agile refined maximum likelihood algorithm," *IET Radar Sonar & Navigation*, vol. 11, no. 3, pp. 491–497, 2017.

[160] D. Dardari, A. Conti, U. J. Ferner, A. Giorgetti, and M. Z. Win, "Ranging with ultrawide bandwidth signals in multipath environments," *Proceedings of the IEEE*, vol. 97, no. 2, pp. 404–426, 2009.

[161] Y. Wang, "Seismic impedance inversion using ℓ_1-norm regularization and gradient descent methods," *Journal of Inverse and Ill-posed Problems*, vol. 18, no. 7, pp. 823–838, 2010.

[162] Y. Liu, B. Jiu, H. Liu, L. Zhang, and Y. Zhao, "Compressive sensing for very high frequency radar with application to low-angle target tracking under

multipath interference," in *2016 4th International Workshop on Compressed Sensing Theory and its Applications to Radar, Sonar and Remote Sensing (CoSeRa)*, 2016.

[163] L. Wang, R. C. de Lamare, and M. Haardt, "Direction finding algorithms with joint iterative subspace optimization," *IEEE Transactions on Aerospace and Electronic Systems*, vol. 50, no. 4, pp. 2541–2553, 2014.

[164] Y. Kinugasa, Y. Itoh, M. Kobayashi, Y. Fukui, and J. Okello, "A study on the step size of cascaded adaptive notch filter utilizing allpass filter," in *Circuits and Systems, 2003. ISCAS '03. Proceedings of the 2003 International Symposium on*, 2003.

[165] H. Tang, "DOA estimation based on MUSIC algorithm," 2014.

[166] Z. Lei, K. Yang, and Y. Ma, "Passive localization in the deep ocean based on cross-correlation function matching," *The Journal of the Acoustical Society of America*, vol. 139, no. 6, pp. EL196–EL201, 2016.

[167] A. Weiss and E. Weinstein, "Fundamental limitations in passive time delay estimation Part I: Narrow-band systems," *IEEE Transactions on Acoustics, Speech, and Signal Processing*, vol. 31, no. 2, pp. 472–486, 1983.

Publication List

Journal Paper

[J1] L. Sun, X. Liu and J. Liu, "Determination of model structure via cyclo-stationarity based neural network", *International Journal of Innovative Computing, Information and Control*, Vol.16, No.2, pp.585-595, April, 2020.

[J2] L. Sun, X. Liu and A. Sano, "Model structure identification and parameter estimation for unstable process in closed-loop", *ICIC Express Letters*, Vol.13, No.7, pp.625-633, July, 2019.

[J3] X. Liu and L. Sun, "Recursive identification algorithm based on cosine basis for rapid time-varying systems", *International Journal of Innovative Computing, Information and Control*, Vol.15, No.2, pp.617-628, April, 2019.

Conference Paper with Review

[P1] L. Sun, X. Liu and J. Zeng, "Recursive identification of time-varying systems with rapid changing", in *Proceedings of 15th International Conference on Innovative Computing, Information and Control*, September, 2021.(8 pages)

[P2] L. Sun, R. Uto, X. Liu and A. Sano, "Multi-point search based identification under severe numerical conditions", in *Proceedings of IFAC-PapersOnLine*, pp. 468-473, July, 2020.

[P3] X. Liu, L. Sun and J. Liu, "Trigonometric basis functions based time-varying identification algorithm with output weight factor", in *Proceedings of 2019 12th Asian Control Conference (ASCC)*, pp.1072-1077, June, 2019.

[P4] X. Liu and L. Sun, "Recursive identification algorithm based on basis functions for time-varying system", in *Proceedings of 13th International Conference on Innovative Computing, Information and Control*, August, 2018.(8 pages)